1-1-2014

Alterations In The Mouse Striatum Following Acute And Repeated Ethanol Exposure

Brooke D. Newman
Wayne State University,

ALTERATIONS IN THE MOUSE STRIATUM FOLLOWING ACUTE AND REPEATED ETHANOL EXPOSURE

by

BROOKE DANIELLE NEWMAN

DISSERTATION

Submitted to the Graduate School

of Wayne State University,

Detroit, MI

in partial fulfillment of the requirements

for the degree of

DOCTOR OF PHILOSOPHY

2014

MAJOR: CHEMISTRY (Biochemistry)

Approved by:

_____

Advisor Date

_____

_____

_____

DEDICATION

This dissertation is dedicated to my parents, husband, and extended family that were always motivating and supporting me whenever I needed it.

ACKNOWLEDGEMENTS

I would to thank my advisor Dr. Tiffany Mathews for introducing me to the field of neuroscience and addiction, a field that was never on my radar and that I now enjoy very much. I would like to thank my committee members Dr. Mary Kay Pflum, Dr. Tamara Hendrickson, and Dr. Alana Conti for their guidance and support. I would especially like to thank Dr. Conti for allowing me to collaborate on a project with her. Dr. Conti's willingness to help me whether or not it was related to our collaborative project was greatly appreciated.

I would also like to thank Dr. Kelly Bosse whose guidance, support, and friendship over the years has been amazing, even when we didn't see eye to eye. Dr. Bosse also contributed experimentally to the DID project as well as the DKO project when they were started. I also would like to thank Dr. Madiha Khalid for not only her friendship and support but also for all of the chapters she read for me. I would also like to recognize the members of the Hendrickson and Conti labs for helping the biochemist in the analytical lab!! Thank you also to the Conti lab for welcoming me and including me in conference travel so I was not alone, it really meant a lot to me. Finally all of the undergraduate students: Christopher Rogalla, Hany Eraqi, Michelle Colombo, Douglas Mack (Cresyl violet staining Chapter 2.5), Megan Jang, and Stephanie Goddens. These students taught me a lot about being a mentor and helped me over the years on various projects, as well as taking on the task of helping to wean mice and genotype them.

Finally I need to express my appreciation and love for my parents, husband, in-laws, extended family and friends. The support and words of encouragement from these people pushed me to keep going when I felt like giving up. Their support, guidance, words of encouragement and even tough love helped me get here and I will forever be appreciative of that.

TABLE OF CONTENTS

LIST OF TABLES

LIST OF FIGURES

LIST OF ABBREVIATIONS

Abbreviation	Meaning	Abbreviation	Meaning
AC	Adenylyl cyclase	**GABA**	gamma-aminobutyric acid
aCSF	Artificial cerebrospinal fluid	**GPCR**	G-protein coupled receptor
AMPA	Amino-3-hydroxy-5-methyl-4-isoxazolepropionic acid	**HPLC**	High performance liquid chromatography
ANOVA	Analysis of variance	**HVA**	Homovanillic acid
AP	Anterior/posterior	**LORR**	Loss of righting reflex
ATP	Adenosine triphosphate	**MAPK**	Mitogen-activated protein kinase
AUDs	Alcohol use disorders	**METH**	Methamphetamine
BDNF	Brain derived neurotrophic factor	**ML**	Medial/lateral
$BDNF^{+/-}$	BDNF heterozygous	**MRI**	Magnetic resonance imaging
BSA	Bovine serum albumin	**NAc**	Nucleus accumbens
cAMP	Cyclic adenosine monophosphate	**NIDA**	National Institute on Drug Abuse
CPu	Caudate putamen	**NMDA**	*N*-methyl-D-aspartate
CREB	cAMP response element binding protein	**PCR**	Polymerase chain reaction
DA	Dopamine	**PET**	Positron emission tomography
DA_{ext}	'true' extracellular DA concentration	**p-FL-TrkB**	Phosphorylated full length tyrosine kinase B receptor
DA_{in}	Perfused DA concentration	**PI3K**	Phosphatidylinositol-3-OH kinase
DA_{out}	Dialysate DA concentration	**PKA**	Protein kinase A
DAT	DA transporter	**PLCγ**	Phospholipase Cγ
DID	Drinking in the dark	**PMSF**	Phenylmethanesulfonyl fluoride
DKO	AC1 and AC8 double knockout	**p-T-TrkB**	Phosphorylated truncated tyrosine receptor kinase B
DLS	Dorsolateral striatum	**RCF**	Relative centrifugal force
DMS	Dorsomedial striatum	**SDS**	Sodium-dodecyl sulfate
DOPAC	3,4-dihydroxyphenylacetic acid	**SPSS**	Statistical package for the social sciences
DV	Dorsal/ventral	**TrkB**	Tyrosine kinase receptor B
ECL	Enhanced chemiluminescence	**T-TrkB**	Truncated tyrosine receptor kinase B
EDTA	Ethylenediaminetetraacetic acid	**VMAT**	Vesicular monoamine transporter
ELISA	Enzyme linked immunosorbent assay	**VTA**	Ventral tegmental area
EtOH	Ethanol	**WT**	Wild-type
FL-TrkB	Full length tyrosine kinase B receptor		

CHAPTER 1

Background and Introduction

1.1 Addiction

The National Institute on Drug Abuse (NIDA) defines addiction as a chronic, relapsing brain disease that is characterized by compulsive drug seeking and use, despite harmful consequences [1]. NIDA defines physical dependence as the development of neuronal adaptations to repeated drug exposure with normal function occurring only in the presence of the drug [1]. When the drug is withdrawn, several physiologic side effects can occur, such as seizures, when alcoholics abruptly stop drinking [2, 3]. While addiction and dependence are defined separately and are likely mediated in part by different brain regions, they are also connected with one another in that dependence often leads to addiction. In 2010, an estimated 9% of the population had a substance abuse or dependence problem [4]. The ability of drugs of abuse to change a person's brain and essentially rewire it to require or want those abused substances, make it almost impossible for an addict to stop without therapeutic intervention [5]. Any individual that tries a drug, legal or illegal, could become addicted, thus it is important to understand how various substances of abuse cause alterations to the brain [1, 2]. The only way to ensure that an individual does not become addicted is if he or she never takes any type of drug, including prescribed pain medication for serious injuries. As that is an unlikely scenario, it is important to continue the efforts to understand the complex problem that is addiction.

Alcohol in particular is a substance of interest due to its widespread availability and because it has been shown to be one of the first substances abused in adolescence [1]. In 2012, 88% of people age 18 and older have consumed alcohol in their lifetime [6]. Any of those people have the potential to become addicted, which could have a number of deleterious effects on their lives and those around

them, including untimely death. In the United States approximately 18 million people are affected by alcohol abuse or alcohol dependence annually, referred to collectively as alcohol use disorders (AUDs) by the National Institute on Alcohol Abuse and Alcoholism [7]. Despite the belief that addiction is an individual's problem, AUDs have high societal costs, from the cost of treatment due to health challenges and increased death rates; these issues are further support for the continued study of these disorders for successful rehabilitation [7]. To better understand what environmental and genetic factors lead to the development of AUDs, extensive research has focused on identifying risk factors predisposing one to AUDs. Continued efforts are needed to understand how to best treat individuals with different genetic backgrounds and predispositions that make them more susceptible to a loss of control over alcohol.

1.2 Fundamentals of Neuroscience and Dopamine Neurotransmission

The brain is a complex network of billions of neurons and neuromodulators working together and communicating in elaborate circuitries to maintain normal biological function. The different regions of the brain are made up of subsets of specialized neurons that serve different functions; for example the region of the amygdala is important in emotion and another region the cortex is responsible for initiation of movement [8]. Neurons communicate with one another via intercellular signaling using a variety of small chemical messengers called neurotransmitters (Table 1.1). One neurotransmitter of importance, which is targeted in some way by all substances of abuse, is dopamine (DA) [5]. DA, a catecholamine, is in the monoamine family of neurotransmitters and is synthesized in the neuron from the amino acid L-tyrosine (Figure 1.1). DA is involved in a vast array of physiological functions, including motor coordination, learning, memory, and drug reward [8].

Table 1.1 Common neurotransmitters organized by classification. This table is not comprehensive but provides an appreciation for the complexity of communication occurring in the brain between different neuron sub-types [8, 9].

Neurotransmitter Type	Neurotransmitters Included
Individual Neurotransmitters	Acetylcholine, Histamine
Biogenic Amines	Dopamine, Epinephrine, Norepinephrine, and Serotonin
Amino Acids	Glutamate and γ-amino butyric acid (GABA)
Purinergic	Adenosine triphosphate and Adenosine
Peptides	Families: Opioid, Hormones, Tachykinins, Neurotensin, Orexins, Neuropeptide Y, Calcitonins, and VIP-Glucagon
Soluble Gases	Nitric oxide, Carbon Monoxide, and Hydrogen Sulfide

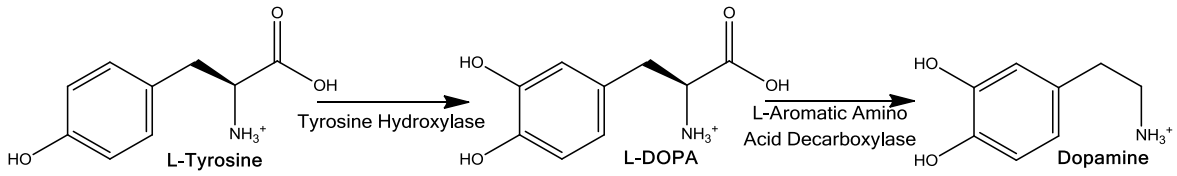

Figure 1.1 Synthesis of DA from L-tyrosine. Step one is hydroxylation of tyrosine by tyrosine hydroxylase to produce the intermediate L-DOPA. This reaction is the rate-limiting step. Subsequent decarboxylation of L-DOPA then yields DA.

1.2.1 Brain Regions

There are three important pathways for DA neurotransmission, the nigrostriatal pathway, the mesolimbic pathway, and the mesocortical limbic pathway (Figure 1.2, [8, 10]). The nigrostriatal pathway consists of DA neurons that project from the substantia nigra (SN), located in the midbrain, to the dorsal striatum or caudate-putamen (CPu) in the forebrain. The mesolimbic pathway refers to midbrain neurons from the ventral tegmental area (VTA) that project to the ventral striatum or nucleus accumbens (NAc). Neurons that originate in the VTA and project to the cortex make up the mesocortical pathway. The CPu (dorsal) and NAc (ventral), which together comprise the striatum, each serve slightly different physiological functions. The CPu can be further divided into two regions: the dorsolateral striatum (DLS) and

the dorsomedial striatum (DMS) [11]. Growing bodies of evidence suggest that each of these 3 regions (DMS, DLS, NAc) have their own specific function in the role of alcohol use and dependence [3, 11, 12]. The DLS is implicated in habitual use, while the DMS is involved in controlling goal-directed behavior, and the NAc is important in environmental control of consumption and relapse [11]. The DLS and DMS are typically grouped together as the CPu in rodent models, however in larger mammals as well as in humans the two subsections can be more easily distinguished by their medial/lateral position from midline. The NAc is involved in memory and motivational processes and has been established as the drug reward center of the brain [8]. Research involving drugs of abuse often focuses on the NAc [3, 8, 13], while the CPu in the past has had more attention with regard to neurodegenerative disorders such as Parkinson's disease, due to its involvement in motor coordination [12, 14]. More recently, the CPu has been gaining attention in later stages of addiction, when drug use is more compulsive and drug seeking has more of a habitual pathology [3, 15, 16]. Initially, drug seeking is likely mediated by the NAc and the motivation for a pleasurable effect, however over time substance abuse leads to neuroadaptations which can lead to habitual behavior mediated by the CPu [3, 12]. The roles of both the NAc and CPu are important and therefore efforts should continue to understand both as a means to determine the mechanism neuroadaptations associated with long term drug use and abuse.

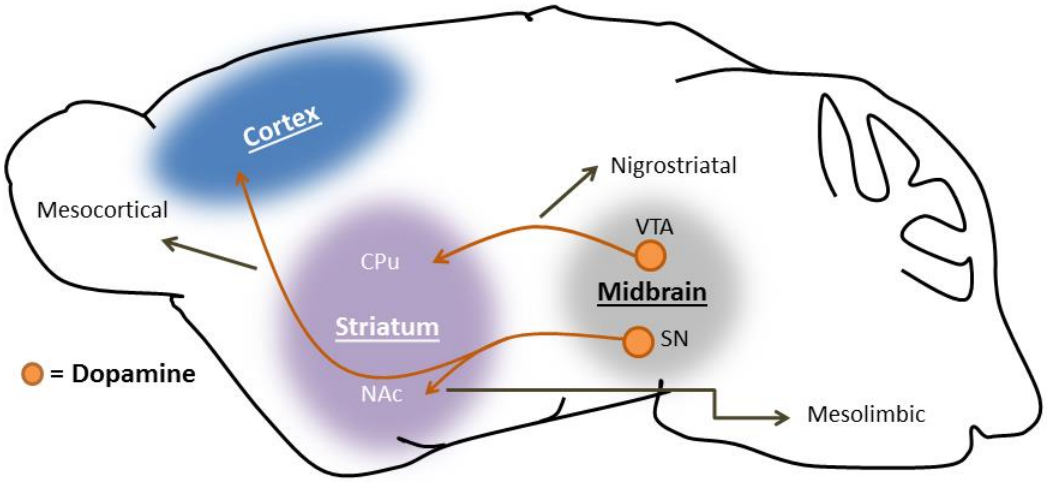

Figure 1.2 Representation of the major DA pathways from a sagittal view of a rodent brain, inspired from ([8, 10]).

1.2.2 Neuronal Communication

Most neurons communicate with each other by forming very close connections known as synapses in which various extracellular proteins join two neurons [8]. Neurons are made up of 4 main components: the dendrites, which receive information, the soma (cell body), a single axon which propagates processed information from the soma and finally nerve terminals (Figure 1.3). The axon of a pre-synaptic neuron creates a synapse with the dendrites of the post-synaptic neuron. Intercellular communication between neurons is accomplished by the release of neurotransmitters such as DA into the synaptic cleft, which is the small gap between synapsed neurons (Figure 1.4). After DA is synthesized, it is packaged into vesicles by vesicular monoamine transporters (VMATs, Figure 1.4, [8]). Following stimulation, neurons depolarize causing Ca^{2+} influx through voltage-sensitive Ca^{2+} channels, which stimulates release of DA through exocytosis during which the vesicles fuse to the membrane to release the stored neurotransmitter [8]. Released DA in the extracellular space can be taken back into the neuron by the DA transporter (DAT), to be recycled, or it can undergo catabolism to generate several

metabolites such as homovanillic acid (HVA) and 3,4-dihydroxyphenylacetic acid (DOPAC). The primary action of DA is to act on DA receptors found on the postsynaptic and/or presynaptic neuron. DA elicits its effects through activation of one of five receptor sub-types, the D1-Like (D1, D5) and D2-Like (D2, D3, D4) receptors [8]. The D1 and D2-like receptors are G-protein coupled receptors (GPCRs) that are differentiated based on the type of G-protein they activate: D1-like are associated with G_s and D2-like are associated with G_i/G_o [8]. The activation of the D1- or D2-like receptors regulate cyclic adenosine monophosphate (cAMP) production by stimulating or inhibiting adenylyl cyclase (AC), respectively (cAMP signaling is discussed in more detail in section ***1.2.4*** [10]). Two of the D2-like receptors, D2 and D3, are also located on the pre-synaptic DA neuron, where they function as auto-receptors to regulate DA synthesis and DA release [10].

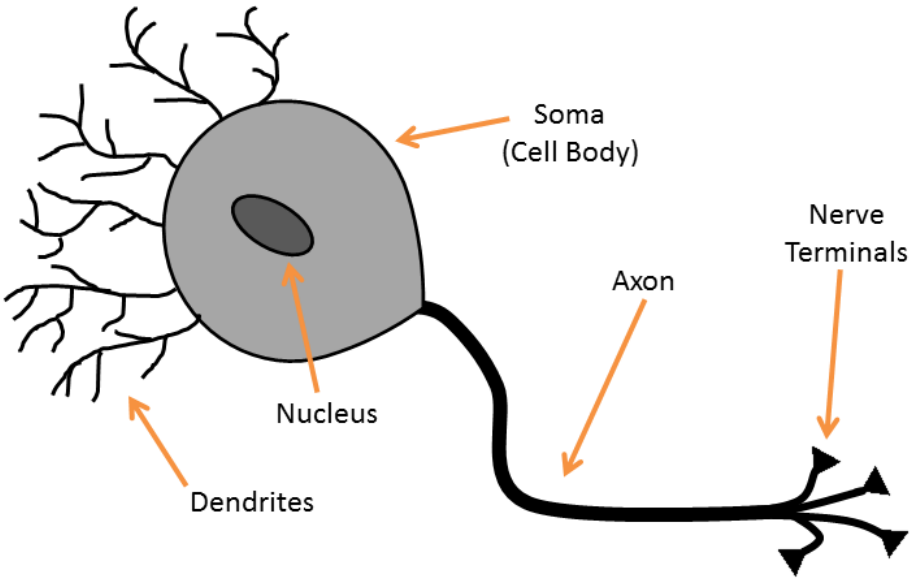

Figure 1.3 Schematic of the four major components of projection-type neurons such as DA neurons (inspired from [8]).

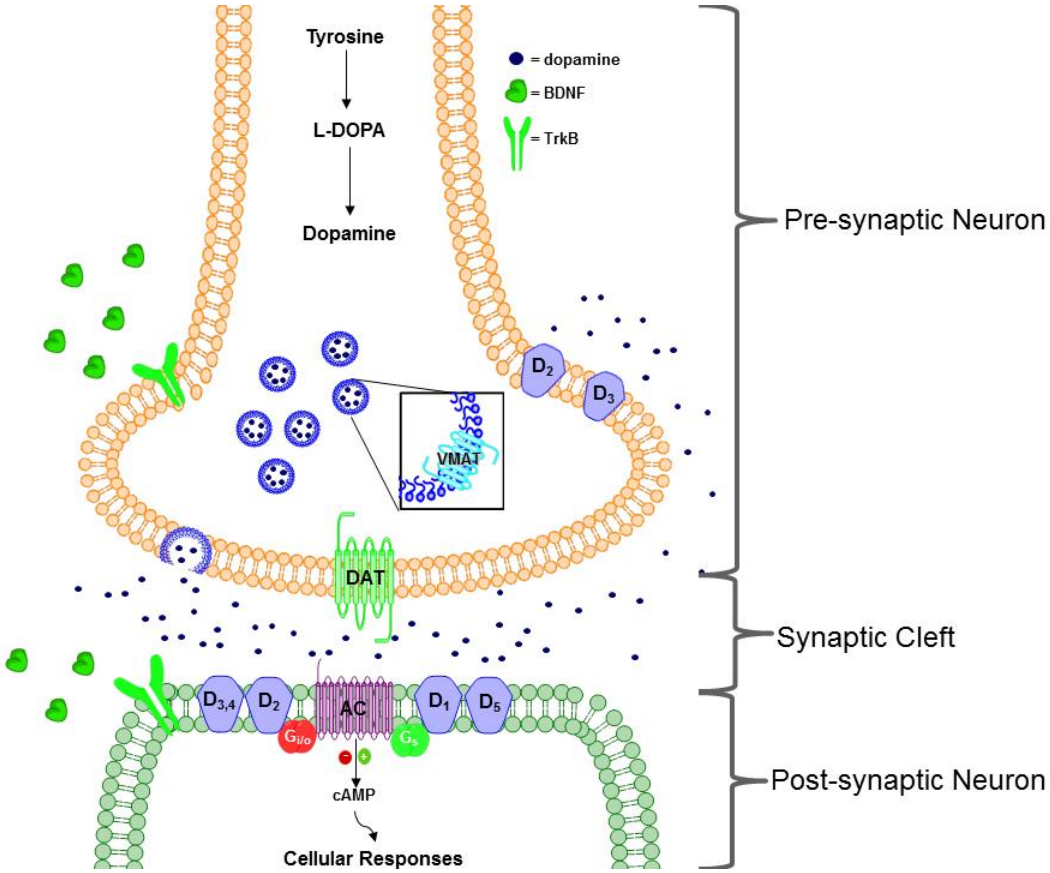

Figure 1.4 Depiction of a DA synapse showing the nerve terminal of the pre-synaptic neuron and the dendrite of the post-synaptic neuron. The space between the two neurons is the synaptic cleft, which is about 20 nm in size [17]. Also represented is the release of DA through fusion of the vesicle (blue) with the neuron membrane (orange). After release DA transmission occurs through interaction with D1- and D2-like receptors. Adenylyl cyclase (AC) is a target of D1-like and D2-like receptor activation with the D1- being stimulatory and the D2- being inhibitory. The DA transporter (DAT) shown on the nerve terminal is important in recycling and regulation of extracellular DA concentrations. The vesicular monoamine transporter (VMAT), responsible for the packaging of DA, is highlighted on the DA vesicles. Finally, the protein brain-derived neurotrophic factor (BDNF) is also depicted, as well as its receptor tyrosine kinase B (TrkB). (Modeled from [8]).

1.2.3 Amino Acid Neurotransmitters

The amino acid neurotransmitters γ-amino butyric acid (GABA) and glutamate are also involved in the nigrostriatal and mesolimbic DA pathways. Typically glutamate and GABA are respectively referred to as the excitatory and inhibitory amino acids. There are several

glutamate receptor subtypes; two of relevance here are *N*-methyl-D-aspartate (NMDA) and α-amino-3-hydroxy-5-methyl-4-isoxazolepropionic acid (AMPA, [8]). The GABA receptors are divided into two main groups, the $GABA_A$ and $GABA_B$ families [8]. The glutamate and GABA amino acid neurotransmitters are important because they converge, are connected with, and regulate DA neurotransmission. About 95% of the neurons in the striatum (NAc and CPu) are GABAergic medium-sized spiny projection neurons [13], which receive input from glutamate neurons of the cortex and DA neurons of the midbrain (Figure 1.5). Figure 1.5 shows an updated representation of the DA pathways, this time including the connections of the amino acid neurotransmitters in these particular brain regions. Together these neurotransmitters have a mutual relationship in their ability to modulate the neurotransmission of one another. Although the consideration of only DA makes experimental interpretation in relation to alcohol dependence simpler, the other neurotransmitters need to be considered as well. The amino acid receptors NMDA and $GABA_A$ are both targets of ethanol [10], which complicates the understanding of whether DA observations are primary or secondary effects of ethanol.

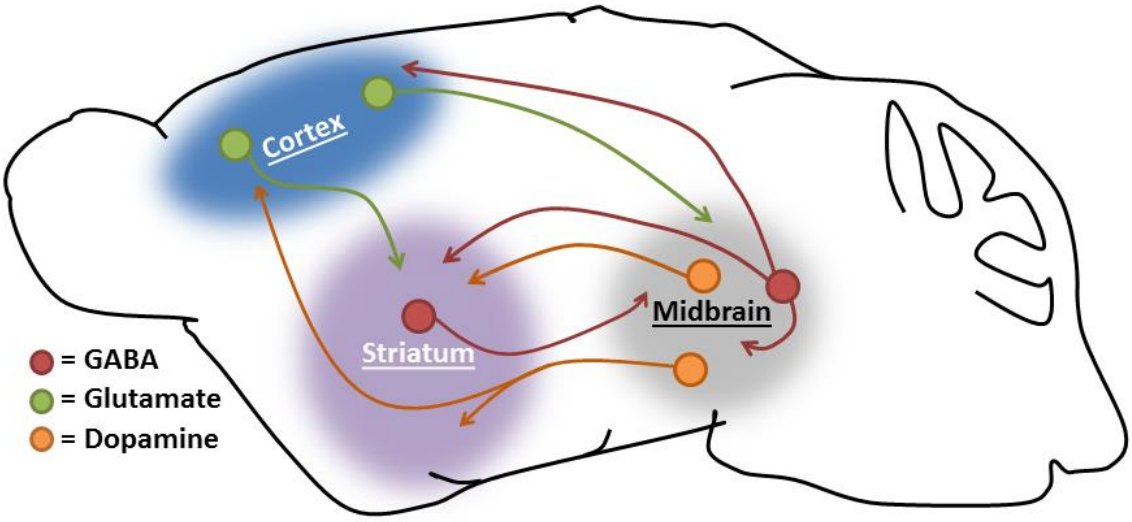

Figure 1.5 A simplified representation of the innervation of DA from the midbrain to the striatum and cortex. There is also mixed innervation from the amino acid neurotransmitters glutamate (excitatory) and GABA (inhibitory) in these three regions [18, 19].

1.2.4 Intracellular Signaling

In addition to the intercellular signaling that occurs across complex networks of neurotransmitters, there is also a vast amount of intracellular signaling taking place in these neuronal sub-populations. There are several small molecule, peptide, and protein neuromodulators that can alter the communication between different types of neurons. Two of those relevant for this dissertation are cAMP and brain-derived neurotrophic factor (BDNF).

cAMP is an important second messenger with its signaling being involved in learning and memory; as such it is also of interest with regard to drugs of abuse and addiction [10, 20]. Adenosine triphosphate is converted to cAMP through the action of ACs [10]. There are 10 mammalian AC isoforms that have variable distributions in different brain regions and neuron types, allowing cAMP-signaling to serve multiple distinct functions [10]. Increases in cAMP promote dissociation of protein kinase A (PKA) regulatory subunits from the catalytic subunits

leading to further phosphorylation of downstream targets, one of which is the cAMP response element binding (CREB) protein [10]. Activation of CREB stimulates gene transcription, which produces various physiological outputs, such as enhanced neuroplasticity through increased expression of structural proteins [8]. The role of CREB in learning is still under investigation in mammalian models but in *Drosophila*, CREB mutants showed deficits in learning and memory [8, 10].

BDNF is a 14 kDa protein in the neurotrophin family important for neuronal survival, differentiation, and plasticity [21]. BDNF binds as a dimer to its receptor, tyrosine kinase B (TrkB), causing internalization and auto-phosphorylation (Figure 1.6, [20]). Several signaling cascades are then activated through recruitment of adapter proteins, such as mitogen-activated protein kinase (MAPK), phosphatidylinositol-3-OH kinase (PI3K), and phospholipase Cγ (PLCγ) (Figure 1.6, [21]). One outcome of activation of these pathways is enhancement of CREB regulated gene transcription, yielding diverse biological outcomes such as enhanced synaptic plasticity (the strengthening of synapses). Furthermore, BDNF itself is a target of CREB and its transcription is regulated by it [20]. In addition to the trophic function of BDNF it, like cAMP, is important in learning and memory and, as such, is of interest in substance abuse studies.

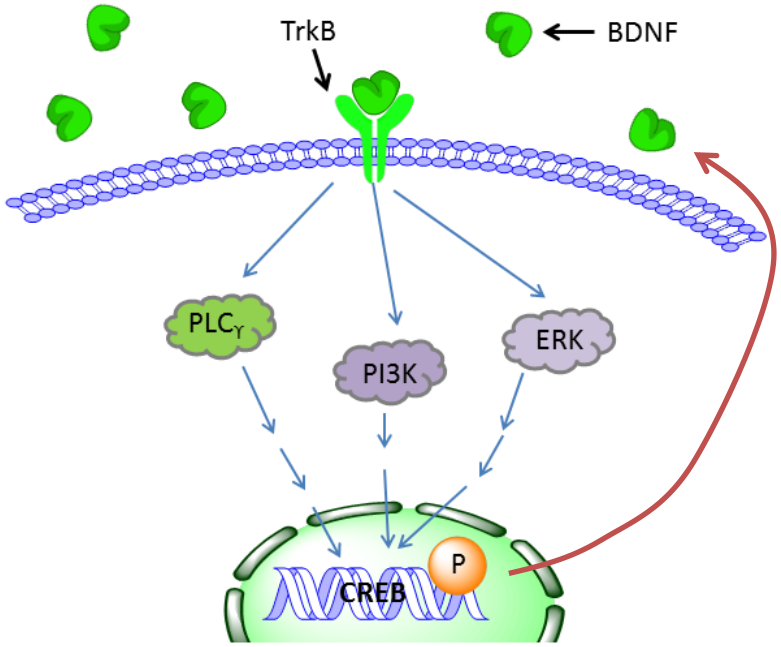

Figure 1.6 Schematic of BDNF-signaling initiated by binding with its receptor TrkB and subsequent activation of kinase signaling cascades to regulate the CREB transcription factor. Also depicted is the CREB regulation of BDNF transcription.

1.3 BDNF and Ethanol

There is a body of evidence suggesting the comorbidity of psychiatric disorders in people suffering from alcohol dependence, which makes understanding the motivation for alcohol consumption all the more complicated [21, 22]. In a clinical study by Goldstein *et al.*, a variety of disorders such as anxiety, depression, and schizophrenia were shown to pre-dispose patients to ethanol abuse [22]. BDNF is a common factor that has been implicated in psychiatric disorders and addiction and has been investigated in an effort to elucidate its role in both [21]. In humans, mutations in the BDNF gene have been linked to increased vulnerability and relapse to alcoholism [21, 23, 24]. A region on chromosome 11, which contains the BDNF gene, has been associated with increased vulnerability to polysubstance abuse, including alcohol, in humans

[23]. Polymorphisms in the BDNF gene have also been associated with an earlier onset of alcohol abuse and a faster rate of relapse in alcoholics [24]. Additionally, decreased plasma BDNF levels have been observed clinically in alcoholics [25]. In rodent models, BDNF-deficient mice consumed more alcohol than control mice and pharmacologic manipulations in control animals that reduced BDNF levels also led to increased consumption; together evidencing a role for BDNF to influence alcohol consumption and preference [26-28]. Further studies to determine the relationship between BDNF and ethanol have also revealed the ability of ethanol to alter BDNF protein and mRNA expression [20, 21, 26, 29]. In mouse models, acute administration of ethanol reduced BDNF protein levels in the striatum [29] and increased BDNF mRNA levels [26]. The mRNA levels of the TrkB receptor of BDNF are also altered following exposure to ethanol [21, 30]. Taken together, it is clear that BDNF plays a role in alcohol consumption and dependence. Conflicting reports of ethanol's effect on BDNF expression [26, 29], together with the reciprocal relationship of BDNF and ethanol, merit further investigations to understand the exact roles of BDNF and the mechanisms through which it carries out its function.

1.4 Dopamine, Ethanol, and BDNF

Thus far evidence has been given for BDNF's role in alcohol consumption and dependence, as well as the importance of the neurotransmitter DA in substance abuse. BDNF alters DA transmission through direct stimulation of DA release and by reduced DA release in BDNF-deficient mice, which can be rescued by BDNF perfusion [31-33]. Ethanol increases DA in both regions of the mouse striatum following intraperitoneal (i.p.) administration [5, 29, 34, 35]. Previous studies, using BDNF-deficient mice, have shown that ethanol stimulated DA release is blunted in the deficient mice compared to wild-type (WT) mice [29]. Further evidence for the

importance of DA in ethanol consumption and dependence is found in alcoholic patients who have less DA D2 receptors compared to non-alcoholic patients, which could either be a factor for predisposition to alcoholism or a result of repeated ethanol exposure [36-38]. Investigations of the D2 receptor after ethanol exposure have shown variable results in D2 function or localization depending on the type of assay, method of ethanol exposure, and animal model [39]. The D2 receptor appears to regulate ethanol consumption, as shown in D2 receptor knock-out mice that are devoid of the long-form of the receptor [40]. The knockout of long form D2 receptor causes up-regulation of the short form D2 receptor and these animals consume more ethanol than control mice [40]. Again, BDNF could be an important factor mediating not only the release of DA in the presence of ethanol but also alterations in the D2 receptor.

1.5 Dissertation Specific Aim

The interactions of BDNF, DA, and ethanol in the brain are incredibly complex given the reciprocal relationships of these molecules and the other neuronal systems implicated with ethanol use and exposure. The purpose of this study was to determine the effect of ethanol on the CPu in the presence of low endogenous BDNF levels to gain a better understanding of how a mutation in an individual's BDNF gene may promote their loss of control over alcohol use. This goal was achieved using genetically altered mice that have a 50% reduction in BDNF protein and mRNA levels ($BDNF^{+/-}$, BDNF heterozygous) and achieving ethanol exposure through the use of a voluntary ethanol consumption protocol, drinking in the dark (DID). After 7 days of exposure, DA neurotransmission, as well as BDNF-signaling, was assessed in the striatum of WT and $BDNF^{+/-}$ mice. The findings presented herein show significant striatal alterations after just 7 days of ethanol exposure and provide important and new information regarding this DID model.

CHAPTER 2

Methods and Methodological Considerations

This chapter provides a detailed description of methods used for the experiments throughout this dissertation, as well as some background discussion on select techniques.

2.1 Animals

Wild-type (WT, strain: C57BL/6J) and brain derived neurotrophic factor (BDNF) deficient mice ($BDNF^{+/-}$, strain: B6.129S4-Bdnftm1Jae/J) were originally purchased from The Jackson Laboratory (Bar Harbor, ME) at the age of 3-5 weeks. $BDNF^{+/-}$ mice have a normal appearance and behavior despite a 50 % reduction in both mRNA and protein levels of BDNF. $BDNF^{-/-}$ mice which are complete knockout animals and are not used because they are not viable past 21 days. Upon acclimation (2 weeks), male $BDNF^{+/-}$ mice were placed with 1-2 C57BL/6J female mice for breeding. At 21 days of age, offspring were marked using an ear punch and tail biopsies were collected for PCR determination of genotype. Animals were housed in groups of 4-6, separated by gender, on a 12-hour light/dark cycle (0600 lights on). Cages were outfitted with corn cob bedding and Nestlets™ for environmental enrichment with food and water available *ad libitum.* Mice were used at about 4-6 months of age, and were moved to a different room for drinking studies carried out on a reverse light/dark cycle. All procedures were designed and conducted to minimize pain and discomfort to the animals. Animal care and use was in accordance with the National Institutes of Health Animal Care guidelines and approved by the Wayne State University Institutional Animal Care and Use Committee.

2.2 Genotyping

Tail biopsies were processed into smaller pieces using a razor blade to chop the tail into 6-8 individual pieces. The pieces were incubated overnight in a water bath at 55 °C in a lysis buffer containing: 0.1 M Tris base, 5 mM ethylenediaminetetraacetic acid (EDTA), 0.2% sodium-dodecyl sulfate (SDS), 0.2 M NaCl and 0.1 mg/mL proteinase K (New England BioLabs, Ipswich, MA). After 15-24 hours samples were vortexed and centrifuged (16 minutes, 20,000 RCF). The supernatants were transferred to a second set of tubes containing 500 µL of isopropyl alcohol each. These tubes were mixed by inversion, and centrifuged (16 minutes, 20,000 relative centrifugal force (RCF)). The supernatants were removed and 500 µL of 75% (v/v) ethanol was added to each pellet. Again the tubes were mixed by inversion and centrifuged (5 minutes, 20,000 RCF). The supernatants were removed and 6 µL of water was added, after which the tubes were placed in a vacuum desiccator to remove ethanol. The pellets were reconstituted in 85 µL of TE buffer (10 mM Tris base and 1 mM EDTA, pH 8.5) and stored at 4 °C until polymerase chain reaction (PCR) amplification was carried out.

Each mouse had two PCR reactions using its DNA, one for the WT primer and one for the $BDNF^{+/-}$ primer. Initially, the PCR procedure required making our own master mix containing: 1.28 mM $MgCl_2$, 0.48X PCR Buffer A (10 mM Tris-HCl, 1.5 mM $MgCl_2$, 50 mM KCl; pH 9.0), 0.096 mM dNTPs, and 1 µM control (or common) primer (ATGAAAGAAGTAAACGTCCAC). This master mix, 1 unit *Taq* DNA Polymerase and either 1 µM $BDNF^{+/-}$ (GGGAACTTCCTGACTAGGGG) or WT primer (CCAGCAGAAAGAGTAGAGGAG) was added to 4 µL of a DNA sample. Primers were purchased from Invitrogen (Grand Island, NY) and were designed based on The Jackson Laboratories (Bar Harbor, ME) recommendation for this mouse strain. The PCR reaction was performed using a thermocycler (Robocycler® gradient 96, Stratagene/Agilent, Santa Clara, CA).

The conditions were 94 °C for 2 minutes, followed by 35 cycles of 94 °C, 55 °C, and 72 °C for 30 seconds each, and a final 2 minute cycle at 72 °C. This method was useful but inconsistent because it often required troubleshooting in an effort to pinpoint the reagent that was causing problems. Additionally, this approach involved the addition of very small quantities of *Taq* Polymerase, which likely contributed to the poor dependability of the reaction due to inaccuracies in pipetting.

In an effort to improve the throughput of genotype analysis, a commercially available master mix, GoTaq® Hot Start Green Master Mix, from Promega (Madison, WI) was tested. The only additions required to this mix were DNA, water, and primers. This approach proved to be a much simpler reaction preparation and thus far has been more robust for continued genotypic analysis. The same cycling conditions on the thermocycler were used for both reactions. This master mix also simplified gel analysis because loading dye was already mixed in, minimizing another pipetting step in our analysis.

PCR products were electrophoresed on a 2% agarose gel containing 0.02% ethidium bromide in 1X TBE buffer (2.5 mM NaOH, 89.2 mM Tris Base, 89.0 mM boric acid, and 2.5 mM EDTA). The gel was prepped by heating the agarose and TBE buffer mixture (above) in the microwave until agarose was fully dissolved. After a brief cooling period ethidium bromide was added and the gel was poured into a rig with the comb in place. Once cooled the gel was placed in the running rig which was filled with the 1X TBE running buffer. 6 µL of sample were loaded on the gel with the WT reaction first, followed by the mutant reaction (Figure 2.1). The gel was electrophoresed at 125-135 V for about 45 minutes and imaged on a Typhoon 9210 scanner (Amersham Biosciences, Pittsburg, PA) at a fluorescence of 500 nm. WT mice were those with

only one DNA product; BDNF$^{+/-}$ mice also contained a second larger band from the PCR reaction using the mutant primer (Figure 2.1).

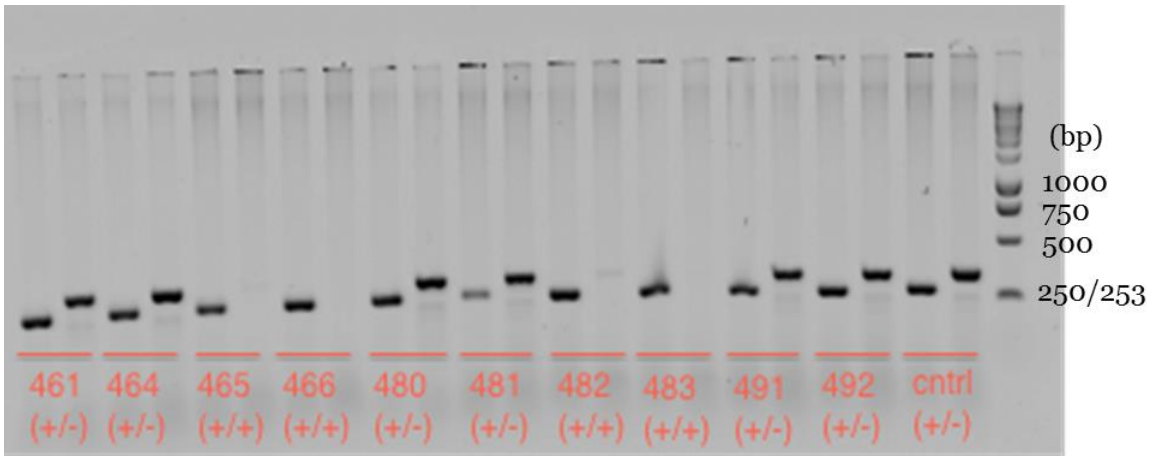

Figure 2.1 Representative agarose gel image used for the determination of mouse genotypes as WT or BDNF$^{+/-}$. The numbers across two lanes refer to the animal number that is defined during weaning when the tail biopsies are collected. The (+/-) notation indicates a BDNF$^{+/-}$ mouse given that there is a 250 bp band in the first (WT) lane for that mouse and a ~300 bp band in the second (BDNF$^{+/-}$ or mutant) lane. The (+/+) means the animal is a WT because no reaction occurred with the BDNF$^{+/-}$ primer.

2.3 Ethanol Consumption

2.3.1 Drinking Models

Mouse models are often used in neuroscience research because of the speed of reproduction, minimal expense, and ease of genetic modification, compared to other models [11]. When using animal models to represent human problems, the route and frequency of exposure is an important consideration. Routes of ethanol exposure include involuntary exposure through injection or vapor chamber or voluntary consumption through different drinking models. Some research has shown evidence that the involuntary routes of exposure do not activate the same neuronal pathways, such as those for habit-formation, in the same way as voluntary consumption protocols [41]. A subsequent challenge using voluntary consumption

models is replicating the human condition, which varies not only with age but also by the stage of addiction [42]. Heavy or excessive alcohol consumption is considered an important characteristic of alcohol dependence and addiction, as such this is a desirable feature of a drinking model [42]. A commonly used model of voluntary ethanol consumption is referred to as the 2-bottle choice assay in which animals have access to water and a solution of ethanol for 24 hours. The two-bottle choice assay allows for assessment of preference because animals have a choice. One drawback is that, due to the extended period of exposure, it is unclear if pharmacologically relevant blood alcohol levels are reached [42]. A recently developed model known as drinking in the dark (DID) promotes excessive 'binge'-like consumption to produce pharmacologically relevant blood alcohol levels (80.0 mg/dL) [43]. The DID protocol requires reversing the mouse's light/dark cycle and giving it limited access to only ethanol for 2-4 hours, starting 3 hours into the dark cycle, which resulted in higher consumption compared to starting at 1 or 2 hours into the dark cycle [43]. Ethanol consumption using the DID model was unaltered by varying the ethanol concentration and remained stable for up to 14 days [43]. The use of the C57BL/6J strain of mice was also important in achieving these high levels of consumption, as assessed in the study by Rhodes *et al*. [44]. 'Binge'-like consumption has been given far less attention in studies of addiction despite the fact that it may be an important factor in the development of dependence, and as such, it should be investigated along with acute and chronic models of ethanol exposure [45, 46]. Information and considerations for the DID model have been reviewed previously (see [47]) and findings thus far from its use in rodent models have also been reviewed recently (see [46]).

2.3.2 Drinking in the Dark Protocol

The overall goal of this work was to assess the effects of ethanol on the striatum in a mouse model with low endogenous BDNF levels by using the voluntary ethanol consumption DID model for 7 days. Animals were acclimated to a reverse light/dark cycle (0600 lights off) for a minimum of 2 weeks before drinking exposure. Animals were also habituated to the single-housed conditions required for the procedure for about 1 week before DID started. On ethanol drinking days, 3 hours into the dark cycle the home cage water bottle was removed and replaced with a pre-weighed bottle containing a 15 % ethanol (v/v) solution in tap water. Mice were left undisturbed with ethanol bottles for two hours. At the end of the DID session, the bottles were removed and weighed. The grams of ethanol consumed were calculated and normalized to the kilograms of mouse weight (reported as ethanol intake g/kg). On the seventh day of DID, animals either underwent surgery, were sacrificed for tissue, or remained in the animal room for 24 hours and then sacrificed for tissue. The mice that underwent surgery on the last day of DID were used for neurochemical characterization by microdialysis the following day, 24 hours after the last drinking session.

2.4 Microdialysis

2.4.1 Techniques for In Vivo Neurotransmitter Analysis

Monitoring neurotransmitters in humans poses a unique challenge as the brain is not easily accessible for measurements from an alive and intact system. The immense cross-talk between different neuron types and brain regions require an intact system to properly understand human conditions. For example the amino acid neurotransmitters that are targeted by ethanol and also regulate DA neurotransmission, these systems project across several brain regions and act in concert with each other highlighting the importance of an intact system.

Scientific advancements have provided solutions to these challenges with tools to measure neurotransmitter function in both human and animal models. These techniques include imaging with contrast agents, biosensors, microelectrodes, and *in vivo* sampling techniques [9, 48].

In humans and animals, positron emission tomography (PET) or magnetic-resonance imaging (MRI or functional MRI) can be used to determine receptor activity or general brain size and function [48]. For example, in a study by Childress *et al.,* detoxified cocaine users were compared to cocaine naïve individuals. Their cerebral blood flow was measured using PET imaging while watching a cocaine video [49]. The cocaine users experienced increased blood flow in some regions and decreased flow in other regions; these changes were not observed in the cocaine naïve individuals [49]. This experiment demonstrates how valuable these techniques can be for understanding brain function; however they do not always provide the required spatial or temporal resolution to understand dynamic processes in the brain.

Many neuroscience methods rely heavily on animal models for multiple reasons, including the relative cost and tendency for breeding; mice specifically are desirable for the ease with which they can be manipulated genetically. In animal models, advancements in neurotransmitter analysis have come in the form of biosensors, microelectrodes, sampling techniques and separation methods. Microelectrodes and biosensors can be used directly in the brain provided they are designed to be selective for the analyte of interest and maintain proper function in the brain tissue [9, 48]. Another common method is to use a sampling technique such as microdialysis to collect fluid from the extracellular space. In addition to being used directly in the brain, biosensors and microelectrodes can also be used with samples collected via microdialysis.

Microdialysis allows for the collection of a mixture of small molecules from the extracellular space from awake and freely moving animals. Microdialysis probes are equipped with a semi-permeable membrane with a molecular weight cut-off to exclude larger molecules, producing inherently clean samples (Figure 2.2). First, a guide cannula is inserted into the brain, which directs the microdialysis probe to a region of interest. Perfusion of the probe with a buffer similar to the biological matrix, termed the perfusate, produces a concentration gradient around the probe. Small molecules travel down the generated concentration gradient and into the probe for collection. Perfusate exiting from the probe is termed dialysate and can be processed in several ways. Initially analysis of dialysate is achieved by separation using liquid chromatography or capillary electrophoresis to separate the complex mixture. After separation, a multitude of detection schemes can be used to quantify the analyte of interest based on its chemical properties. Catecholamines such as dopamine (DA) are electroactive and are typically quantified via electrochemical detection, whereas non-electroactive neurotransmitters (*e.g.* amino acids) are usually derivatized so that fluorescence or electrochemical detection can be used [9, 48]. For this work, the analyte of interest was DA, and high performance liquid chromatography (HPLC) with electrochemical detection was used.

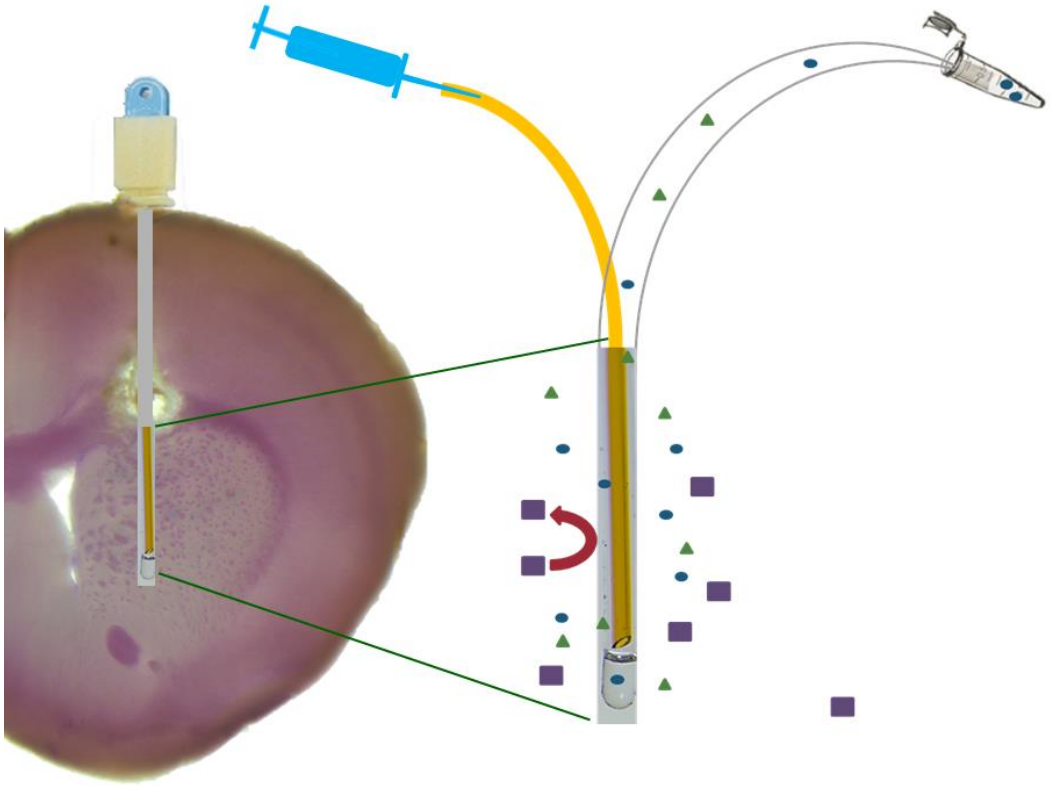

Figure 2.2. Diagram of an inserted microdialysis probe in the CPu (left) using a stained mouse slice. The expansion of a microdialysis probe (on the right) highlights the diffusion of small molecules (triangles and circles) into the probe and the exclusion of larger molecular weight molecules (squares).

2.4.2 Surgical Details

On days of surgery in preparation for microdialysis experiments, animals were moved from the colony to the laboratory, which had a separate room dedicated to surgical procedures, and allowed to acclimate. Mice were anesthetized using isoflurane inhalation, delivered with medical grade O_2 (g). Animals were induced in a chamber at 3% isoflurane delivery and subsequently transferred to a nose piece and maintained at 1.5-3% isoflurane. The animals were maintained in a surgical plane of anesthesia, which was verified by assessing the pedal withdrawal reflex. Before the procedure began, animals were injected with 0.2 mL of sterile

saline (0.9% NaCl) to aid in recovery from the procedure. In addition, sterile ophthalmic ointment was applied to the eyes to retain moisture and mice were placed on an isothermal heating pad to maintain body temperature.

The top of the head was shaved using a Remington beard and mustache trimmer so that the scalp could be cleaned. The incision area was cleaned three times, alternating between Betadine and 70% ethanol, followed by subcutaneous injection, in an elliptical pattern, of a local analgesic (0.5 mg/kg lidocaine + 1.5 mg/kg bupivacaine). A small circle of skin was then incised. A solution of 10% (v/v) hydrogen peroxide was applied to dissolve the perosteum and expose the skull to make the markings of bregma more defined. The bregma is the T-shaped intersection, which is the result of different skull sections fusing together and is used as an anatomical marker to target specific brain regions. Mice were placed on a stereotaxic frame (Figure 2.3) to achieve a flat and level skull surface. The guide cannula was positioned over bregma to read the associated anterior/posterior (AP) and medial/lateral (ML) coordinates. After applying the correction to target for the brain region of interest, a mark was made on the skull. Using a drill, a small burr hole was made to fit the guide cannula and, in the opposing quadrant, another small hole was made for placement of a bone anchor. The guide cannula was placed over the hole and the coordinates were recorded again. This time a dorsal/ventral (DV) reading was taken, and, as before, a correction was applied to insert the cannula to the proper depth. The guide cannula was secured in position using dental cement and the animal was allowed to recover on a heating pad.

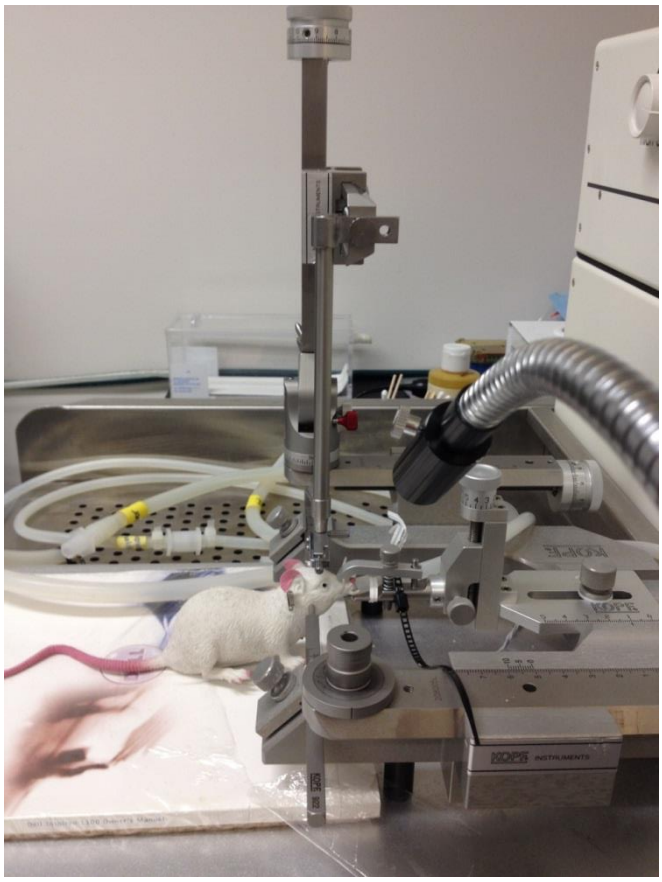

Figure 2.3. Picture of the stereotaxic frame used for surgeries with a mock animal in place.

Once the mice regained consciousness, they were transferred to a cylindrical bucket equipped for *in vivo* microdialysis. Two to four hours after surgery the 'dummy' probe was removed from the cannula and the CMA/7 2 mm microdialysis probe (0.24 mm diameter, Cuprophane, 6 kDa cut-off, Harvard Apparatus Inc) was inserted. Microdialysis lines and probes were cleaned offline using the antimicrobial ProClin® (BASi, West Lafayette, IN) and 70% ethanol (v/v), followed by perfusion with sterile artificial cerebrospinal fluid (aCSF, composition: 145 mM NaCl, 3.5 mM KCl, 2.0 mM Na_2HPO_4, 1.0 mM $CaCl_2$, 1.2 mM $MgCl_2$, pH = 7). ACSF was continuously perfused at a flow rate of 1.1 µL/min overnight and experiments were started the next day.

During microdialysis sampling, fractions were collected every 20 minutes, providing about 21 µL of dialysate for analysis per sample. Most dialysis experiments herein involved pharmacologic manipulation of some form. For such experiments, 3 baseline fractions were collected providing uncorrected extracellular DA levels, followed by drug treatment and subsequent fraction collection. All samples either pre- or post-drug were normalized to the 3 averaged baseline samples (set to 100%). The baseline correction achieved by normalizing values to the averaged baseline allows for individual variability between mice to be accounted for. Pharmacological treatment using microdialysis was carried out in several ways including systemic injection of the drug or targeted application through retrodialysis (perfused through probe) of the drug mixed into the aCSF. Baseline correction of experiments allows for variability in baseline DA levels to be accounted for between mice.

2.4.3 Zero Net Flux

As mentioned above, typically extracellular DA levels are determined without assessing the recovery of the microdialysis probe. However, there are some instances where determining the 'true' extracellular DA levels are beneficial to understand. The method of quantitative microdialysis also known as no net flux or zero net flux, allows for the determination of 'true' basal extracellular dopamine levels, which differ from extracellular levels determined directly from dialysate because it accounts for the recovery of the microdialysis probe. When determining 'true' extracellular DA levels it is important to consider that measurements are being made from a dynamic system which undergoes constant fluctuations with both passive (diffusion away from the synapse) and active processes (re-uptake and catabolism) occurring that can affect the diffusion of the analyte into the probe. Several quantitative approaches to determine extracellular DA levels have been assessed, which involve variations in flow rate of

the perfusate or varying concentrations of perfused analyte [50]. Microdialysis is possible because of the diffusion gradient created at the probe; as such, the recovery rate of analytes is dependent on the perfusate flow rate. Lower flow rates yield higher recovery because there is more time for equilibration around the probe. The variable perfusion method extrapolates from DA levels determined at different flow rates to determine the DA concentration at zero flow, which would be when the dialysate is in equilibrium with the extracellular fluid [50]. The drawbacks to the variable flow method are that it requires long sampling times and the determination of extracellular concentration is based off of interpolation of a non-linear curve [50]. The variation in concentration method, described below, is simpler and generates linear curves for interpretation and therefore it was used for this study.

The variation in concentration method, also called the difference method, is commonly referred to as no net flux or zero net flux. Using zero net flux, known concentrations of DA are added to the perfusate that bracket the expected extracellular concentrations. A programmable perfusion pump equipped with a 'Y' connector and two syringes: one with a stock standard of 20 nM DA and another with only aCSF. The pump was programmed such that concentrations of 0, 5, 10, and 20 nM DA were also perfused, for 1.5 hours each. Additionally, the concentrations of 20, 10 and 5 nM were assessed and quantified in an *in vitro* calibration to account for differences in making solutions from experiment to experiment and mixing variations of the perfusion pumps. The perfused DA (DA_{in}) minus dialysate DA output (DA_{out}) were plotted ($DA_{in} - DA_{out}$, y-axis) versus DA_{in} (x-axis) providing four data points (0, 5, 10 and 20 nM DA). A linear regression was run on these points to get a linear equation, $y = mx + b$ where m is the slope and b is the y-intercept. The x-intercept, where there is no loss from the brain or gain to the brain, then represents the 'true' extracellular concentration of DA (DA_{ext}).

The zero net flux difference method also provides an additional piece of information about the *in vivo* recovery of the probe, which indicates DA turnover efficiency [50]. According to a review by J.B. Justice, there are passive and active processes affecting probe recovery [50]. Passive processes include the reduced volume for transport and increased tortuosity (complexity of path analytes must traverse) in the tissue as compared to a homogenous solution [50]. Active processes to consider include metabolism and reuptake, due to their ability to alter concentrations of analytes in the extracellular space being samples from. J.B. Justice assessed data from zero net flux experiments of DA and its metabolite DOPAC, as well as a series of pharmacologic manipulations targeting release, metabolism, and reuptake processes, it was concluded that for neurotransmitters such as DA, the primary component affecting probe recovery was DA reuptake by the transporter [50]. As such, the slopes from the linear regression lines of the zero net flux data can be used to assess DA transporter function.

2.5 Histological Verification of Probe Placement

Confirming placement of the probe after experimentation is important to verify that observations are in fact from the targeted brain region. Compared to the NAc, the CPu probe placement is more easily confirmed by sectioning of the brain due to the large size and anatomical markers present in the tissue itself. It is also less likely that the CPu is missed when doing a surgery; due to its large size and the probe size, there is more room for deviation from the coordinates to target that region. When verifying probe placement in the NAc, additional measures were required to visualize the probe and verify correct placement.

Initially, placement was verified by euthanizing the mouse using CO_2 asphyxiation with the probe still inserted into the brain region of interest. Crystal violet stain (~500 µL) was then manually pushed through the probe. The brain was removed and sectioned on a vibratome.

There were several disadvantages to this verification method, the main one being inconsistency. The dye did not always perfuse out of the probe very well, which led to a poor marking of probe position. The brain tissue was also very fragile to work with. Depending on the brain, the thinnest slices that could be achieved were 400 µm, which is bigger than the probe, meaning the necessary slice was not always obtained. Additionally, this method had to be done immediately following the experiment otherwise the probe became clogged and dye could not be pushed through.

A more convenient alternative method was developed in Dr. Matthew Allen's lab (Wayne State University, Chemistry Department), which involved staining the entire brain [51]. Their method was optimized for our purposes of histological verification of probe placement. The method offered an advantage of experimenter convenience in that it allowed tissue collection and storage so that the staining and probe verification could take place at a later time. Tissue was fixed in formalin (3.7% v/v) and stored at 4 $^{\circ}$C until ready to use. When ready, tissue was rinsed in DI water and the brain was incubated in a solution of cresyl violet (0.2% w/v in an acetic acid (0.2%) and ethanol (98%) aqueous mixture) for 23-24 hours at room temperature. Tissue differentiation occurred using 70% ethanol (v/v, 20–25 mL) for 24 h, and the differentiation fluid was changed once after 3-4 h. After the second differentiation period (20–21 h), the solution was changed to 95% ethanol and differentiated for 30 min. Finally, the brain samples were hydrated in water for 1 h before suspension in agarose gel. Tissue was sliced into 150 µm thick coronal slices for imaging. The fixed tissue and fixation in agarose before slicing provided more durable brain slices and the ability to obtain thinner slices which were ideal for capturing the location of the microdialysis probe.

Figure 2.4 shows a comparison of probe placement verification using the probe perfusion method compared to the whole tissue staining method. Figure 2.4A is an example of the crystal violet perfusion method working well, while Figure 2.4C is an example of one of the many ways it could fail. While both techniques allowed for verification, the latter method was more reliable and the images are consistently comparable to that of Figure 2.4B. The whole brain method also provided enhanced experimenter convenience.

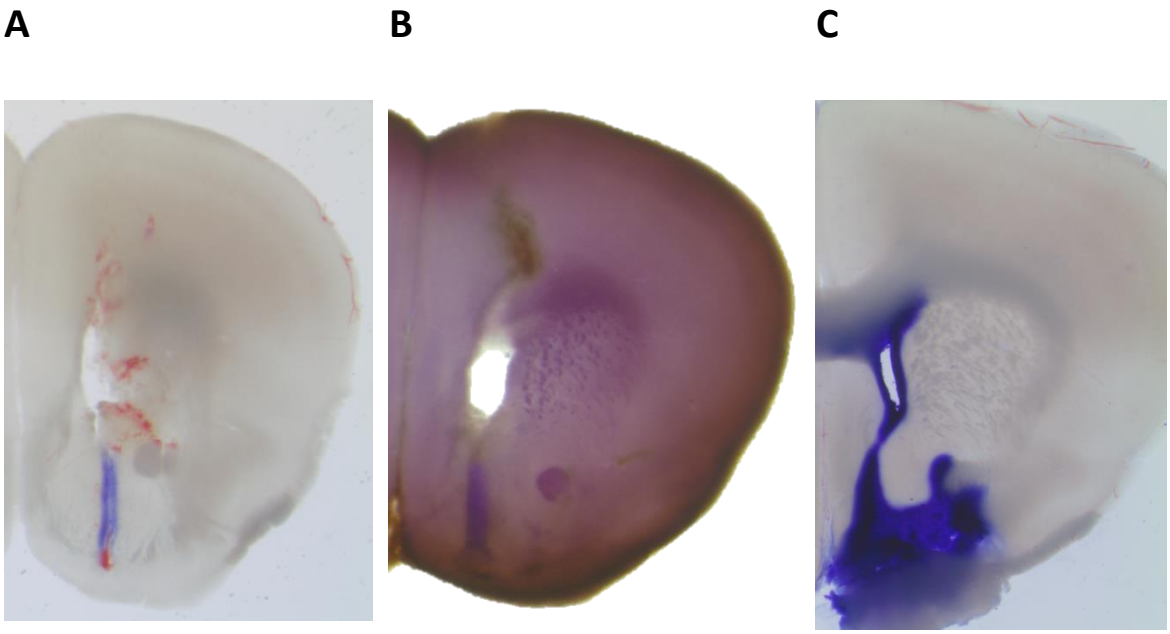

Figure 2.4 Examples of brain slices from probe placement verification using the crystal violet perfusion method and cresyl violet whole brain staining method. **A**) A successful verification with the crystal violet perfusion method where the probe is clearly visualized (purple line). **B**) Representative brain slice for probe placement using the whole brain cresyl violet method; this is consistently what would be observed. **C**) The perfusion method (also in A) was not reliable for various reasons and this is an example of what could go wrong, with the dye spilling out and the probe location not being determined.

2.6 Microdialysis Sample Analysis

As previously mentioned, HPLC coupled with electrochemical detection was used to quantify DA concentrations from dialysate samples collected by microdialysis. An isocratic

Shimadzu LC-20AD HPLC pump delivered mobile phase to a Phenomenex C_{18} (2)-HST HPLC column (100 mm x 3 mm, 2.5 um) at a flow rate of 0.4 mL/min. Mobile phase composition was 75 mM NaH_2PO_4 monohydrate, 1.6 mM 1-octanesulfonic acid, 0.025 mM EDTA, 10% acetonitrile, and 0.002% triethylamine, with a pH of 3 adjusted with 85% phosphoric acid. Samples (20 µL) was injected by overfilling a 20 µL sample loop with the 21 µL dialysate sample and detection occurred with an ESA 5014B microdialysis cell (E1 = - 150 mV, E2 = +220 mV). A guard cell (ESA 5020) set to a potential of + 350 mV was placed in-line before the injection loop. Peak areas were integrated and quantified against known standards using LC Solutions Shimadzu Software.

2.7 Tissue Content Studies

For tissue content studies, animals were euthanized using cervical dislocation followed by excision of the brain. The brain was free-hand dissected into brain regions of interest using anatomical markers visual to the eye and snap frozen in liquid nitrogen. Brain samples were stored at -80 $^{\circ}$C until used. Tissue content studies include: determination of BDNF protein levels using a commercially available ELISA kit (Promega, Madison, WI), the BDNF receptor tyrosine kinase B (TrkB) and its activation by phosphorylation (pTrkB). The latter receptor studies were assessed by measuring protein levels using immunoblotting. *Detailed methods are provided in Chapter 4*

2.8 Data Analysis

Plots of data were created solely using GraphPad Prism v5 software. Statistical analysis was carried out using GraphPad or, when the appropriate statistical functions were not available, Statistical Package for the Social Sciences (SPSS) was used. Most microdialysis experiments and drinking data were analyzed using repeated measures analysis of variance

(ANOVA). Other data were analyzed using an appropriate ANOVA or t-test. In most cases of repeated measures analysis, sphericity was violated due to the pharmacological manipulation in these experiments so the Greenhouse-Geisser correction was used. One caveat of the repeated measures design is that animals are excluded if they are missing any measures over time compared to the rest of the group. When using an *in vivo* animal model, there are a lot of challenges that can be encountered in just collection of the sample, as well as during analysis. As such, there are often samples missing (typically 0-2 samples per mouse). For example in an animal where 12 samples are collected over the course of 4 hours, if the animal gets disconnected for one of the 20 minute samples, the whole animal would be excluded. This exclusion then results in the statistical analysis only including around 20% of the subjects. The field of psychology often uses the repeated measures design where clinical data is used with much larger *n* values so losing a few is insignificant, therefor there is not a standard resolution for missing data in animal models where the groups are much smaller. One possible solution would be to increase group sizes, however when using animal models the goal is always to reduce numbers and minimize usage. The use of unlimited animals for the purposes of collecting complete data sets would be a waste of animal lives and resources. This problem with statistical analysis, is well known however, there is no standard solution in the field. One solution, which is used here, is mathematical modeling and prediction of the missing time points. One model for doing this is the expectation maximization method available in the SPSS software, and from experience working with microdialysis, the predictions made using this model are reasonable. As such, missing value analysis was performed on microdialysis data and DA concentrations from missing time points were predicted for further analysis using the repeated measures ANOVA.

2.9 Chemicals

Reagent kits and enzymes were from various vendors which were specified in the text where they were used. All other chemicals used to make buffers, mobile phase and aCSF were purchased from Fisher Scientific (Ottowa, Ontario), EMD (Darmstadt, Germany), or Sigma-Aldrich (St. Louis, MO) and were of HPLC grade quality.

CHAPTER 3

Striatal Dopamine Tolerance to Ethanol Following Seven Days of Drinking in the Dark

A similar version of this chapter and the data described within is being submitted to the Journal of Neuropharmacology.

3.1 Introduction

Approximately 18 million people annually in the US are affected by alcohol abuse or alcohol dependence, referred to collectively as alcohol use disorders (AUDs) by the National Institute on Alcohol Abuse and Alcoholism [7]. To better understand what environmental and genetic factors lead to the development of AUDs, research has focused on identifying risk factors predisposing one to AUDs. Both clinical and preclinical research has suggested brain-derived neurotrophic factor (BDNF) as a risk factor. In humans, mutations in the BDNF gene are linked to increased vulnerability and relapse to alcoholism [21, 23, 24]. In rodent models, BDNF levels influence alcohol consumption and preference [26-28]. BDNF heterozygous ($BDNF^{+/-}$) mice, which have a 50% reduction in BDNF mRNA and protein, consume more alcohol in a two-bottle choice assay, and show a preference for ethanol in conditioned place preference testing [26, 28]. Additionally, administration of a fusion protein containing RACK1, a scaffolding protein known to increase BDNF levels, attenuated alcohol consumption [26]. Together these data indicate that BDNF plays an important regulatory role in alcohol consumption and long-term usage of alcohol.

BDNF may influence alcohol intake behavior through modulation of the neurotransmitter dopamine (DA), a key component in drug reward and learning processes [8, 31, 32, 52]. DA transmission in striatal pathways innervating the nucleus accumbens (NAc) and

caudate putamen (CPu) is well established in the propagation of addiction related behavior through mediating positive reinforcement and habitual learning, respectively [3, 8]. Similar to other drugs of abuse, ethanol increases DA in both striatal regions of the CPu and nucleus accumbens of the mouse following intraperitoneal (i.p.) administration [5, 29, 34]. Additionally, alcoholic patients have less D2 receptors compared to non-alcoholic patients, with this being a factor for predisposition to alcoholism or a result of repeated ethanol exposure [36-38]. Mouse models using knockouts of the long D2 receptor isoform have suggested that alterations in the ratio of long to short D2 receptors are important in regulating ethanol consumption [40]. D2 receptor expression could be a downstream regulatory target of BDNF, given BDNF's influence on CREB-regulated gene expression and BDNF's influence on the D2-like receptor D3 [27, 53]. BDNF alters DA transmission in neuronal cultures and rescues reduced release of DA in $BDNF^{+/-}$ mice [31-33]. Given the evidence that BDNF can regulate alcohol intake and DA transmission, the current study aims to understand how BDNF influences the response of the DA system to alcohol and how that could modulate alcohol drinking behavior. Additionally, the DA D2 receptor could be a mediator of BDNF to alter this DA response. The potential for the DA system to undergo more or different alterations in an individual with low levels of BDNF (either genetically or environmentally) could be an important factor that may lead one from being a casual drinker to becoming dependent.

The present work serves as an initial investigation to understand how ethanol consumption affects DA transmission in the CPu, specifically aiming to elucidate the role of low endogenous BDNF levels on these changes. A modified voluntary consumption drinking protocol known as drinking-in-the-dark (DID) [43], was used to examine ethanol consumption. The advantage of the DID protocol is it does not require any prior training of the animal or the use of tastants to elicit "binge"-like alcohol consumption with pharmacologically relevant blood alcohol levels.

Wild-type (WT) and BDNF$^{+/-}$ mice were exposed to 7 days of DID after which aspects of the DA system were characterized using pharmacological manipulations using the sampling technique microdialysis. Although both genotypes had similar ethanol consumption, the main finding was that after 7 days of DID ethanol no longer induced increases in DA levels in the striatum of either genotypes. Overall, the BDNF-deficient mice were not subject to more significant alterations of the characterized aspects of the DA system following ethanol exposure.

3.2 Methods

3.2.1 Animals

Animals used were offspring from C57BL/6J females and BDNF$^{+/-}$ male mice (50% reduction in mRNA and protein), originally purchased from Jackson Laboratory (Bar Harbor, ME, USA) that were bred in-house. Genotypes were determined by PCR analysis of tail biopsies as previously described [29]. Mice were housed in groups of 4 - 5 on a regular light/dark cycle (light: 0600 h – 1800 h). Male mice, 4 - 6 months of age, were used for the described experiments. Food and water were available *ad libitum* except during ethanol drinking sessions when mice only had access to food and a single bottle containing ethanol for 2 hours. All procedures were designed and conducted to minimize pain and discomfort to the animals. Animal care and use was in accordance with the National Institutes of Health Animal Care guidelines and approved by the Wayne State University Institutional Animal Care and Use Committee.

3.2.2 Ethanol Consumption

Approximately 3 weeks before starting the drinking study, all experimental mice were moved to reverse light/dark conditions (light: 1800 h – 0600 h); during the last week they were

single housed. Voluntary alcohol consumption was measured using a limited access DID model [43]. Briefly, 3 hours into the dark cycle (0900 h), the standard water bottle from each cage was removed and replaced with a single bottle containing a 15% (v/v in tap water) ethanol solution. The ethanol bottle was left in the cage for 2 hours with the room undisturbed, after which it was removed and the standard water bottle was returned. The ethanol bottle was weighed before and after the drinking session to determine the quantity of ethanol consumed, which was reported as grams of ethanol per kilogram of mouse weight, (which was obtained the day before DID initiated). This procedure was repeated for a total of 7 days.

3.2.3 Blood Alcohol Determination

Blood was collected from the submandibular vein immediately following the last drinking session (day 7). Blood alcohol concentrations were determined using a commercially available enzymatic assay (Pointe Scientific, Canton, MI, USA). The whole blood method was used in which 10 µL blood was homogenized in 90 µL trichloroacetic acid (6.25% w/v). The supernatant from this mixture was used for analysis. Absorbance was determined using a Shimadzu UV-1800 spectrophotometer.

3.2.4 Microdiaysis

Stereotaxic surgeries were performed immediately after the last DID session (day 7) as previously described [29, 33]. Briefly, a surgical plane was achieved using isoflurane (3% induction, 2% maintenance) anesthetic so that a CMA/7 guide cannula (Harvard Apparatus) could be inserted to target the CPu (ML +1.30, AP +1.00, DV -2.50), determined using the mouse atlas [54]. The animal's body temperature was maintained using a heating pad at about 37 $^{\circ}$C. A lidocaine (0.5 mg/kg) and bupivacaine (1.5 mg/kg) mixture was subcutaneously injected around the incision site to minimize pain before tissue was incised to expose skull. Ophthalmic ointment

was applied immediately after anesthetic induction to keep eyes hydrated. The guide cannula was secured using dental cement. Following recovery (~3 - 4 h), a CMA/7 microdialysis probe (2mm length, 0.24 mm diameter, Cuprophane, 6 kDa cut-off, Harvard Apparatus) was inserted and perfused (1.1 µL/min) with sterile artificial cerebrospinal fluid (aCSF; composition: 145 mM NaCl, 3.5 mM KCl, 2.0 mM Na_2HPO_4, 1.0 mM $CaCl_2$, 1.2 mM $MgCl_2$ and pH = 7) continuously until experimental dialysis collection the following day. After overnight perfusion with aCSF, baseline dialysate samples were collected for one hour at 1.1 µL/min prior to all experimental manipulations. After dialysis, brains were removed and sectioned for verification of probe placement.

3.2.4.1 Ethanol and Methamphetamine Microdiaylsis

Following baseline collections, either 2 g/kg ethanol (15% ethanol solution, v/v in 0.9% saline) or 3 mg/kg methamphetamine (METH, Sigma-Aldrich) was injected i.p in mice. Microdialysis samples were collected every 20 minutes for 2 or 3 hours after the ethanol or METH treatment, respectively. DA content was determined with high-performance liquid chromatography (HPLC) equipped with electrochemical detection and results were normalized for each mouse as a percent of their respective baseline values.

3.2.4.2 Quinpirole Microdialysis

To analyze D2 DA auto-receptor functionality, the dose-dependent effect of the D2 receptor agonist quinpirole (Sigma Aldrich, St. Louis, MO) on extracellular DA levels was measured by perfusing increasing concentrations of the drug (10, 100, and 1000 nM) into the CPu using retro-dialysis. Each dose of quinpirole was perfused for one hour during which dialysis samples were collected every 20 minutes. DA levels in the presence of drug were determined

with HPLC coupled to electrochemical detection and results were normalized for each mouse as a percent of their respective baseline values.

3.2.4.3 Zero Net Flux Microdialysis

To determine basal extracellular DA levels, the quantitative microdialysis method of zero net flux was used [50]. After baseline samples were collected, varying concentrations of DA (5, 10, and 20 nM) in aCSF containing 200 µM ascorbic acid were perfused through the probe for 90 minutes per concentration through the use of a CMA/402 programmable gradient infusion pump. The quantity of DA perfused in (DA_{in}) was determined using *in vitro* calibration in which the same concentrations of DA aCSF were similarly perfused and collected with no animal on line [55, 56].

3.2.5 Dialysis Sample Analysis

Following microdialysis collection, DA levels were quantified using HPLC coupled with electrochemical detection. An isocratic Shimadzu LC-20AD HPLC pump delivered mobile phase to a Phenomenex C_{18} (2)-HST HPLC column (100 mm x 3 mm, 2.5 um) at a flow rate of 0.4 mL/min. Mobile phase composition: 75 mM NaH_2PO_4 monohydrate, 1.6 mM 1-octanesulfonic acid, 0.025 mM EDTA, 10% acetonitrile, and 0.002% triethylamine, with a pH of 3 adjusted with 85% phosphoric acid. A microdialysis sample (20 µL) was injected and DA was measured with an ESA 5014B microdialysis cell (E1 = - 150 mV, E2 = +220 mV). A guard cell (ESA 5020) placed in-line before the injection loop was set to a potential of + 350 mV. Peak areas were integrated and quantified against known standards using LC Solutions Shimadzu Software.

3.2.6 Data Analysis

For the DID data, values are reported as grams of ethanol consumed per kilogram of mouse weight. For ethanol, METH, and quinpirole dialysis experiments, the percent change in DA levels in the presence of drug for each mouse were normalized to their respective baseline values (baseline set to 100%). For the zero net flux experiment, a plot was created of the concentration of DA_{in} (x-axis) versus the difference between recovered DA (DA_{out}) and DA_{in} on the y-axis ($DA_{in} - DA_{out}$). This plot had four points, one for each DA_{in} concentration which included 0, 5, 10, and 20 nM DA, which then had a linear regression fitted to it to give a $y = mx + b$ equation. The apparent extracellular concentration of DA (DA_{ext}) was determined by the x-intercept of that line [50]. The extraction fraction (E_d) was given by the slope (m), which was used to assess the *in vivo* recovery of DA [57]. DA_{ext} and E_d values taken from the linear regression lines were summarized in bar graphs for statistical testing.

Data were plotted using GraphPad Prism (GraphPad Software v4) and statistical analysis was performed using SPSS (IBM Statistics). Values are reported as mean ± standard error of the means (SEMs), with the criteria for statistical significance being $p < 0.05$. Statistical analysis was performed with two-way repeated measures ANOVA for the microdialysis experiments and one-way repeated measures ANOVA for the drinking data plotted by day. When sphericity was violated, the Greenhouse-Geisser correction was used. Two-tailed independent *t*-tests were used for the blood ethanol concentrations and the average daily consumption comparison. Finally a two-way independent ANOVA was used to compare the slopes and C_{ext} bar graphs from the zero net flux experiment. For repeated measure analysis, missing values were handled using SPSS missing value analysis and imputation using the expectation maximization model (EM) method.

3.3 Results

3.3.1 Limited Access Ethanol Intake was Comparable Between WT and BDNF$^{+/-}$ Mice

To assess how alterations in BDNF can influence binge-like drinking in a limited access model, DID intake was evaluated in BDNF$^{+/-}$ mice compared to WT littermates. WT and BDNF$^{+/-}$ mice were given access to a 15% (v/v in tap water) ethanol solution for 2 hours each day for 7 days [43]. The average daily consumption (Figure 3.1B) across the 7 days was 2.97 ± 0.19 g/kg for WT mice and 2.95 ± 0.13 g/kg for BDNF$^{+/-}$ mice, with no difference observed by an independent *t*-test ($t(12) = 0.081$, $p = 0.937$, $n = 13$/group). No between-subjects effect was observed in consumption over the time course of 7 days between genotypes ($F(1, 24) = 0.130$, $p = 0.722$, Figure 3.1A). However, there was a significant within-subjects effect of time observed by one-way repeated measures ANOVA with Greenhouse-Geisser correction ($F(3.46, 83.06) = 6.83$, $p < 0.001$, $n = 13 – 15$/group), which was comparable with respect to genotypes (Time x Genotype interaction, $F(3.46, 83.06) = 0.510$, $p = 0.702$) . Because of this difference over time, we compared the intake levels of WT and BDNF$^{+/-}$ mice on day 1 and day 7 (Figure 3.1C). Two-way ANOVA of the day 1 to day 7 comparison showed a main effect of time ($F(91,24) = 33.51$, $p < 0.001$) with WT and BDNF$^{+/-}$ mice increasing consumption from 2.17 ± 0.21 to 3.43 ± 0.24 g/kg, and 2.28 ± 0.14 to 3.09 ± 0.20 g/kg, respectively. BEC values were also not different according to the independent t-test, with WT mice at 110.39 ± 30.26 mg/mL and BDNF$^{+/-}$ mice at 76.82 ± 21.31 mg/mL ($t(8) = 0.907$, $p = 0.391$, $n = 5$/genotype, data not shown).

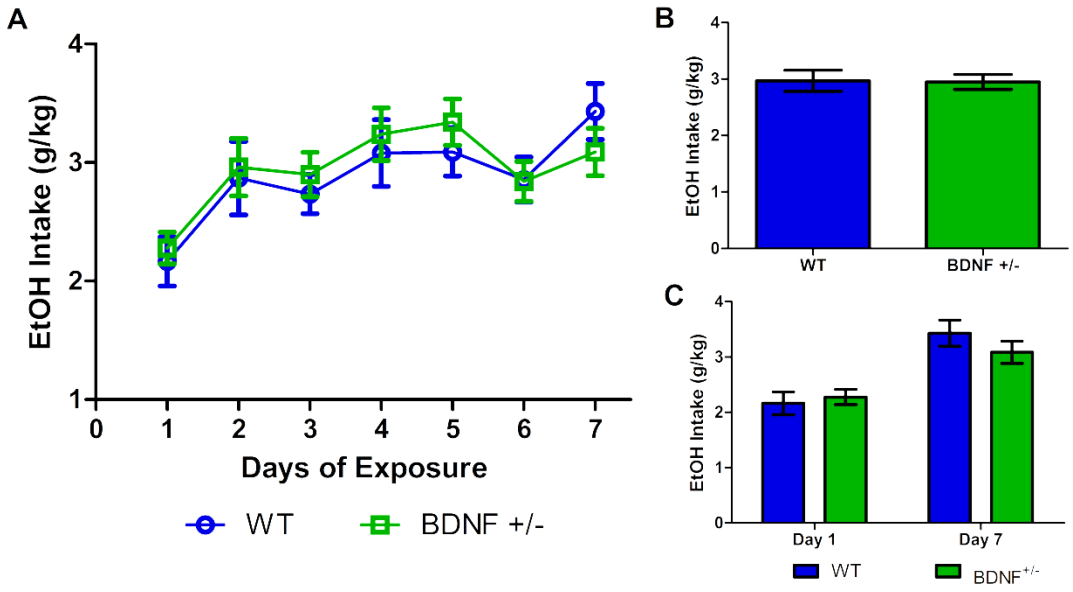

Figure 3.1 Summary of ethanol consumption during DID (n = 13/group) reported as mean ± SEMs. Data for these plots can be found in Table A.1 of the appendix. **A**) Average daily consumption in grams/kilogram of 15 % (v/v) ethanol during the 2 hour DID session over the course of seven days. No difference was observed between BDNF$^{+/-}$ and WT mice. There was however a main effect of time $p < 0.001$. **B**) Average ethanol intake during the entire 7 days of DID in g/kg of WT and BDNF$^{+/-}$ mice. **C**) Comparison of increased consumption from day 1 to day 7 in WT and BDNF$^{+/-}$ mice where there was a main effect of time $p < 0.001$.

3.3.2 Ethanol Induced Increase in DA is No Longer Observed Following Repeated Exposure to Voluntary DID Ethanol Consumption in Either WT and BDNF$^{+/-}$ Mice

DA levels were quantified following an acute injection of 2 g/kg (i.p.) ethanol in naïve and 7 day DID WT and BDNF$^{+/-}$ mice. In naïve (control) animals, ethanol treatment similarly increased DA levels to about 20 - 25 % over baseline in both WT and BDNF$^{+/-}$ mice (Figure 3.2). Baseline DA levels before ethanol was administered were 2.9 ± 0.5 nM and 3.2 ± 0.5 nM in WT and BDNF$^{+/-}$ mice, respectively. After ethanol was administered, there was an approximate increase in DA from 100 % to 126 ± 9 % and 120 ± 14 % over baseline at 120 minutes in WT and BDNF$^{+/-}$ mice, respectively. In mice given 7 days limited access to ethanol in the DID procedure, there was no change in uncorrected baseline values of DA from control mice (1. 7 ± 0.4 nM for

WT and 2.5 ± 0.4 nM for BDNF$^{+/-}$ mice). However, an acute injection of ethanol no longer elevated DA levels in either genotype (Figure 3.2A & B, *n* = 7-12/group). Two-way repeated measures ANOVA with the Greenhouse-Geisser correction showed no within-subjects effect of time ($F(4.53, 149.46) = 1.41$, $p = 0.227$) and no interactions between time and genotype ($F(4.53, 149.46) = 0.697$, $p = 0.612$). There was a significant within-subjects interaction between time and DID treatment ($F(4.53, 149.46) = 3.51$, $p < 0.01$). Between-subjects effects were observed for DID treatment ($F(1, 33) = 10.07$, $p < 0.01$) but not for genotype ($F(1, 33) = 0.019$, $p = 0.892$), and there was no genotype x treatment interaction ($F(1, 33) = 0.130$, $p = 0.721$)). In naïve WT and BDNF$^{+/-}$ animals ethanol is able to increase extracellular DA levels, however after the mice have consumed alcohol for 7 days during 2 hour DID sessions ethanol is no longer able to induce this increase in DA levels.

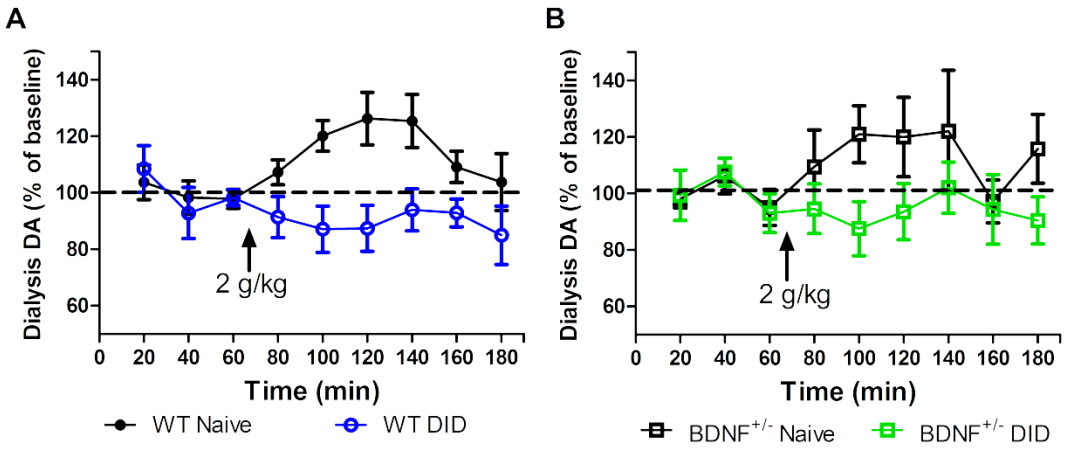

Figure 3.2 Ethanol challenge following 7 days of DID had a within-subjects interaction between time and treatment ($p < 0.01$, n = 7-12/group) and a between-subjects effect of treatment ($p < 0.01$). DA response to ethanol challenge reported as mean ± SEMs of DA percent of baseline following 2 g/kg ethanol challenge. Data for these plots are located in Table A.2 of the appendix. **A**) Naïve WT mice show an increase in DA about 26 % over baseline and WT DID mice show no change in DA levels following ethanol challenge. **B**) Naïve BDNF$^{+/-}$ animals exhibited an increase in DA levels of about 20 % over baseline and DID animal show no change.

3.3.3 Dopamine Release Stimulated by the Psychostimulant METH was Unaltered Following 7 Days of DID Ethanol Consumption

Given that an ethanol challenge did not promote DA release in DID exposed mice, a similar experiment was performed with the psychostimulant METH to determine if this tolerance to DA stimulation was specific to ethanol. In this experiment, METH was administered (3 mg/kg, i.p.) to WT and $BDNF^{+/-}$ naïve mice and mice exposed to 7 days of voluntary DID ethanol drinking (Figure 3.3, n = 6 - 12/group). In naïve WT mice, an acute injection of METH enhanced DA levels from 1.7 ± 0.3 nM to 20.2 ± 3.2 nM, a 1470 ± 370 % increase relative to baseline. METH elicited a similar increase in DA levels, from 2.3 ± 0.5 nM to 23.8 ± 11.1 nM, in naive $BDNF^{+/-}$ mice (1120 ± 740 % of baseline). Across the genotypes, mice exposed to 7 days of DID ethanol intake showed similar levels of METH-stimulated DA release as naïve controls. WT mice following DID had an 1840 ± 480 % increase (from 2.2 ± 0.3 nM to 33.6 ± 6.2 nM) and $BDNF^{+/-}$ mice had a 900 ± 300 % increase (from 2.17 ± 0.38 nM to 25.82 ± 6.66 nM) in DA over baseline after acute METH treatment. Analysis by two-way repeated measure ANOVA with the Greenhouse-Geisser correction gave a significant within-subjects effect of time (F(1.46, 46.79) = 35.27, $p < 0.001$). Within-subjects there was no interaction between time and genotype (F(1.46, 46.79) = 2.20, p = 0.135), or time and DID treatment (F(1.46, 46.79) = 0.339, p = 0.647). Between-subjects there was no significant main effect for genotype (F(1, 32) = 2.41, p = 0.130), DID treatment (F(1, 32) = 0.259, p = 0.614), and no interaction between genotype and treatment (F(1, 32) = 0.442, p = 0.511). The lack of DA release following ethanol in DID mice of either genotype appears to be ethanol specific given that METH was able to increase extracellular DA levels in these mice.

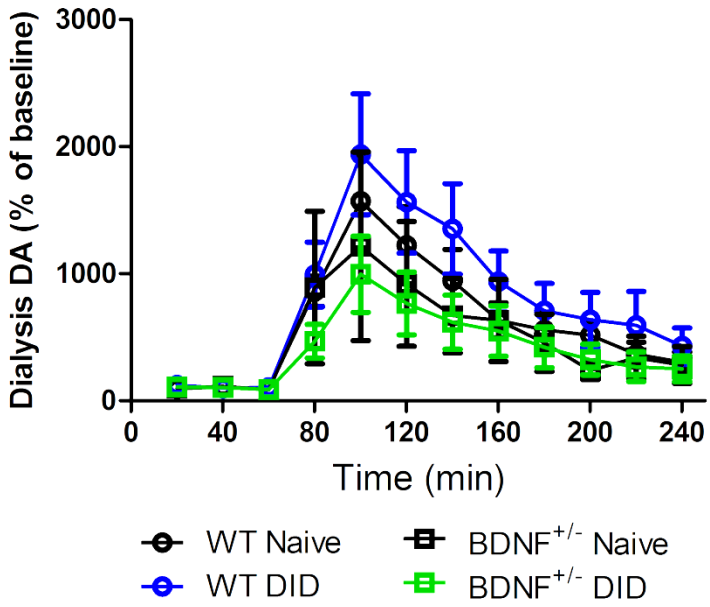

Figure 3.3 METH challenge following 7 days of DID (*n* = 6 - 12/group). DA response to a 5 mg/kg i.p. injection of METH given at 60 minutes reported as mean ± SEMs of DA percent of baseline. Maximal increases over baseline were WT naïve: 1470 ± 370 %, WT DID: 1840 ± 480 %, $BDNF^{+/-}$ naïve: 1120 ± 740 % and $BDNF^{+/-}$ DID: 900 ± 300 %. Responses to METH challenge were not different for any of the groups. Data used to create this graph are located in Table A.3 of the appendix.

3.3.4 Corrected Basal Extracellular DA Levels and D2-like Auto-receptor Activity Are Not Affected by 7 Days of DID Ethanol Consumption in Either Genotype

Zero net flux was used to determine the apparent basal extracellular DA levels (DA_{ext}) based on the x-axis intercept of the linear regressions run on plots of recovered DA ($DA_{in} - DA_{out}$) versus perfused DA (DA_{in}) (Figure 3.4A, *n* = 5 - 6/group). Corrected baseline values of DA were similar for all groups regardless of DID treatment or genotype (Figure 4B; WT naïve: 9.0 ± 1.6 nM, WT DID: 8.8 ± 2.2 nM, $BDNF^{+/-}$ naïve: 8.4 ± 1.8 nM, and $BDNF^{+/-}$ DID: 8.6 ± 1.8 nM) as confirmed by two-way independent ANOVA (Figure 3.4B) showing no main effect of genotype ($F(1, 22) = 0.59$, $p = 0.810$), DID treatment ($F(1, 22) = 0.00$, $p = 0.999$), and no interaction of

genotype and treatment ($F(1, 22) = 0.14$, $p = 0.906$). The E_d did not differ across genotype or treatment groups (Figure 3.4C; independent two-way ANOVA, no main effect of genotype ($F(1, 22) = 0.000$, $p = 0.999$), DID treatment ($F(1, 22) = 0.09$, $p = 0.767$), or interaction ($F(1, 22) = 0.36$, $p = 0.554$)).

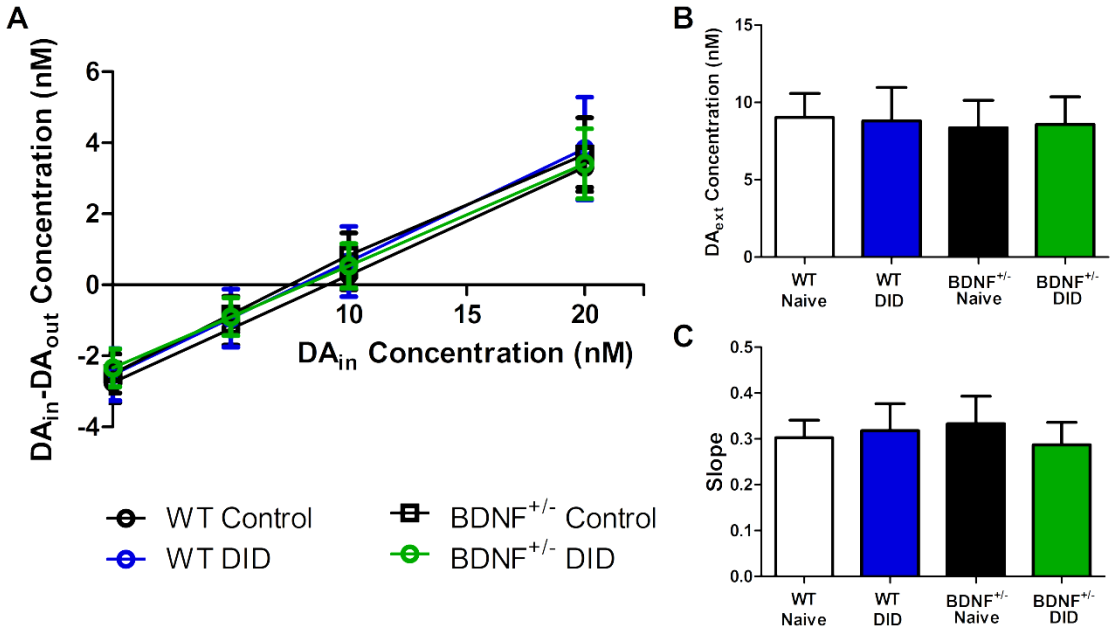

Figure 3.4 Zero net flux data to determine apparent extracellular DA levels (n = 6 - 8/group). Data for these plots is described in Table A.4 of the appendix. **A)** DA_{in}-DA_{out} plotted versus DA_{in} for the zero net flux microdialysis experiment. Above the x-axis there is a net loss of DA from the probe to the brain and below there is a net gain of DA into the probe from the brain. The x-intercept is the apparent extracellular DA concentration (DA_{ext}). **B)** Summary of DA_{ext} values with no effect for genotype or treatment. **C)** Summary of the slopes from the zero net flux regression lines to indicate DA clearance, again with no affect for genotype or treatment.

The DA D2 receptor has also been implicated in alcohol consumption and dependence in both human and mouse studies [39, 40, 58]. Thus far, the mechanistic role of the D2 receptor in the pre- and post-synaptic effects of ethanol is unclear. To isolate the presynaptic activity of the D2 auto-receptor, the current study evaluated the effect of a D2 agonist quinpirole to attenuate

basal DA levels with local perfusion in the CPu using *in vivo* microdialysis. Quinpirole perfusion dose-dependently decreased baseline dialysate DA levels (WT naïve: 1.7 ± 0.3 nM, WT DID: 1.3 ± 0.1 nM, $BDNF^{+/-}$ naïve: 1.6 ± 0.2 nM, and $BDNF^{+/-}$ DID: 1.7 ± 0.3 nM), with little to no decrease at the lowest concentration (10 nM), a ~ 25 % reduction at 100 nM, and a ~ 50% reduction at 1000 nM (Figure 3.5, n = 7 - 12/group). The quinpirole-mediated reduction in DA levels was similar between WT and $BDNF^{+/-}$ naïve mice and mice exposed to 7 days of DID voluntary ethanol consumption, indicating that repeated limited access to ethanol drinking did not significantly alter auto-receptor activity. Two-way repeated measures ANOVA with the Greenhouse-Geisser correction showed a within-subjects effect of time ($F(6.33, 189.88) = 32.41$, $p < 0.001$), but no interaction between time and genotype ($F(6.33, 189.88) = 0.908$, $p = 0.494$) or time and DID treatment ($F(6.33, 189.88) = 1.14$, $p = 0.339$). Between-subjects analysis established no main effects for genotype ($F(1, 30) = 0.59$, $p = 0.447$), DID treatment ($F(1, 30) = 0.70$, $p = 0.409$), or interaction ($F(1, 30) = 2.68$, $p = 0.107$). The DA system in the CPu appears normal in DID of both genotype given that the extracellular levels are not altered and the D2 auto-receptor function is normal.

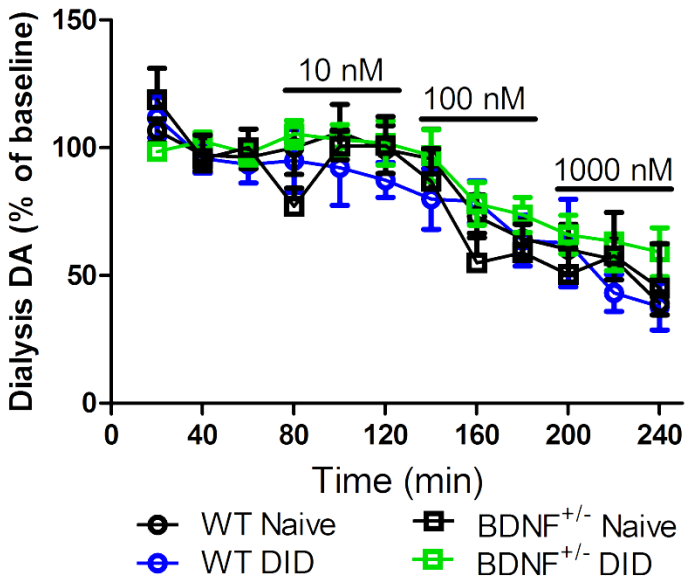

Figure 3.5 DA D2-autoreceptor dose-response curves using the agonist quinpirole (*n* = 7-12/group). DA response to drug concentrations were reported as mean ± SEMs of DA percent of baseline (first hour). Increasing concentrations of quinpirole and the time it was applied are indicated on the graph. No genotype or treatment effect was observed but, as would be expected, there was a within-subjects effect of time ($p < 0.001$). Data for this graph are located in Table A.5 of the appendix.

3.4 Discussion

Given the previously demonstrated role of BDNF in alcohol consumption and addiction [21, 23, 24, 26, 29], the present work sought to investigate how alterations to the striatal DA system following ethanol consumption may be affected by endogenous BDNF levels. To investigate this potential interaction, $BDNF^{+/-}$ mice with a 50% reduction in BDNF protein levels, were compared to WT littermates following a well-characterized limited access voluntary ethanol consumption protocol, DID. This is the first study to our knowledge that has characterized the striatal DA system following repeated voluntary DID ethanol access. Twenty-four hours after 7 days of DID, WT and $BDNF^{+/-}$ mice were affected similarly by the repeated exposure to ethanol. Basal DA levels and D2 auto-receptor function appear normal for both

genotypes. There was a loss of ability of ethanol to stimulate DA release after repeated exposure that was also similar between genotypes. The lack of ethanol stimulation after 7 days of DID highlights how quickly ethanol can cause adaptations in the striatum. Further investigations will seek to understand behaviorally what this tolerance means and how BDNF levels are affected under similar exposure conditions.

3.4.1 DID Consumption is Similar for WT and BDNF$^{+/-}$ Mice

BDNF$^{+/-}$ mice have increased preference for ethanol, and increased consumption, when tested with a 2-bottle choice drinking protocol [26, 28]. Alternatively, the current study, using a limited access DID consumption model, did not reveal genotypic differences in ethanol intake or the subsequent BEC levels (Figure 3.1). One potential reason for similar consumption between genotypes is our use of C57BL/6J mice derived from breeding with BDNF$^{+/-}$ mice as WT controls, since this is the background strain of the BDNF$^{+/-}$ mice. The C57BL/6J strain is known to exhibit high ethanol intake behavior [44]. The DID model, designed to promote binge-like drinking and pharmacologically relevant elevations in blood alcohol levels [47] may mask any elevations in drinking behavior driven by BDNF deficiency as animals are reaching a threshold level of drinking. Additionally, the limited access to ethanol used in this model is not readily amenable to measuring preference due to the animals not having a choice what to drink, which was largely altered in previous studies in BDNF$^{+/-}$ mice [26, 28]. Of note, the similar consumption observed between WT and BDNF$^{+/-}$ mice (Figure 3.1) does allow for any differential changes in neurochemistry following DID to be more easily attributed to endogenously reduced BDNF levels, rather than differences in the level of ethanol exposure.

3.4.2 There are No Ethanol Induced Increases in DA Following DID for Either WT and BDNF$^{+/-}$ Mice

Systemic administration of 2 g/kg ethanol in naïve animals elicits an increase in DA levels in both striatal regions of the NAc and CPu [29, 34, 35, 59, 60]. The DA increase in the CPu of BDNF$^{+/-}$ mice following ethanol challenge is blunted compared to WT littermates [29]. In this experiment, DA levels were monitored following an i.p. injection of 2 g/kg ethanol for 2 hours similar to the aforementioned study ([29]). Both WT and BDNF$^{+/-}$ control animals showed a 20-25% increase in DA levels following ethanol injection (Figure 3.2). The lack of genotypic differences compared to those previously observed [29] is likely due to differences in experimental design. Due to the use of the DID model, all of the neurochemical measurements currently presented were conducted during the dark cycle, whereas previous measurements were carried out during the light cycle [29]. It is well established that neurochemicals experience diurnal variation [61, 62], therefore this change in when experiments were carried out relative to light cycles may have contributed to the disparate results. Another potential explanation for the genotypic differences no longer being observed is the anesthetic used to perform the surgery, which was isoflurane inhalation in the current study and the injectable Avertin previously [33]. Although both anesthetics are CNS depressants, there are numerous unknowns regarding their molecular targets and their lasting effects [63, 64]. It is plausible that each anesthetic could be producing different neuroadaptations before neurochemical measurements were made [65, 66]. A major finding of this study was that 7 days of voluntary DID ethanol consumption caused alterations in the DA response to a subsequent ethanol challenge, so that ethanol-induced DA release was no longer observed in either WT or BDNF$^{+/-}$ mice as compared to naïve animals (Figure 3.2). This lack of response to the DA stimulatory effect of ethanol is consistent with data that has shown repeated exposure to limited access DID drinking results in

a behavioral tolerance to ethanol [67]. In a study by Linsenbardt *et al.*, footslips were counted following a 1.5 and 1.75 g/kg ethanol challenge after 16 days of DID consumption: DID exposed animals exhibited improved motor performance, in that they demonstrated less hind footslips, than their water drinking counterparts [67].

In contrast to the lack of ethanol response to DA in DID exposed mice, acute administration of the psychostimulant METH produced a robust increase in DA in the CPu, which was comparable between DID drinking and naïve WT and BDNF$^{+/-}$ mice. Ethanol has been shown to increase DA through enhanced neuronal firing as well as through modulation of other neurotransmitters that subsequently act to increase DA [5, 52]. In contrast, METH is a DA transporter (DAT) and vesicular monoamine transporter substrate, which together lead to reverse transport of DA through DAT, leading to large increases in extracellular DA [5]. The observation of METH-induced DA release following DID consumption indicates that the DA system is relatively intact and that the tolerance of the DA response to ethanol is specific to the pharmacological mechanism underlying DA stimulation by ethanol. While our observation that the 'tolerance' to the ethanol-evoked DA response was similar in both WT and BDNF$^{+/-}$ mice following DID does not implicate a role for BDNF, future studies are planned to understand the mechanism underlying this observation.

3.4.3 Basal DA function is Not Changed Following DID Exposure in Either Genotype

The DID procedure is often referenced to promote high ethanol intake over a short period of time, reflective of a 'binge' pattern of drinking [46, 47]. Few studies to date have measured the impact of this pattern of voluntary ethanol consumption on striatal dopaminergic function [40, 46, 68]. Additionally, acute ethanol exposure has been shown to alter BDNF mRNA and protein expression [26, 29] and BDNF is identified as an important modulator of DA

neurotransmission [33]. Taken together, it is reasonable to hypothesize that 7 days of voluntary ethanol exposure in the DID model would likely produce alterations in the DA system that would be modulated by BDNF.

First, basal extracellular DA levels were measured using the microdialysis method of zero net flux. There was no difference in extracellular DA concentration observed between WT and $BDNF^{+/-}$ mice or following DID for either genotype (Figure 4A & B). The fact that DA levels in control WT and $BDNF^{+/-}$ animals were not different was unexpected, as previous studies have shown a strong genotype dependent difference [33]. The lack of genotypic differences in basal levels compared to those previously observed are likely due to differences in experimental design as previously discussed (light/dark cycle, surgical anesthetic). Overall, the key finding from this characterization was that the DID model of ethanol consumption did not affect extracellular DA levels in the CPu.

In a second set of experiments to assess DA system function, autoreceptor activity was evaluated using retro-dialysis of the D2 agonist quinpirole (Figure 5). Alterations in D2 receptor levels have been previously reported after ethanol exposure [39, 58], the current experiment would isolate the study of presynaptic DA D2 auto-receptor activity changes apart from postsynaptic contributions. The maximal effect of D2 autoreceptor inhibition at 1000 nM quinpirole infusion resulted in a 50% reduction in dialysis DA levels below baseline. As observed with basal DA levels, no difference in DA D2 autoreceptor functionality in the CPu was found between genotypes or as a result of DID treatment. A previous study in the NAc reported reduced D2 auto-receptor function that was only observed following moderate doses (1.0 g/kg) of acute ethanol, but not higher doses (2.0 g/kg); these observations were also true for up to 5 days of ethanol treatment [39]. The quantity of ethanol consumed using the DID model in the

present study (Figure 3.1) is within the higher end of dosing that did not elicit any D2 changes in the study by Franklin *et al.* [39]. The similar DA D2 presynaptic receptor function after DID is consistent with our observation that basal extracellular DA levels with zero net flux also remain normal. Taken together, 7 days of DID ethanol intake does not have a prolonged effect on tonic DA transmission measured 24 hours after the last drinking session.

3.5 Conclusion

Several studies have employed the use of the limited access DID voluntary ethanol consumption model to assess the neurobiology of 'binge'-like drinking as this model produces a pharmacologically significant elevation in blood alcohol levels. This study aimed to elucidate the neurochemical impact of several days of DID drinking on the DA system in the CPu and evaluate the role of BDNF to influence DA transmission after ethanol consumption using BDNF-deficient mice. While the current study did not observe any specific changes in drinking behavior or DA system function in $BDNF^{+/-}$ mice compared to WT littermates, to support an influence of BDNF on 'binge'-like intake, repeated access to voluntary DID ethanol drinking produced a lack of effect in ethanol-stimulated DA release in both WT and $BDNF^{+/-}$ mice. Given the role of striatal DA in promoting ethanol drinking behavior, the long-term goal of this work is to understand a mechanism for how causal drinking transitions to alcohol dependence in an individual. The DA tolerance observed could be an important mediator in the similar consumption observed over repeated drinking sessions carried out for several days. If initial drinking sessions produced positive effects for the animal, then enhanced consumption in subsequent sessions could be a result of the animal trying to attain those positive effects again. Overall the hypothesis that $BDNF^{+/-}$ mice would have more significant alterations to their DA system was no supported,

however there are neuroadaptations to the DA system that warrant further investigation to understand.

CHAPTER 4

Assessment of BDNF-TrkB Signaling in BDNF$^{+/-}$ and WT Mice Following 7 Days of DID

4.1 Introduction

As a trophic factor, brain-derived neurotrophic factor (BDNF) mediates its responses by activation of tropomyosin-related kinase B receptor, also referred to as the tyrosine receptor kinase B (TrkB) [10]. Binding of BDNF with the full length (FL) TrkB (FL-TrkB) receptor induces dimerization and auto-phosphorylation, which subsequently activates several signaling pathways, most notably mitogen-activated protein kinase (MAPK), phosphatidylinositol-3-OH kinase (PI3K), and phospholipase Cγ (PLCγ) [20, 21]. There is also a truncated TrkB receptor (T-TrkB) whose mode of action is not well understood, however there is evidence for its potentiation or attenuation of the FL-TrkB receptor activation depending on localization [21, 69, 70]. BDNF has been a protein of interest as a risk factor for alcohol use disorder (AUDs), due to the previously discussed findings of its alterations in human alcoholics and regulation of ethanol consumption in rodent studies (Chapters 1 and 3). BDNF's signaling through activation of TrkB and downstream targeting of gene transcription make it important in learning and memory processes which also make BDNF of interest in addiction research.

There have been contradicting reports on the effect of ethanol on BDNF protein and BDNF mRNA expression levels [26, 29]. A series of investigations from the laboratory of Dorit Ron led to the hypothesis that BDNF serves a neuroprotective role by preventing the reinforcing alterations of ethanol through increased BDNF-signaling [26, 27, 71]. The caveat of these studies is that they only measured BDNF mRNA, while increased mRNA does not necessarily lead to increased protein. Additionally it is important to assess the TrkB receptor levels and activation, rather than to infer that increases in BDNF mean enhanced receptor activation. In the study by Baek *et al.*, chronic ethanol exposure led to reductions in BDNF mRNA in the hippocampus of rats; however there was an up-regulation of the TrkB

receptor [30]. The mechanisms behind interactions of BDNF and ethanol are complex and to better understand the role of BDNF further investigations should focus on gene and protein expression of the protein and its receptor TrkB.

The goal of this study was to evaluate BDNF and TrkB following 7 days of binge-like drinking using the drinking in the dark (DID) model to understand how low endogenous BDNF levels may lead to a propensity for addiction. To this end, mice with a 50 % reduction in the BDNF protein ($BDNF^{+/-}$) were compared to wild-type (WT) littermates following ethanol exposure. The immediate effects were tested by assessing changes 30 minutes after the last DID session and lasting effects were assessed 24 hours after the last drinking session. Following 7 days of DID, WT mice have reduced BDNF protein levels and TrkB activation, whereas the $BDNF^{+/-}$ mice did not exhibit these alterations. These results were surprising as we would have expected more alterations from the $BDNF^{+/-}$ mice. The results from this study may suggest important implications for the use of the DID model that we had not anticipated.

4.2 Methods

4.2.1 Animals

C57BL/6J (WT) and $BDNF^{+/-}$ mice purchased from The Jackson Laboratory (Bar Harbor, ME, USA) were bred in-house and offspring from these breeders were used. The average ages of the male and female mice used were 4 – 6 months of age. Genotypes were determined by PCR analysis of tail biopsies as previously described (Chapter 2, [29]). Mice were housed in groups of 4 - 5 and maintained on a light/dark cycle (light 0600 – 1800 h). Food and water were available *ad libitum* except during ethanol drinking sessions where for 2 hours only ethanol and food were available. All procedures were designed and conducted to minimize pain and discomfort to the animals. Animal care and use was in accordance with the National Institutes of Health Animal Care guidelines and approved by the Wayne State University Institutional Animal Care and Use Committee.

4.2.2 Ethanol Consumption

Ethanol exposure was achieved using the drinking in the dark (DID) model as previously described (Chapter 2). About 2-3 weeks before ethanol exposure, animals were put on a reverse light/dark cycle (lights off 0600 h); one week before experiments, animals were placed in singly housed conditions for acclimation. Three hours into the dark cycle on DID days the home-cage water bottle was removed and replaced with a bottle containing 15 % ethanol (v/v in tap water) for 2 hours per day for 7 consecutive days. Bottles were weighed before and after DID to determine the grams of ethanol consumed per kilogram of mouse weight for each session.

4.2.3 Tissue Collection

Animals were sacrificed by cervical dislocation and subsequent dissection of the brain to isolate the caudate putamen (CPu), a sub-region of the striatum. The brain was removed and placed on a petri dish covered with an artificial cerebrospinal fluid soaked paper towel. Spatulas and a straight razor were then used to section the tissue based on anatomical markers visual to the eye. Tissues were flash frozen in liquid nitrogen and stored at -80 $^{\circ}$C until needed for analysis. The time points at which tissues were collected from DID mice was 30 minutes and 24 hours after the 7th DID session. Tissue from control mice was collected after they had been singly housed for two weeks similar to the DID animals.

4.2.4 BDNF Protein Quantification

BDNF protein levels were determined using a commercially available ELISA assay (Promega, Madison, WI). Tissue samples were weighed and homogenized using an ultrasonic cell disruptor. Lysis buffer (4 mL/sample) contained: 100 mM PIPES (pH 7.0), 500 mM NaCl, 0.2% (v/v) Triton X-100, 0.1% (w/v) NaN_3, 2% bovine serum albumin (BSA), 2 mM EDTA and various protease inhibitors (200 µM phenylmethanesulfonyl fluoride (PMSF, Sigma, St. Louis, MO), 10 µM leupeptin (Sigma), 0.3 µM

aprotinin (Sigma), and 1 µM pepstatin A (Sigma)). After homogenization, samples were centrifuged and the supernatants were removed and stored at -80 °C until analysis.

Sample analysis was carried out according to the Promega (Madison, WI) kit instructions, with each sample analyzed in triplicate. A 96-well plate was incubated overnight at 4 °C with the anti-BDNF monoclonal antibody diluted 1:1000 in carbonate coating buffer (0.025 M sodium bicarbonate and 0.025 M sodium carbonate, pH 9.7). The following morning the plate was washed once with TBST wash buffer (20 mM tris-HCl pH 7.6, 150 mM NaCl, and 0.05% (v/v) Tween 20) and blocked for 1 hour at room temperature in 1X sample and block buffer (diluted from 5X stock in kit, cat no. G3311). After blocking the plate was washed once with TBST wash buffer before samples (100 µL each) were added. Rows B-H of the plate had 100 µL of 1X sample buffer to them and 200 µL of the highest standard (500 pg/mL) was added to the standards wells of row A. A 1:2 serial dilution was preformed down the rows of the plate to obtain different concentrations of standards for the standard curve (0, 7.8, 15.6, 31.3, 62.5, 125, 250, and 500 pg/mL). After standard and sample addition the plate was sealed and incubated for 2 hours at room temperature with shaking. The plate was then washed 5 times with TBST wash buffer before the anti-human BDNF polyclonal antibody (diluted 1:500 in 1X sample buffer) was added (100 µL) and incubated for 2 hours at room temperature with shaking. Again 5 washes with TBST were done and 100 µL/well of the next antibody was added (anti-IGY horseradish peroxidase conjugate; diluted 1:200 in 1X sample buffer) and incubated for 1 hour at room temperature with shaking. During this time the 3,3´,5,5´-tetramethylbenzidine (TMB) one solution was equilibrated to room temperature. The plate was washed 5 times with TBST buffer before the horseradish peroxidase substrate (TMB one solution) was added at 100 µL per well and incubated at room temperature for 10 minutes with shaking. Finally the reaction was stopped with the addition of 100 µL/well of 1 N HCl and the plate was read on a plate reader at 450 nM. From the ELISA assay the concentration of BDNF was determine in units of pg/mL, which was multiplied by (4 mL) to determine the pg quantity of BDNF in the sample. The amount of

BDNF (in ng) was then divided by the tissue wet weight (ww) recorded before homogenization. The ng BDNF quantity divided by the ww (in mg) provided the raw values plotted in Figure 4.2. WT and $BDNF^{+/-}$ mice were run on separate plates and kits, thus raw data and values for DID animals normalized to percent of control (no ethanol) were both plotted to assess the effects of DID on BDNF levels.

4.2.5 TrkB Activation and Levels

Total TrkB levels and TrkB phosphorylation were determined using immunoblotting. Tissue homogenization was achieved using sonication in 100 µL lysis buffer. Lysis buffer contained: 20 mM Tris (pH 7.5), 150 mM NaCl, 2 mM EDTA, 1% Triton X-100, 10% glycerol, protease inhibitors, and phosphatase inhibitor cocktails II and III. As before, after homogenization the supernatant was collected and stored at -80 $^{\circ}$C until needed.

Total protein levels of the homogenates were determined using the enhanced protocol of the Pierce™ BCA Protein Assay Kit from Thermo Scientific (Waltham, MA). Samples were diluted 1:100 in phosphate buffered saline (140 mM NaCl, 2.7 mM KCl, 10 mM Na_2HPO_4, 1.8 mM KH_2PO_4, pH 7.3) before use in the assay. Samples were run according to the kit directions in duplicate and transferred to a 96-well plate and read on a Molecular Devices plate reader at 562 nm. Based on the concentrations obtained from the protein assay, samples were diluted in additional lysis buffer such that each sample was at a concentration of 2 µg of protein/µL.

Samples were mixed with 6X sample buffer/dye (3 g glycerol, 900 mg SDS, 228 mg Tris, and 1.5 mL beta-mercaptoethanol diluted to 5 mL with water), boiled for 5 minutes at 100 $^{\circ}$C, and loaded onto NuPage® pre-cast 4–12% Bis-Tris gels (Life Technologies, Carlsbad, CA). Gels were run in 1X NuPage® MOPS (Life Technologies, Carlsbad, CA) running buffer (20X stock: 1.0 M 3-(N-morpholino) propane sulfonic acid, 1.0 M tris base, 69.3 mM SDS, and 20.5 mM EDTA) at +127 V for about 1.5 hours. Proteins were transferred to a nitrocellulose membrane using a semi-dry transfer apparatus run at +15 V for 40

minutes. Membranes were blocked overnight in 5% BSA at 4 °C. The following day membranes were labeled with the primary antibody anti-phospho-NTRK2 (pTyr705) (Sigma-Aldrich, St. Louis, MO) diluted 1:1000 in 5% BSA overnight at 4 °C. The secondary anti-rabbit IgG (Cell Signaling, Beverly, MA) HRP-linked antibody was incubated for one hour the next morning, diluted 1:1000 in 5% BSA. Thermo Scientific™ SuperSignal™ West Dura Substrate (Waltham, MA), a luminol-based enhanced chemiluminescence (ECL) HRP substrate, was used for detection. The chemiluminescence signal was documented on film, which was developed and scanned for band quantification. Blots were stripped using Pierce Restore™ PLUS (Thermo Scientific, Waltham, MA) and were blocked for one hour in 5% milk. The Neuromics TrkB primary antibody (Edina, MN) was incubated overnight in 5% milk (1:4000 dilution). Secondary anti-goat (1:4000, Santa Cruz, Dallas, TX) was added for 1 hour and detected as before with Thermo Scientific™ SuperSignal™ ECL reagent. The signal for TrkB was too intense for film documentation so after a brief 30 second wash a Kodak Imager was used to capture the signal. The blot was again stripped with Pierce Restore™ Plus and blocked overnight in 5% milk. The final western was for the loading control actin. The actin primary antibody (Sigma-Aldrich, St. Louis, MO) was incubated for 1 hour diluted 1:5000 in 5% milk and the secondary anti-rabbit, also in 5% milk (1:2000), was incubated for 30 minutes. Enhanced chemiluminescence reagent was again used and documented using film.

4.2.6 Statistical and Data Analysis

BDNF levels were normalized to tissue wet weight, TrkB levels were normalized to actin or as a ratio of phosphorylated to total levels and DA tissue content concentrations were normalized to total protein levels. Bands for the Western blots were quantified using ImageJ software (NIH, Bethesda, MD). GraphPad Prism v5 software was used to create graphs and run statistical analysis using two-way ANOVA, with significance set to $p < 0.05$.

4.3 Results

4.3.1 Ethanol Consumption

Ethanol consumption over the course of 7 days of DID was similar between WT and $BDNF^{+/-}$ mice (Figure 4.1). Analyzing all DID consumption data together (Figure 4.1A, repeated-measures two-way ANOVA) there was a within-subjects effect of time ($F(6,210) = 3.01$, $p < 0.01$). Together there was also a between-subjects effect of gender ($F(1,35) = 16.95$, $p < 0.001$) and genotype ($F(1,35) = 5.27$, $p < 0.05$). The within-subjects effect of time is attributed to the males based on a separate analysis of the genders showing a significant effect for males only ($F(6,114) = 3.09$, $p < 0.01$, Figure 4.1B). The genotypic effect can be attributed mainly to the female animals (Figure 4.1C) as a separate genotype analysis on males ($F(1,19) = 1.01$, $p = 0.33$) and females ($F(1,14) = 3.90$, $p = 0.07$) did not show significance for either gender, but there was a trend with females based on their *p*-values.

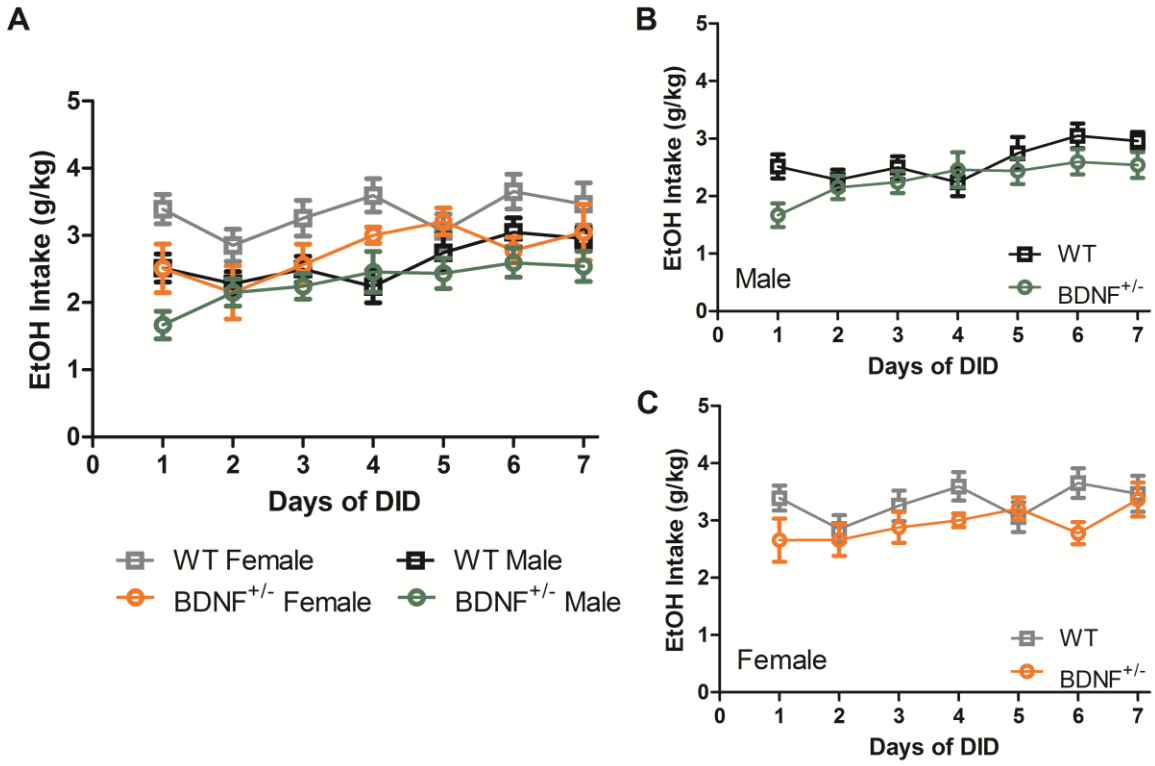

Figure 4.1 Ethanol intake during the 7 days of DID in grams (g) of ethanol consumed per kilogram (kg) of mouse weight (n = 9–13/group). **A**) All genotypes and genders plotted together showing a main effect of gender ($p < 0.001$) and genotype ($p < 0.05$). **B**) Ethanol intake for male mice only with a main effect of time ($p < 0.01$). **C**) Ethanol intake for female mice with a trend towards genotypic differences ($p = 0.07$). Data to create these plots can be found in Table A.6 and A.7 of the appendix.

4.3.2 BDNF Levels

BDNF levels were determined using an ELISA assay. Due to the variability in assay kits and the fact that different kits were used for WT and BDNF$^{+/-}$ mice, raw values and values as percent of control for naïve animals were calculated to better assess the effect of DID. BDNF levels plotted for both genders as ng BDNF/mg wet weight (ww) show a reduction in BDNF levels in both genotypes (Figure 4.2A). Two-way ANOVA illustrated a main effect of treatment ($F(2,46) = 3.70$, $p < 0.05$) and of genotype ($F(1,46) = 31.08$, $p< 0.001$). Bonferroni post-test revealed that WT controls were significantly different from the 24 hour treatment group ($p < 0.05$). Plotting the data as percent of control for naïve animals of

their own genotype (Figure 4.2B), the effect of genotype was no longer observed (as expected) but the confidence of the main effect of treatment increased ($F(2,45) = 6.43$, $p < 0.01$). Normalized data gives a clearer indication of the effect of DID, which was similar for both WT and $BDNF^{+/-}$ mice. In WT animals there was an almost 25% reduction in BDNF levels 30 minutes after the last DID session which was further attenuated 24 hours after the last DID session. $BDNF^{+/-}$ mice had reduced BDNF levels (~60 % of baseline) 30 minutes after the last DID session; a similar reduction was observed at 24 hours as well.

The aforementioned data included both genders for each genotype. Figure 4.2C-F shows similar comparisons of raw versus normalized data with the genotypes also separated out by gender. WT males and females appear to undergo similar reductions in BDNF levels, however in $BDNF^{+/-}$ mice the previously observed reductions of BDNF are clearly attributed to the females. Figure 4.2C, comparing raw values of male WT and $BDNF^{+/-}$ mice shows that there was a main effect of genotype ($F(1,25) = 18.87$, $p < 0.001$) and the difference between WT mice from the control group and the 24 hours group was significant (Bonferroni post-test, $p < 0.05$). In the normalized data set, (Figure 4.2D), the main effect of genotype was not observed but the reduction in 24 hour WT animals was still significant (Bonferroni post-test, $p < 0.05$). Raw BDNF levels for female animals (Figure 4.2E) had a main effect of genotype only ($F(1,13) = 9.22$, $p < 0.01$). WT females had a similar trend in attenuated BDNF levels following the DID protocol as the male WT mice. However, the female $BDNF^{+/-}$ mice appeared to be more heavily impacted by DID than their male $BDNF^{+/-}$ counterparts. When BDNF levels were normalized for female mice (Figure 4.2F) there was a significant main effect of treatment ($F(2,13) = 15.32$, $p < 0.001$) and genotype ($F(1,13) = 5.46$, $p < 0.05$). Female $BDNF^{+/-}$ mice had a significant reduction in BDNF at 30 minutes and 24 hours as compared to their controls (Bonferroni post-test, 30 minutes $p < 0.05$, 24 hours $p < 0.001$).

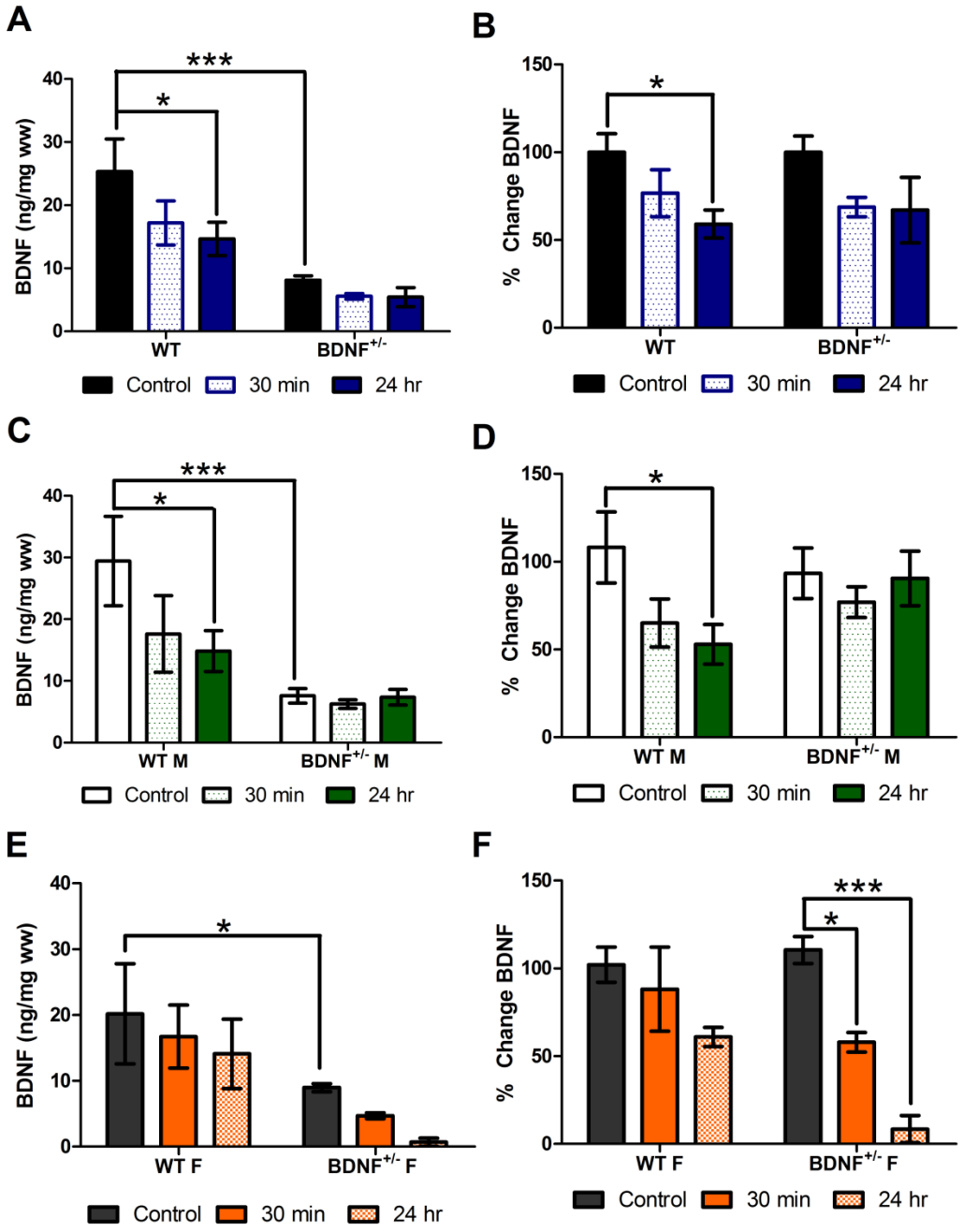

Figure 4.2 BDNF levels reported as raw values (ng BDNF/wet weight (ww) of tissue) and normalized based on assay plate to control animals. Mixed gender (A&B, n = 6-8/group) and separate gender plots (C-F, n = 2-5/group). Significant differences observed by Bonferroni post-test are displayed on graphs (* $p < 0.05$, *** $p < 0.001$). **A**) WT and BDNF$^{+/-}$ levels of BDNF protein with mixed gender. There was a main effect of treatment ($p < 0.05$) and of genotype ($p < 0.001$). **B**) Mixed gender plot of BDNF levels normalized to control animals for each genotype where a main effect of DID treatment was observed ($p < 0.01$). **C**) BDNF levels for male animals only, where there was a main effect of genotype ($p < 0.001$). **D**) Normalized BDNF levels for male mice. **E**) BDNF levels in female mice where there was a main effect of genotype ($p < 0.01$). **F**) Normalized BDNF levels in female mice with a main effect of genotype ($p < 0.05$) and treatment ($p < 0.001$). Data to create these plots can be found in Table A.8 of the appendix.

4.3.3 TrkB Levels and Activation

TrkB levels and activation were assessed using two separate blots for male vs. female animals. Each genotype/treatment group contained 2–3 mice. Activation was assessed by determining phosphorylated levels of TrkB (p-TrkB), which were observed for both the T-TrkB (truncated) and FL-TrkB (full length). Total truncated and full length levels of TrkB were also evaluated. Figures 4.3 and 4.5 summarize each of these protein measurements, which were normalized to the actin loading control for male and female mice, respectively. Figures 4.4 and 4.6 summarize the ratios between phosphorylated TrkB to total TrkB for both truncated and full length for male and female mice, respectively. Additionally, the ratios of the phosphorylated (Figure 4.4C and 4.6C) and total levels (Figure 4.4D and 4.6D) of the two receptors are also plotted.

4.3.3.1 Males

Phosphorylation of FL-TrkB was similar for all groups of male WT and BDNF$^{+/-}$ mice with no main effects (two-way ANOVA, Figure 4.3A) of treatment or genotype observed, however there was a significant reduction of p-FL-TrkB 30 minutes after DID for the WT animals only (Bonferroni post-test, $p < 0.05$). Total FL-TrkB levels are not different for either genotype (Figure 4.3C). Activation of T-TrkB had a divergent pattern at the 30 minute time point, with a decrease in WT and an increase in BDNF$^{+/-}$ mice (Figure 4.3B). There was a main effect of genotype ($F(1,10) = 7.52$, $p < 0.05$) on p-T-TrkB and a significant interaction of genotype x treatment ($F(2,10) = 7.39$, $p < 0.05$). The reduction of p-T-TrkB observed in WT male's was not statistically different in the post-test but the increase at 30 minutes in BDNF$^{+/-}$ mice was significant (Bonferroni, $p < 0.05$). For both WT and BDNF$^{+/-}$ male mice p-T-TrkB levels returned to control by 24 hours after DID. Finally, for total T-TrkB (Figure 4.3D), there was an increase in levels at the 30 minute and 24 hour time point for WT mice as compared to control (Bonferroni post-test, 30 minute $p < 0.01$, 24 hour $p < 0.05$), leading to a main effect of treatment ($F(2,10) = 7.403$, $p < 0.05$) and genotype ($F(1,10) = 9.43$, $p < 0.05$) in the two-way ANOVA. Additionally based on the increases in T-TrkB following

DID in the WT and no change in the BDNF$^{+/-}$ mice there was a significant treatment x genotype interaction ($F(2,10) = 5.75$, $p < 0.05$).

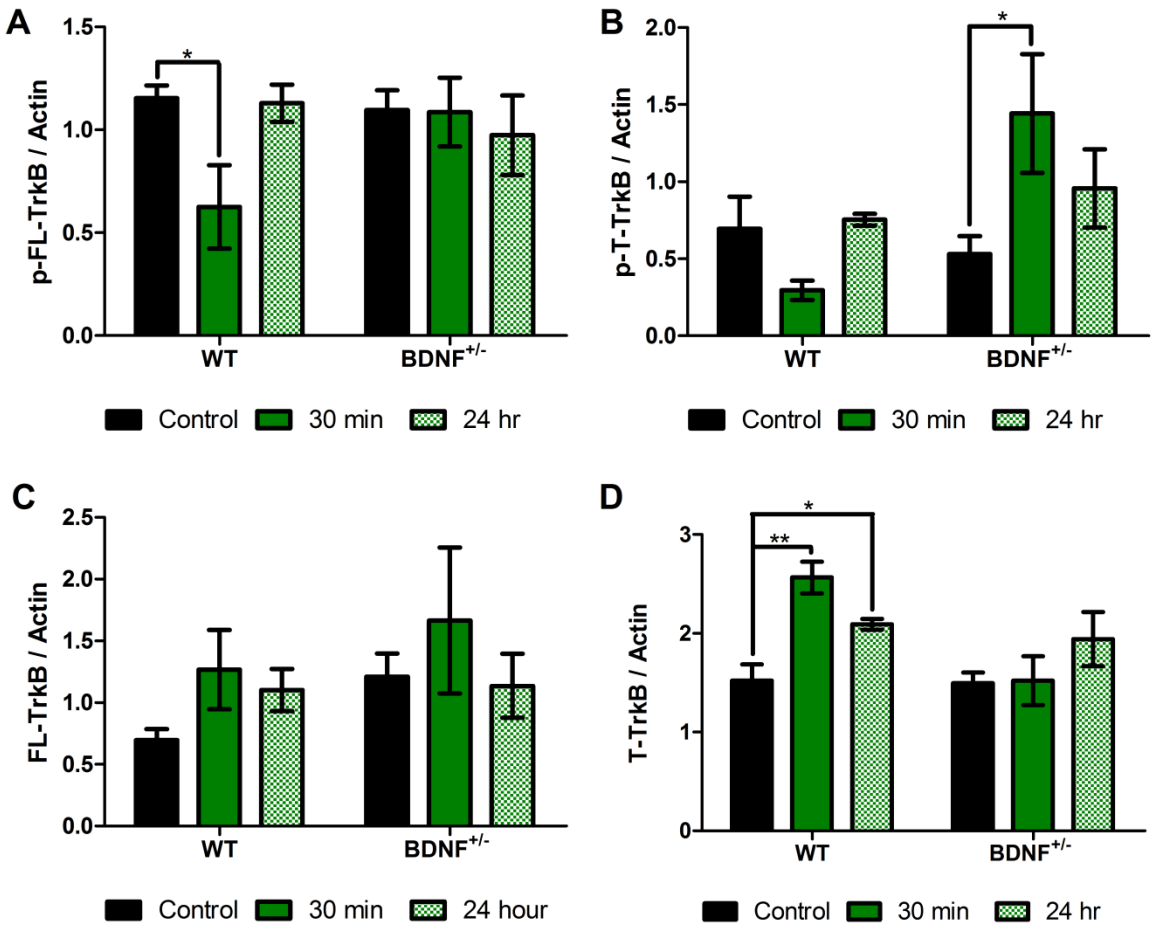

Figure 4.3 Phosphorylation of full-length and truncated TrkB receptor, as well as total levels observed from western blot analysis, all normalized to actin in male animals (n = 2-4/group). Only significant differences observed by post-test are displayed on graphs (* $p < 0.05$, ** $p < 0.01$). **A**) Phosphorylated levels of the full length TrkB receptor (p-FL-TrkB). **B**) Phosphorylation of the truncated receptor (p-T-TrkB) in which there was a main effect of genotype ($p < 0.05$) and a genotype x treatment interaction ($p < 0.05$). **C**) Total full-length TrkB levels in which no statistical significance was observed. **D**) In total truncated receptor levels (T-TrkB) there was a main effect of treatment ($p < 0.05$), genotype ($p < 0.05$) and treatment x genotype interaction ($p < 0.05$). Data to create these plots can be found in Table A.9 and Figures: A.1, A.3 and A.5 of the appendix.

To assess receptor activation, the ratios of p-T-TrkB/total T-TrkB and p-FL-TrkB/total FL-TrkB were calculated. The ratio of p-FL-TrkB/total FL-TrkB was reduced at 30 minutes in WT mice (Bonferroni, $p < 0.05$, Figure 4.4A) however there was no main effect of treatment. There was also a reduction in p-FL-TrkB/total FL-TrkB in BDNF$^{+/-}$ control mice compared to WT controls that also did not produce any main effect of genotype ($p = 0.094$, Figure 4.4A). The ratio of p-T-TrkB/total T-TrkB (Figure 4.4B) appear to trend toward a decrease in WT mice and increased in BDNF$^{+/-}$ mice at 30 minutes (Bonferroni, $p < 0.05$) and levels are comparable to control by 24 hours. This divergent response led to a main effect of genotype ($F(1,10) = 8.48$, $p < 0.05$) and interaction between genotype x treatment ($F(2,10) = 8.14$, $p < 0.01$). The ratio of p-FL-TrkB to p-T-TrkB was calculated and no statistically significant changes were detected (Figure 4.4C), however there is trend towards BDNF$^{+/-}$ mice having a smaller ratio (p-FL-TrkB/p-T-TrkB) due to the increases of the p-T-TrkB observed after DID at both 30 minutes and 24 hours. Finally, the ratio of total TrkB receptor was determined for FL-TrkB compared to T-TrkB and there was a main effect of genotype (Figure 4.4D, $F(1,10) = 8.01$, $p < 0.05$), based on the increase in BDNF$^{+/-}$ controls compared to WT controls and also the increased levels at 30 minutes in the BDNF$^{+/-}$ mice.

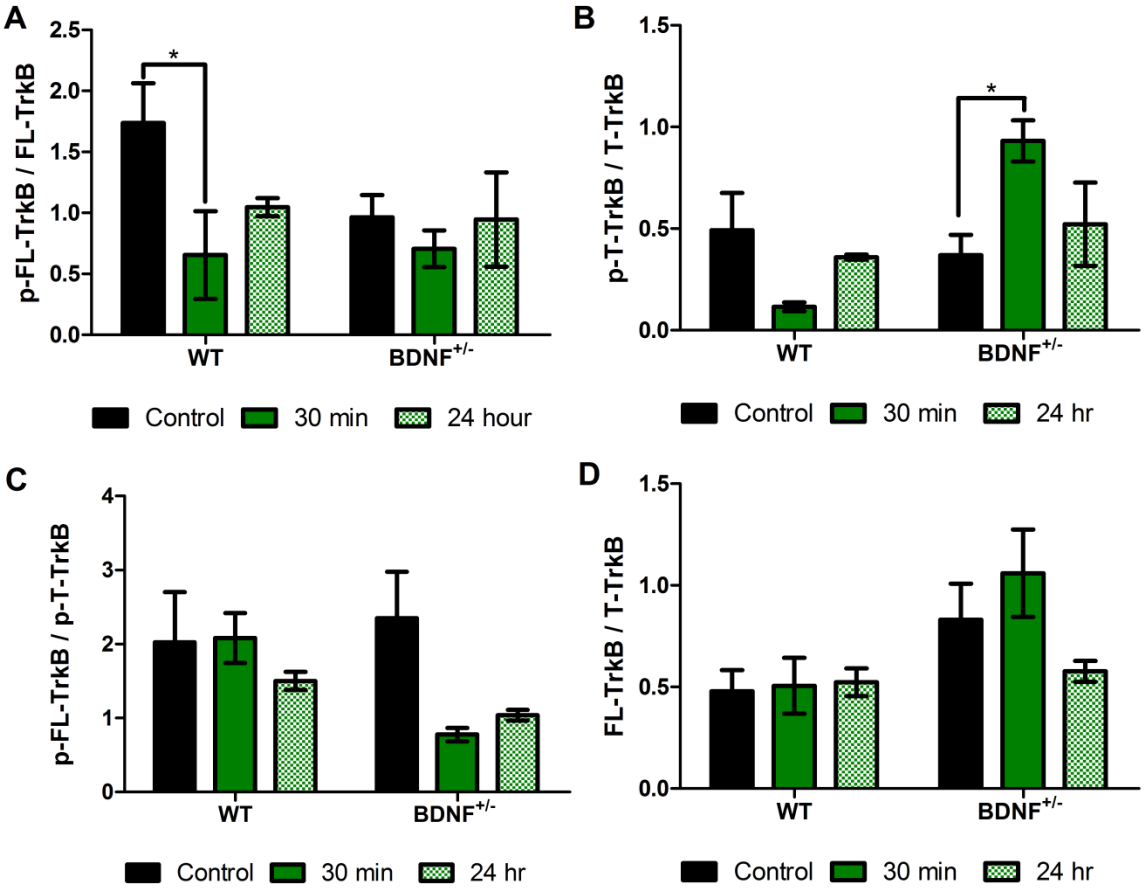

Figure 4.4 Receptor activation in male mice indicated by the ratio of the phosphorylated receptor to the total receptor levels. Separate ratios of phosphorylated receptors and total levels are also shown (males, n = 2-4/group). Only significant differences as determined by post-test are displayed on graphs (* $p < 0.05$). **A**) Phosphorylated levels of the full length TrkB receptor (p-FL-TrkB) divided by total full length levels (FL-TrkB). **B**) Phosphorylation of the truncated receptor (p-T-TrkB) divided by total truncated receptor (T-TrkB) levels where there was a main effect of genotype ($p < 0.05$) and a genotype x treatment interaction ($p < 0.01$). **C**) Ratio of full length (p-FL-TrkB) to truncated (p-T-TrkB) phosphorylated receptors. **D**) Ratio of total receptor levels full length (FL-TrkB) to truncated (T-TrkB) where there was a main effect of genotype ($p < 0.05$). Data to create these plots can be found in Table A.9 and Figures: A.1, A.3 and A.5 of the appendix.

4.3.3.2 Females

Given the gender differences observed in the BDNF levels, and the space constraints of the protein gel, TrkB levels were assessed separately for the female mice. Female $BDNF^{+/-}$ mice had slightly lower levels of phosphorylation of FL-TrkB compared to WT mice (two-way ANOVA main effect of genotype, $F(1,12) = 14.16$, $p < 0.01$, Figure 4.5A). There was no statistically significant effect of treatment on p-FL-TrkB, however, at the 30 minute and 24 hour time points, p-FL-TrkB levels did show a trend toward reductions in female $BDNF^{+/-}$ mice. With respect to total FL-TrkB levels in females (Figure 4.5C) the changes were similar yet more pronounced than the male mice. In female WT mice, total FL-TrkB levels were increased at the 30 minute and 24 hour DID groups (Bonferroni, 30 minute $p < 0.05$, 24 hour $p < 0.01$). $BDNF^{+/-}$ control mice had enhanced levels of FL-TrkB compared to WT controls and also had increase total FL-TrkB 30 minutes after DID as compared to $BDNF^{+/-}$ control (Bonferonni, $p < 0.001$). These changes in total FL-TrkB led to a main effect of treatment ($F(1,12) = 16.63$, $p < 0.001$), genotype ($F(1,12) = 8.58$, $p < 0.05$), and a genotype x treatment interaction ($F(2,12) = 7.57$, $p < 0.01$) in the two-way ANOVA (Figure 4.5C). With respect to phosphorylation of the T-TrkB receptor (Figure 4.5B), there was a main effect of genotype ($F(1,12 = 81.06$, $p < 0.001$), as well as a genotype x treatment interaction ($F(2,12) = 8.70$, $p < 0.01$). In female $BDNF^{+/-}$ control mice p-T-TrkB levels were reduced compared to WT animals, and there was a significant reduction in p-T-TrkB levels at 30 minutes and 24 hours after DID (Bonferroni, 30 minutes $p < 0.05$, 24 hours $p < 0.01$). Total T-TrkB levels were similar for control animals, but there was a main effect of treatment (Figure 4.5D, $F(2,12) = 12.56$, $p < 0.01$) given the increase in total T-TrkB levels following DID, which were more pronounced in $BDNF^{+/-}$ mice at both 30 minutes and 24 hours after DID (Bonferroni, 30 minute $p < 0.01$, 24 hours $p < 0.001$).

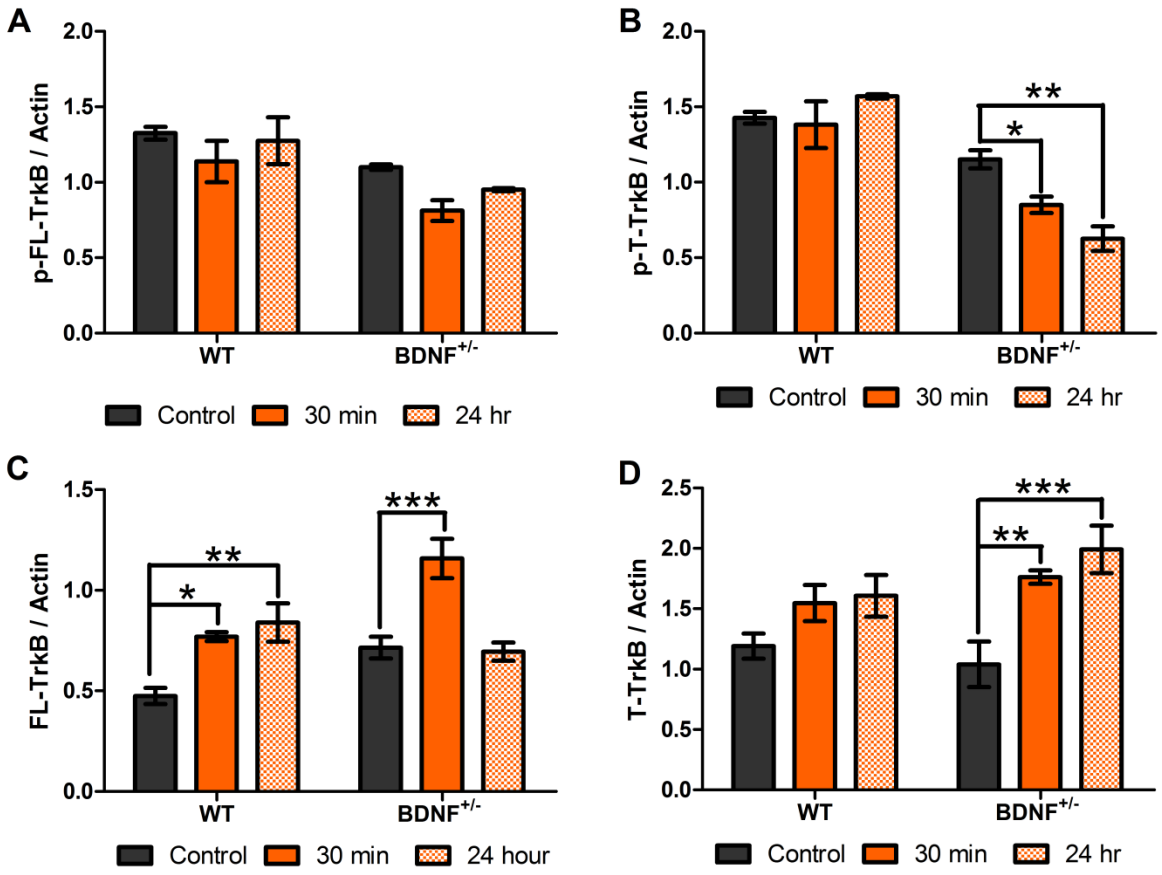

Figure 4.5: Phosphorylation of full-length and truncated TrkB receptor, as well as total levels observed from western blot analysis, all normalized to actin in female animals (n = 2-4/group, Bonferroni post-test, * $p < 0.05$, ** $p < 0.01$, *** $p < 0.001$). **A**) Phosphorylated levels of the full length TrkB receptor (p-FL-TrkB), where there was a main effect of genotype ($p < 0.01$). **B**) Phosphorylation of the truncated receptor (p-T-TrkB), where there was a main effect of genotype ($p < 0.001$) and a genotype x treatment interaction ($p < 0.01$). **C**) Total full-length TrkB (FL-TrkB) levels where there was a main effect of treatment ($p < 0.001$), genotype ($p < 0.05$) and treatment x genotype interaction ($p < 0.01$). **D**) Total truncated receptor levels (T-TrkB) in which there was a main effect of treatment ($p < 0.01$). Data to create these plots can be found in Table A.10 and Figures: A.2, A.4 and A.6 of the appendix.

The activation of the FL-TrkB, as assessed by the ratio of p-FL-TrkB to total FL-TrkB (Figure 4.6A), exhibited a main effect of genotype ($F(1,12) = 25.83$, $p < 0.001$), treatment ($F(2,12) = 21.98$, $p < 0.001$), and an interaction of genotype x treatment ($F(2,12) = 4.65$, $p < 0.05$). Post-hoc analysis revealed a significant reduction of FL activation (p-FL-TrkB/FL-TrkB) at the 30

minute time point for both genotypes, where in the WT mice this reduction was persistent for up to 24 hours. The ratio of p-T-TrkB to total T-TrkB had a main effect of genotype ($F(1,12) = 13.06$, $p < 0.01$) and treatment ($F(2,12) = 12.66$, $p < 0.01$) with post-tests showing a statistically significant reduction of p-T-TrkB/T-TrkB at 30 minutes and 24 hours after DID in female $BDNF^{+/-}$ mice. The ratios of p-FL-TrkB to p-T-TrkB were unaltered for WT mice, while in female $BDNF^{+/-}$ mice they were increased only 24 hours after DID (Figure 4.6C, Bonferroni post-test, $p < 0.001$). Due to the increase in p-FL-TrkB/p-T-TrkB at 24 hours for the female $BDNF^{+/-}$ there was a main effect of genotype ($F(1,12) = 23.78$, $p < 0.001$), treatment ($F(2,12) = 7.71$, $p < 0.01$) and genotype x treatment interaction ($F(2,12) = 11.89$, $p < 0.01$). The ratios of the total FL-TrkB levels to total T-TrkB (Figure 4.6D) had a significant interaction of genotype x treatment only ($F(2,12) = 6.77$, $p < 0.052$) due to the divergent pattern of: increases in female WT treated animals versus decreases in treated $BDNF^{+/-}$ mice at 24 hours. The post-hoc analysis revealed a statistical difference from control to 24 hours in the $BDNF^{+/-}$ mice ($p < 0.01$).

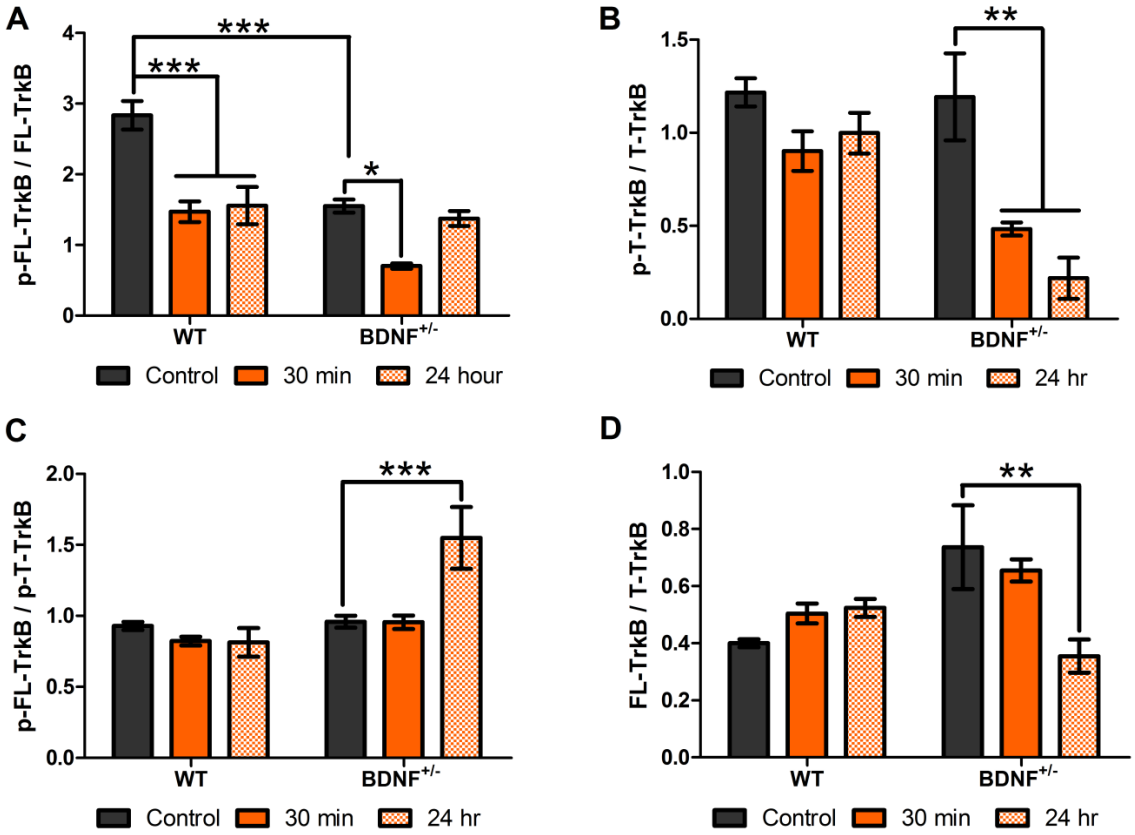

Figure 4.6: Receptor activation indicated by the ratio of the phosphorylated receptor to the total receptor levels. Separate ratios of phosphorylated receptors and total levels are also shown (females, n = 2-4/group). Only significant differences observed by post-test are displayed on graphs (* $p < 0.05$, ** $p < 0.01$, *** $p < 0.001$). **A**) Phosphorylated levels of the full length TrkB receptor (p-FL-TrkB) divided by total full length levels (FL-TrkB) where there was a main effect of genotype ($p < 0.001$), treatment ($p < 0.001$) and a genotype x treatment interaction ($p < 0.05$). **B**) Phosphorylation of the truncated receptor (p-T-TrkB) divided by total truncated receptor levels (T-TrkB) where there was a main effect of genotype ($p < 0.01$) and treatment ($p < 0.01$). **C**) Ratio of phosphorylated full length (p-FL-TrkB) to truncated (p-T-TrkB) receptors, where there were effects of genotype ($p < 0.001$), treatment ($p < 0.01$), and a genotype x treatment interaction ($p < 0.01$). **D**) Ratio of total receptor levels, full length (FL-TrkB) to truncated (T-TrkB), where there was a treatment x genotype interaction ($p < 0.05$). Data to create these plots can be found in Table A.10 and Figures: A.2, A.4 and A.6 of the appendix.

4.3.3.3 Summary Tables

Tables 1–4 summarize the aforementioned differences observed in total receptor levels, activation and the various ratios determined. The smaller symbol size in these comparison tables indicates a trend towards differences. Fluctuations that were not statistically significant but appear qualitatively different (by visual observation) are highlighted in red.

Table 4.1 Summary of changes in BDNF and its receptor TrkB for male $BDNF^{+/-}$ controls and DID WT animals as compared to male WT control animals.

Protein Measure	BDNF+/- Control	WT 30 min	WT 24 hour
BDNF	↓	↓	↓
Total Truncated TrkB	=	↑	↑
Total Full Length TrkB	↑	↑	↑
pTrkB (truncated)	=	↓	=
pTrkB (full length)	=	↓	=
p-FL/Total FL TrkB	↓	↓	↓
p-T/Total T TrkB	=	↓	=
pFL/pT	=	=	↓
FL/T	↑	=	=

Table 4.2 Summary of changes in BDNF and TrkB for male $BDNF^{+/-}$ DID mice as compared to control animals.

Protein Measure	BDNF+/- 30 min	BDNF+/- 24 hour
BDNF	=	=
Total Truncated TrkB	=	↑
Total Full Length TrkB	=	=
pTrkB (truncated)	↑	↑
pTrkB (full length)	=	=
p-FL/Total FL TrkB	=	=
p-T/Total T TrkB	↑	=
pFL/pT	↓	↓
FL/T	=	↓

Table 4.3 Summary of changes in BDNF and TrkB for female $BDNF^{+/-}$ controls and DID WT animals as compared to female WT control animals.

Protein Measure	BDNF+/- Control	WT 30 min	WT 24 hour
BDNF	↓	↓	↓
Total Truncated TrkB	=	↑	↑
Total Full Length TrkB	↑	↑	↑
pTrkB (truncated)	↓	=	↑
pTrkB (full length)	↓	=	=
p-FL/Total FL TrkB	↓	↓	↓
p-T/Total T TrkB	=	↓	↓
pFL/pT	=	=	=
FL/T	↑	↑	↑

Table 4.4 Summary of changes in BDNF and TrkB for female $BDNF^{+/-}$ DID animals as compared to control animals.

Protein Measure	BDNF+/- 30 min	BDNF+/- 24 hour
BDNF	↓	↓
Total Truncated TrkB	↑	↑
Total Full Length TrkB	↑	=
pTrkB (truncated)	↓	↓
pTrkB (full length)	↓	↓
p-FL/Total FL TrkB	↓	=
p-T/Total T TrkB	↓	↓
pFL/pT	=	↑
FL/T	=	↓

4.4 Discussion

The data obtained from the various tissue content analyses allows for genotypic comparisons of the effect of DID on BDNF-TrkB signaling, as well as the role of gender in these alterations. The primary goal of these experiments was to understand how voluntary ethanol consumption through DID influences BDNF-TrkB signaling in mice with low endogenous BDNF levels compared to normal (WT) mice. Understanding how ethanol may alter BDNF-deficient mice differently than WT mice may lead to a better understanding of the risk associated with humans having mutations in their BDNF gene. An additional piece of information was assessed

in these studies to determine if gender may lead to different alterations in the effects of DID on WT and BDNF$^{+/-}$ mice. The four groups under study, male WT, male BDNF$^{+/-}$, female WT and female BDNF$^{+/-}$, all seem to have slightly different alterations to BDNF and TrkB following 7 days of DID. The changes observed help to understand the role of low endogenous BDNF levels by suggesting that corresponding TrkB changes also occur; but also highlight a need to study both sexes in order to better relate to the human condition.

4.4.1 DID Behavior is Similar Between WT and BDNF$^{+/-}$ Mice

Ethanol consumption was assessed for 7 days, after which protein measures were made to determine BDNF-TrkB signaling function. WT and BDFN$^{+/-}$ mice exhibited similar ethanol consumption however there were some gender based differences. The main effect of genotype observed when all mice were assessed together (statistically) was likely attributed to the female WT mice because of their higher consumption on days 1 – 4. By the end of the 7 days however, consumption for all of the groups was similar. For the present study the focus was on genotype and the male and female mice were assessed separately, therefore there is less emphasis on drinking differences observed between male and female mice.

4.4.2 DID Induced Reductions in BDNF Levels Lead to Reductions in Activation of the TrkB Receptor

BDNF levels were initially analyzed with the intention of using male and female mice together to assess the effect of DID (due to limited availability from the mouse colony), however other experimental factors led us to assess gender separately (see following). Initially, it appeared that BDNF levels were reduced to about 60% of baseline for both WT and BDNF$^{+/-}$ mice (Figure 4.2A & B). However, separation of data obtained from male and female mice indicated that the reduced BDNF levels following DID in BDNF$^{+/-}$ mice were primarily due to the

response of the female mice (Figure 4.2D & F), since a 50% (30 minutes) and 90% (24 hours) decrease was observed in females with no change in the males. In contrast, in the WT animals the reductions in BDNF levels were attributed mainly to male animals, especially at 30 minutes after the 7th DID session.

For the TrkB receptor, investigations primarily focused on the ratio of p-FL-TrkB to total FL-TrkB; with this ratio considered as activation of TrkB signaling by BDNF. The changes in receptor activation (p-FL-TrkB/FL-TrkB) were consistent with the changes observed in BDNF protein levels. In both male and female WT mice, there was a reduction in receptor activation at both 30 minutes and 24 hours after the 7th DID session. Although the mechanism of how the ratios of p-FL-TrkB/FL-TrkB are reduced to indicate attenuated TrkB activation in WT mice are different. The levels of phosphorylation (p-FL-TrkB) are consistent following treatment, whereas the amount of total receptor (FL-TrkB) was increased. This trend of stable p-FL-TrkB and increased FL-TrkB was true except at the 30 minute time point in male WT mice, where phosphorylation is reduced leading to the reduction in p-FL-TrkB/FL-TrkB. For BDNF$^{+/-}$ control mice of both genders, there was a reduction of FL-TrkB activation compared to WT animals and this reduction was a result of increased levels of total FL-TrkB. In BDNF$^{+/-}$ male mice there was no difference in BDNF levels or FL-TrkB activation following DID exposure. BDNF$^{+/-}$ females had attenuation in BDNF levels: to 50% at 30 minutes and 10% at 24 hours, compared to BDNF$^{+/-}$ controls. Interestingly, reductions in FL-TrkB activation for female BDNF$^{+/-}$ mice were only observed at the 30 minute time point due to slightly lower p-FL-TrkB levels and increased total FL-TrkB. By 24 hours, the total FL-TrkB levels are back to control levels suggesting that reduced BDNF levels 24 hours after the last DID session are not translating to alterations in signaling. The gender differences observed with regard to BDNF and TrkB levels in BDNF$^{+/-}$ mice only could likely be a result of differences in gene expression due to estrogen regulation, which has

previously been shown [72]. Further experiments should verify the gender differences observed in $BDNF^{+/-}$ mice by increasing the *n*-values in the study for example. Overall these data suggest that the reduced BDNF levels, whether endogenous or as a result of DID exposure, yield reductions in receptor activation due primarily to increases in the total amount of FL-TrkB expression.

The role for BDNF in mediating ethanol's action and the affect ethanol has on BDNF is difficult to understand due to seemingly conflicting evidence. First, numerous studies have pointed to a neuroprotective role for BDNF due to its increased expression following ethanol exposure, as well as reductions in BDNF leading to enhanced ethanol consumption [26, 28]. However, many of the studies indicating increased BDNF levels following ethanol exposure examined only mRNA levels, not protein. When acute ethanol has been administered, BDNF protein levels are reduced 45 minutes after administration [29]. The divergence in mRNA and BDNF protein levels could be a result of ethanol's action on different neuronal sub-populations. For instance, despite the diffuse expression of BDNF throughout the brain, the main source of BDNF in the CPu is from glutamatergic cortical afferents [73]. One molecular target of ethanol is the glutamatergic *N*-methyl-D-aspartate (NMDA) receptor, which leads to neuronal inhibition [74], through which BDNF levels in the CPu could be reduced (recall Figure 1.5). With regard to enhanced BDNF mRNA following acute ethanol, it has been established that TrkB activation can be switched from a transient to sustained activation mode when coupled with neuronal depolarization [75]. Acute administration of ethanol increases extracellular DA levels in the CPu which could lead to sustained activation of TrkB, despite reduced BDNF levels. This sustained activation of TrkB could lead to increased BDNF mRNA expression through its downstream target of the CREB transcription factor which can regulate BDNF transcription. Together these

studies suggest that despite the conflicting mRNA and protein measures of BDNF, following ethanol exposure the neuroprotective pathway for BDNF in response to ethanol is still valid.

Given the hypothesis that BDNF is serving a neuroprotective role in acute ethanol exposure, what does it mean when WT mice have reduced BDNF and TrkB activation following repeated ethanol exposure with 7 days of DID? The immediate and sustained reductions in BDNF and TrkB activation in WT mice following 7 days of DID shown here suggest that the DID model may be promoting an alcohol dependent phenotype in the WT animals. A study by Logrip *et al.* used a variation of the DID procedure, where mice had 4-hour daily DID sessions with access to water and ethanol for 6 weeks [76]. Key findings were increased ethanol preference over time in WT animals, and disruption in the proposed BDNF protective pathway [76]. Initially, after 1 day of modified DID consumption BDNF mRNA was increased in the CPu only, however after 6 weeks there were no longer any differences observed in BDNF mRNA in the CPu and there was reduced expression in the cortex [76]. The reduced BDNF-TrkB signaling in our WT mice may indicate an earlier onset of dysfunction in the protective BDNF pathway than the aforementioned 6 weeks. Additionally the inherent nature of the DID procedure to produce excess ethanol consumption and blood alcohol concentrations, could result in initiating an addiction or dependence in the WT animals. If dependence in WT animals is being induced this complicates our use of the $BDNF^{+/-}$ mice to assess the role of low endogenous BDNF levels to make one more susceptible to alcohol dependence because we have caused dysfunction in our control group that we are comparing too. The goal of using the $BDNF^{+/-}$ mice was to understand how alterations may occur faster or to a greater extent than their WT counterparts, however if our use of the DID model for 7 days is rendering a dysfunction in the WT animals than this model or exposure length may not be optimal for our purposes. Further support for the 7 days of DID producing a dependence-like phenotype can be found when considering the enhanced

preference for ethanol consumption in the $BDNF^{+/-}$ mice. Other ethanol consumption models have shown increased preference and consumption in the $BDNF^{+/-}$ mice [26, 28] likely due to their already altered BDNF-TrkB signaling as compared to WT. The increase in ethanol preference observed in WT mice by Logrip *et al*. after 6 weeks in a modified DID protocol, together with alterations in the neuroprotective BDNF pathway [76], suggest that DID is producing a similar phenotype to the $BDNF^{+/-}$ mice. Although, further investigations are required to assess these hypotheses, together the present investigations and previous studies show that disruptions in BDNF-TrkB signaling have an impact on ethanol consumption and conversely ethanol causes alterations to the important neurotrophic factor BDNF.

An essential component to further studies which could test the hypothesis of 7 days of DID causing addiction/dependence in WT animals, would be to incorporate a behavioral assessment of the preference for or the seeking of ethanol in WT or $BDNF^{+/-}$ mice. If the goal is to understand what neuroadaptations switch a casual drinker to a dependent (or addicted) drinker, than assessing the animals after they have become addicted is not as useful. Future studies should focus on intermediate time points throughout the DID exposure, as well as a behavioral component to assess the animals preference for ethanol in order to infer if an addiction/dependence is being created in the animal. Another consideration is the numerous intracellular signaling cascades induced by TrkB activation and the different biological responses resulting from those pathways. There is evidence that different cascades are affected differently by ethanol and as such in order to truly understand the implications of altered BDNF-TrkB signaling, the specific downstream pathways up-regulated or down-regulated must be investigated in detail [21]. Finally, most of the reductions in TrkB activation resulted from increases in total FL-TrkB levels; therefore, when repeated ethanol exposure down-regulates BDNF protein levels, it would be important to understand what specific mechanism is

responsible for enhanced TrkB receptor expression. Similarly there should be a confirmation that the reduced activation observed in the ratios, actually leads to attenuation of the pathways downstream of TrkB.

4.4.2.1 An Alternative Explanation for the Alterations in BDNF-TrkB Signaling.

Most studies discuss the outcome of enhanced BDNF-TrkB signaling and how this promotes synaptic plasticity and learning [77]. It is possible that the reductions in BDNF-TrkB signaling in WT animals are actually serving to reduce synaptic plasticity in the presence of repeated exposure to ethanol to prevent reinforcement of its addictive properties. Despite the fact that BDNF-TrkB signaling is reduced in $BDNF^{+/-}$ males compared to WT, 7 days of DID did not cause further attenuations, which could indicate their genetic susceptibility to addiction. If reductions in BDNF-TrkB signaling were considered protective then the unchanged BDNF-TrkB signaling in the male $BDNF^{+/-}$ mice following DID may indicate that they are more amenable to the re-enforcing properties of ethanol. Future studies could investigate this behaviorally by assessing learning and memory in the WT and $BDNF^{+/-}$ males following 7 days of DID.

4.4.3 Differences in T-TrkB Are Acute and Less Dependent on BDNF Levels

There is less known about the T-TrkB receptor, its activation, and what that activation means for cellular responses. Although the role of the T-TrkB receptor is not well understood, we chose to pursue assessing T-TrkB levels to provide additional insight into the interactions of BDNF and ethanol. T-TrkB receptor activation was not different between control WT and $BDNF^{+/-}$ mice, whereas FL-TrkB receptor activation was reduced in the $BDNF^{+/-}$ controls compared to WT. In WT males there was a trend toward reduced activation (p-T-TrkB/T-TrkB) at only 30 minutes due to reduced phosphorylation and increased total T-TrkB levels. In female WT animals, there was a slight reduction in T-TrkB activation due to increased total T-TrkB levels. $BDNF^{+/-}$ males

have enhanced T-TrkB activation only at the 30 minute time point, which appears to be due to increased phosphorylation (p-T-TrkB). Female BDNF$^{+/-}$ mice have attenuated T-TrkB activation at both 30 minutes and 24 hours, which is a combined effect of reduced phosphorylation with increased total T-TrkB levels. Taken together these data suggest that T-TrkB alterations are not directly correlated to BDNF levels due to the lack of genotypic difference in controls and the lack of pattern between reductions in BDNF and a corresponding change in the T-TrkB. Additionally, the alterations observed in T-TrkB seem to be an acute effect as a direct result of consumption due to the fact that changes were only observed at the 30 minute time point with the exception of female BDNF$^{+/-}$ mice. The T-TrkB receptor is hypothesized to inhibit the FL-TrkB receptor by binding with it to form an inactive receptor complex [70]. Although there may be support for this hypothesis here, further investigations would be required to confirm it. The levels of p-FL-TrkB (normalized to actin) are attenuated 30 minutes after DID in the male WT mice; together with increases in total FL-TrkB, this change led to reduced activation. At the same time there were increases in total levels of T-TrkB. Similar trends were observed in female mice of both genotypes as well. It is logical to associate the reduction in activation of FL-TrkB to a direct result of the reduced BDNF levels, however it is possible that the changes in T-TrkB receptor levels are contributing to this attenuation. The important consideration though is that the function of T-TrkB is dependent on its localization to the FL-TrkB receptor [69, 70]. Our work made no distinction in localization so further investigations would be required to elucidate what role, if any, the T-TrkB receptor is playing in the differences observed for the FL-TrkB activation following ethanol exposure.

4.5 Conclusions

The results of the investigation of BDNF-TrkB signaling in WT and BDNF$^{+/-}$ mice following 7 days of DID are interesting and have set a foundation to continue to explore down the signaling pathways to determine molecular mechanisms. From Tables 1 - 4 it is clear that male WT mice undergo more alterations following DID compared to male BDNF$^{+/-}$ mice. Female WT mice undergo similar alterations to their male WT counterparts, while female BDNF$^{+/-}$ mice also undergo similar alterations to the male and female WT mice. Two opposing hypotheses were given above as to what the reductions in BDNF-TrkB signaling following DID could mean. One is that the BDNF neuroprotective role is significantly altered in the WT animals causing 'dependence'; the other is that the reduced BDNF-TrkB signaling is a positive in that it serves to limit synaptic plasticity following ethanol to reduce reinforcement. Despite the changes observed, there are many more questions generated by these data. Future directions include determining the mechanisms for increased TrkB receptor protein expression, what down-regulations in BDNF-TrkB signaling mean for synaptic plasticity, and what alterations are occurring to BDNF and its receptor in other brain regions that input to the striatum. Also requiring further investigation are the signaling cascades downstream of TrkB and how gender may determine differences in the alterations following DID. Finally, the evidence that an "addicted" brain is created in the WT animals needs to be investigated further with behavioral studies to determine the phenotype of mice after 7 days of DID in order to better interpret what the molecular changes observed mean.

CHAPTER 5

Characterization of the Nucleus Accumbens Dopamine System in Adenylyl Cyclase 1 & 8 Double Knockout Mice

In collaboration with Dr. Alana Conti, Department of Neurosurgery, Wayne State University.

5.1 Introduction

Adenylyl cyclase (AC) is an enzyme responsible for catalyzing the conversion of adenosine triphosphate (ATP) to cyclic adenosine monophosphate (cAMP), an important second messenger involved in synaptic plasticity, learning, memory, and substance abuse, to name a few [10]. AC can be indirectly modulated by ethanol through its actions on other neurotransmitter systems [52]. Ethanol can also have direct action on AC signal transduction for which different AC isoforms show differential sensitivities [52]. Additionally, cAMP signaling has been implicated in regulating the stimulating and sedating properties of ethanol [78-80]. There are ten known ACs, eight of them activated primarily via sub-units of G-protein coupled receptors while the other two, AC1 and AC8, are stimulated by calcium via calmodulin signaling [10, 52, 80]. Mice lacking the AC1, AC8, or both isoforms have different sensitivities to the effects of ethanol [78-80]. Understanding how these molecular components respond to ethanol and cause these altered sensitivities will be important to the development of therapies in the treatment of alcohol use disorders.

Behaviorally, AC1 and AC8 double knock-out (DKO) mice exhibit differences in consumption and sensitivity to ethanol [80]. Using a two-bottle choice assay, Maas *et al*. observed that DKO mice consumed less ethanol than wild type (WT) littermates specifically at

higher concentrations of ethanol [80]. Additionally, they confirmed that these changes were not due to differences in caloric requirements or baseline taste differences [80]. In the same study using the loss of righting reflex (LORR) test, it was also observed that DKO animals were more sensitive to the sedative effects of ethanol [80]. The righting reflex refers to the animal's reflex to correct the body's orientation. In this test, the animal is laid on its back after sedation from a high dose of ethanol and the time required for the animal to regain consciousness and flip itself over is assessed. At higher doses of ethanol, DKO animals were sedated almost twice as long as the WT [80]. Using a lower dose of ethanol, it has been reported by Conti *et al.* that, while WT animals have increased locomotor activity following a 1 g/kg dose of ethanol, DKO animals show no change from baseline locomotor activity [79]. When a dose of 2 g/kg was given, DKO animals did show increased locomotor activity, however it was blunted compared to WT animals [79]. The same dose of 2 g/kg ethanol was also used by Mass *et al*. to study the ataxic effects of ethanol; in which DKO animals were not more sensitive [80]. These studies suggest that at the lower (2 g/kg) dose of ethanol, DKO and WT animals have different sensitivities to ethanol with relation to ethanol stimulation of locomotor movement, but motor coordination is not different [79, 80]. Together, these behavioral and consumption data illustrate that AC1 and AC8 play an important role in the physiological response to ethanol and that role differs depending on the ethanol dose. In this study, neurochemical investigations were carried out to identify potential mechanisms of AC1 and AC8's modulation of ethanol sensitivities.

Assessments of the role of AC1 and AC8 have elucidated a potential function for these isoforms in a homeostatic mechanism in response to ethanol exposure and neuronal inhibition [78, 80]. Ethanol exposure elicits phosphorylation of protein kinase A (PKA) targets. This phosphorylation has been compromised in DKO animals [80]. The AC1 and AC8 dependent changes in PKA phosphorylation are brain region dependent, suggesting that different brain

regions are responsible for the sedative versus ataxic response to ethanol and explaining why enhanced sensitivity is only observed with sedation [80]. AC1 and AC8 dependent cAMP/PKA signaling are important for regulating presynaptic activity through the modulation of exocytotic machinery [78]. Phosphoproteomic techniques used by Conti *et al.* have shown phosphorylation of several proteins involved in vesicular release after ethanol exposure in WT mice that was attenuated in DKO mice [78]. The reduced phosphorylation of these proteins would all contribute to a reduction in exocytotic release. These studies suggest that AC1 and AC8 are involved in a homeostatic response to the inhibitory effects of ethanol on neurotransmission.

Given the aforementioned roles of ACs in mediating ethanol sensitivity as well as the role of cAMP in learning and memory, the goal of this study was to understand if there are also changes in the reward center of the brain in the DKO animals. The ventral striatum (recall from Chapter 1, Figure 1.2), also referred to as the Nucleus Accumbens (NAc), is the reward center of the brain, and is a dopamine (DA) rich region. Considering the established differences in sensitivity to ethanol, it is important to understand if these changes translate to the DA system of DKO animals, as well as how these changes may correlate with changes in behavior. Using the technique of microdialysis to investigate the NAc of these animals, initial experiments sought to determine if there were inherent differences in the DA system between the wild-type (WT) and DKO mice. Subsequent experiments served to probe differences in the presence of ethanol. Finally, an experiment to investigate stimulant drug response in DKO animals was also carried out based on unpublished locomotor activity experiments using methamphetamine (METH).

5.2 Methods

The characterization of the DA response in DKO mice was performed using microdialysis. This method has been described in detail previously (Chapter 2, Section **2.4**), thus this section will only highlight deviations from the previously described methods.

5.2.1 Animals

WT and DKO animals were bred in Dr. Alana Conti's lab (WT x WT and DKO x DKO); WT animals were originally purchased from The Jackson Laboratory (Bar Harbor, ME). DKO animals were offspring of homozygous mutants with a constitutive deletion of both AC1 and AC8. Mice were housed in groups of 4-5 with food and water available *ad libitum*. Animals were maintained on a 12 hour light/dark cycle (0600 lights on) and were between about 4-6 months of age. Animal care and use was in accordance with the National Institutes of Health Animal Care guidelines and approved by the Wayne State University Institutional Animal Care and Use Committee.

5.2.2 Surgery

Investigation of the NAc of AC1&8 DKO animals was performed using microdialysis with sample analysis by HPLC coupled with electrochemical detection. Surgeries were performed as described earlier (Chapter 2, ***2.4.2***), although different coordinates were used to target the NAc. Initial coordinates from the Paxinos and Franklin mouse atlas were (ML +0.75, AP +1.50, DV -3.75) [54]. After several surgeries and histological verification of probe placement, coordinates were optimized to (ML +0.70, AP +2.40, DV -3.60) for the mice used in this study (Figure 5.1). Additionally a smaller dialysis probe (1 mm in length, 240 µm diameter) was used for these experiments, due to the reduced size of the NAc compared to the caudate putamen (CPu)

(Figure 5.1). The brain slice in Figure 5.1 indicates the larger size of the CPu, and this region gets even larger moving to more posterior positions in the brain.

*(For more detailed methods used for histological verification please see Chapter 2, Section **2.5**)*

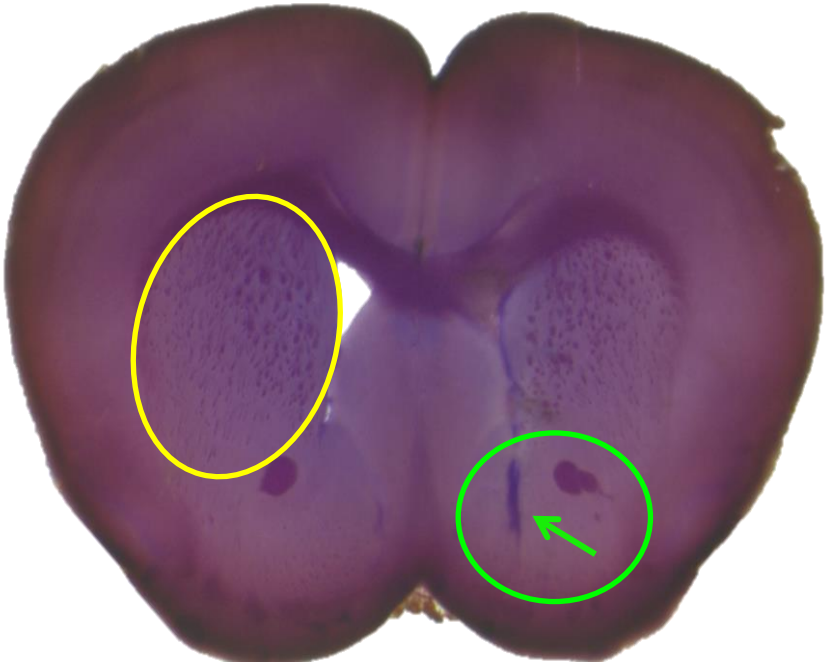

Figure 5.1 A representative brain slice (150 µm) from a microdialysis animal, fixed in formalin and stained with cresyl violet. The green circle indicates the approximate region of the NAc and the dark purple line (green arrow) within that circle is where the probe was for this particular animal. Additionally the yellow circle is indicating the CPu as an illustration of the size difference between the two brain regions.

5.2.3 Microdialysis

In microdialysis the recovery of analytes is affected by the flow rate of the perfusate, with lower flow rates allowing for more analyte recovery [50]. The 1.1 µL/min flow rate traditionally used did provide suitable DA recovery with the smaller probe, thus the flow rate was reduced to 0.8 µL/min. As before, one hour of 20 minute baseline collections were taken

followed by i.p. administration of either ethanol (1 or 2 g/kg) or 5 mg/kg METH. Subsequent 20 minute fractions collected for 1-3 hours after drug were then normalized to baseline values with baseline set at 100%. The zero net flux method was also used to determine 'true' extracellular DA levels (Chapter 2, Section 2.4.3, [50, 55, 56]). For this experiment, there were some changes made to the previous method due to the differences in brain region and experimental challenges with the smaller probe size required for the NAc. Recall that baseline samples were collected followed by perfusion of 3 different DA concentrations meant to bracket the concentration of extracellular levels. Previously each DA concentration was perfused for 1.5 hours, however with the slower flow rate this did not provide enough time for the proper equilibration of the different concentrations of DA to be perfused through. Therefore, each concentration was perfused for one hour and forty minutes (6 fractions) so that each concentration of DA essentially had 2 equilibration samples collected and then 3 samples suitable for quantification. The concentrations of 5, 10 and 20 nM DA proved to be too high as they were all above the extracellular DA levels, so the concentrations were reduced to 2.5, 5, and 10 nM DA. Apart from the changes in perfusion times and DA concentrations used, the experiment was the same as previously described (Section 2.4.3). *In vitro* calibration was performed to determine the concentration of perfused DA (DA_{in}). A plot was constructed of the difference of DA_{in} and the recovered DA (DA_{out}) from the animal, versus the DA_{in}; the x-intercept of the linear regression of these points was indicative of the extracellular DA concentration DA_{ext}. The slope of the regression line was also used to analyze *in vivo* DA recovery and is referred to as the extraction fraction (E_d).

5.2.4 Sample Analysis

Due to the reduced flow rate, only 16 µL of dialysate were collected for each sample. Analysis of a lower sample volume then required optimization of the HPLC method. Initially, a smaller 10 µL loop on the HPLC was used and overfilled. The DA signal was quite low with this method, so an alternative was to add 5 µL of a stabilizing solution, containing 0.2 M perchloric acid, 0.2 µM ascorbic acid, and 0.2 µM EDTA to the sample, bringing the total sample volume to 21 µL, which could then be injected using a 20 µL sample loop [81]. The latter method was preferred based on the resultant improved intensity of the DA peak. Data analysis was completed as before using SPSS and the expectation maximization method to model missing values so that an appropriate repeated measures design could be used for statistical testing (chapter 2, section 8). The Greenhouse-Geisser correction was used in cases where sphericity was violated.

5.3 Results

5.3.1 Extracellular DA Levels in the NAc Determined by Quantitative Microdialysis Were Not Different for WT and DKO Mice

Zero net flux microdialysis was used to determine if there were differences in basal DA levels in the NAc of DKO animals as compared to WT. From Figure 5.2A of the recovered DA (DA_{in} – DA_{out}) versus the DA_{in} plot, it is apparent that the regression lines lie close to one another. In order to statistically compare the extracellular DA concentrations (DA_{ext}, x-intercept) and the slopes of the lines, bar graphs were generated for each (Figure 5.2B and 5.2C respectively). The average extracellular DA concentrations were 3.3 ± 1.6 nM for WT (n = 7) and 2.8 ± 1.2 nM for DKO animals (n = 8), which were not statistically significant as determined by independent t-test ($t(12) = 0.549$, $p = 0.593$). The slopes of the curves provide *in vivo* DA

recovery and indicate DA turnover rate, which signify DA transporter function [50]. The slopes of the zero net flux curves for WT (0.28 ± 0.05) and DKO (0.28 ± 0.04) mice were not different ($t(12) = 0.015$, $p = 0.988$).

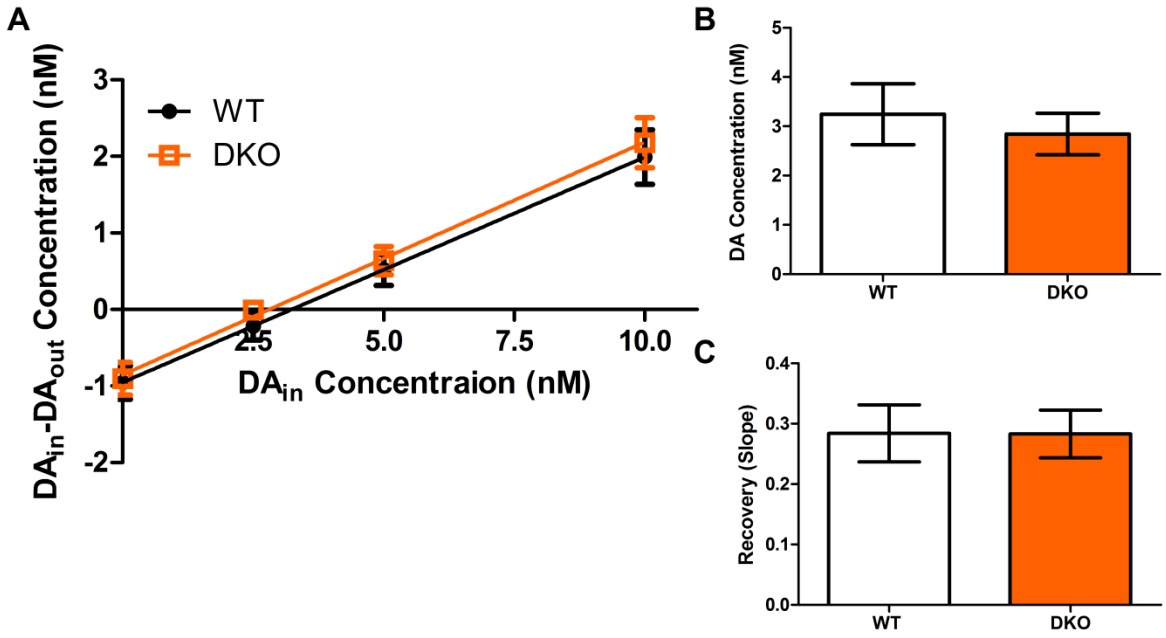

Figure 5.2 Comparison of baseline DA levels and DA recovery in WT and DKO mice (n = 7-8/group) using the method of zero net flux. **A)** Regression lines of DA recovered versus perfused DA in the zero net flux experiment. **B)** Summary of the x-intercept values which indicate extracellular DA concentrations and are not different for WT and DKO mice ($p = 0.593$). **C)** Slopes from lines in **A,** which are not different ($p = 0.988$). Data used to construct these plots can be found in Table A.11 of the appendix.

5.3.2 Dose Dependent Differences in Response to Ethanol: DKO versus WT Controls

Mice were challenged with two different doses of ethanol, both of which are locomotor activating as evidenced by Conti *et al*. [79]. One hour of baseline collections (20 minute fractions) were completed before 1 g/kg ethanol was given systemically. DA levels were subsequently monitored for an additional 100 minutes following injection. One-way repeated measures ANOVA with the Greenhouse-Geisser correction showed no difference within-subjects

effect of time (p = 0.07), although DA levels do appear to be reduced 40 minutes after 1 g/kg ethanol challenge (Figure 5.3A). There was also no within-subjects interaction of time x genotype (p = 0.890), nor a between-subjects effect of genotype (p = 0.760). Observations for the higher 2 g/kg dose of ethanol were quite different compared to the 1 g/kg dose. Approximately 20 minutes after the 2 g/kg ethanol challenge, DA levels in WT mice increased to about 50% greater than baseline whereas the DKO animals, similar to the 1 g/kg dose experiment, showed no difference in DA levels. Interestingly, in DKO animals approximately 80 minutes after ethanol injection a slight reduction in DA levels was observed (Figure 5.3). There was no within-subjects effect of time (p = 0.161) observed for the 2 g/kg ethanol challenge and no interaction of time x genotype (p = 0.093). There was however a significant between-subjects effect of genotype ($F(1, 12) = 6.24$, $p < 0.05$), demonstrating that the genotypes responded differently to ethanol.

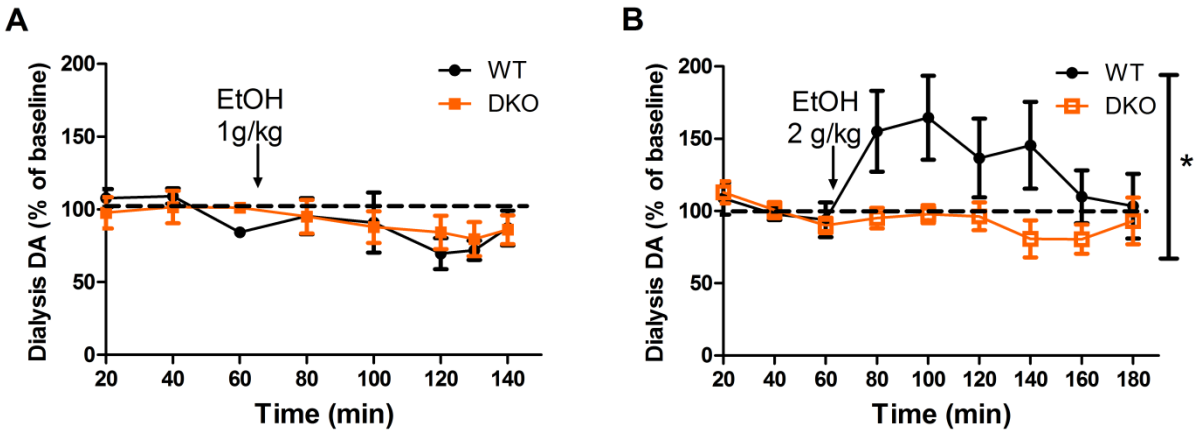

Figure 5.3 DA response to ethanol challenge reported as percent of baseline (n = 5-7 / group) **A)** After 1 g/kg ethanol challenge was not different genotypically different (p = 0.161). **B)** Percent of DA levels after 2 g/kg ethanol challenge, where there was an increase in percent DA in WT animals, while there was no difference in DKO animals (*, $p < 0.05$). Data used to make these plots is outlined in Table A.12 of the appendix.

5.3.3 DKO and WT Show Similar Stimulation Profiles Following a Systemic 5 mg/kg Dose of METH

Unpublished observations personally communicated from Dr. Alana Conti's lab reveal that DKO animals have been observed to have lower METH-stimulated locomotor activity compared to their WT counterparts. Given these differences and that striatal DA neurotransmission is important in motor behavior the DA response to a 5 mg/kg METH i.p. challenge was assessed in the NAc of these mice. The baseline normalized DA response to METH over time in WT and DKO mice appear to be similar (Figure 5.4A). Repeated measures one-way ANOVA with the Greenhouse-Geisser correction showed a significant within-subjects effect of time ($F(1.36, 18.967) = 18.49$, $p < 0.001$) but no interaction of genotype x time ($p = 0.598$). There was also no between-subjects effect of genotype observed ($p = 0.560$). Analyzing the data and the curves, it appears that the extracellular DA levels in DKO animals do not return to baseline as they do in WT animals. From 240 – 300 minutes of collection time, the DA levels of DKOs remain slightly elevated. Due to this observation, an area under the curve analysis of the baseline-corrected data was done and summarized as a bar graph (Figure 5.4B). DKO animals appear to exhibit a larger average area under the curve (230000 ± 53000 arbitrary units) compared to WT littermates (140000 ± 37000 arbitrary units); however, due to large SEMs, this trend is not statistically significant ($p = 0.188$).

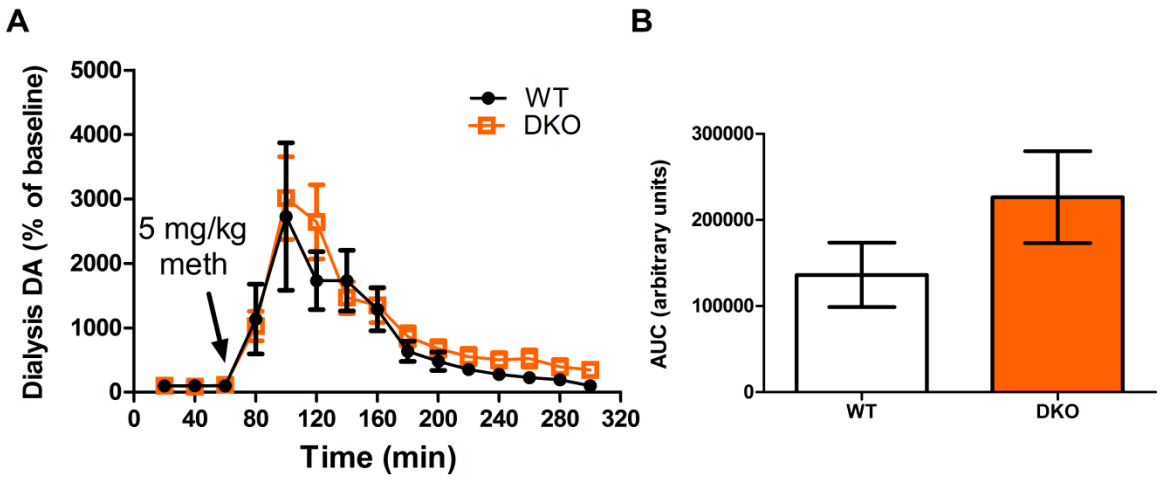

Figure 5.4 DA response to a locomotor activating dose of 5 mg/kg METH reported as percent of baseline (n = 8/group). **A)** Time course of percent DA changes following METH; results were not different between genotypes (p = 0.560). **B)** Summary of area under the curve analysis with plots from **A** where DKOs have a higher average AUC; this average is not statistically significant (p = 0.188). Data to construct these plots can be found in Table A.13 of the appendix.

5.4 Discussion

5.4.1 DKO Animals Display Normal DA Function in the NAc

Before investigating the effect of ethanol on the NAc DA system in DKO animals, it was important to first understand if there were any differences in their naïve DA system. The quantitative microdialysis method of zero net flux showed that DKO mice have similar extracellular DA levels as WT littermates. Additionally, characterization of stimulated DA release and investigation of transporter function carried out using the technique of fast scan cyclic voltammetry in brain slices from DKO and WT mice showed no genotypic differences (*personal communication with Dr. Madiha Khalid*). DA neurotransmission is important in mediating movement and previous work has shown that DKO animals are more active in baseline locomotor activity than their WT littermates [79]. Although presynaptic DA activity does not

always translate directly to locomotor behavior, one may expect to see some changes in DA given the observed behavioral differences. Microdialysis experiments only provide presynaptic information therefore the behavioral changes observed despite the apparently normal functioning DA system suggest that there are changes downstream from DA responsible for those locomotor alterations.

5.4.2 Dose Dependent and Genotypic Differences Observed in the NAc DA System in Response to Ethanol Challenge

At the lower-dose of ethanol administered (1 g/kg), the DA system of WT and DKO animals responded similarly, with no difference in DA levels compared to baseline. However at the higher dose of ethanol (2 g/kg) genotypic differences were observed. Normally a dose of 2 g/kg ethanol elicits an increase in DA in the striatum [34, 35], which was also observed in our study with WT, mice but not with DKO mice. In a study by Conti *et al.,* locomotor behavior was monitored following an ethanol challenge of the same dose (2 g/kg) where DKO mice did exhibit increased activity following ethanol but it was blunted compared to WT mice [79]. The differences in ethanol induced locomotor output are likely due to combined effects of alterations in other systems in the DKO animals and the observed difference in pre-synaptic DA release.

Taking what is known about the proposed role of the AC1 and AC8 in a homeostatic response to ethanol, the alterations in phosphorylation after ethanol that have been observed in the cortex could be important in mediating these different DA responses. After ethanol exposure phosphorylation of several exocytotic proteins is increased in the cortex to promote neuronal activity and this cortical phosphorylation is reduced in DKOs [78]. The circuitry connecting the NAc and the cortex involve the excitatory amino acid glutamate neurons (see

Figure 1.5) which can stimulate DA neurotransmission. The inhibition of glutamate neurons in the cortex of DKO animals (decreased phosphorylation) could prevent ethanol from stimulating the DA release in the NAc, which is observed in WT animals. These hypotheses would need further investigation due to the fact there is limited knowledge on the DA system of the DKO mice and the fact that the investigations of molecular changes in DKOs were carried out using a dose of ethanol that is much higher (4 g/kg) [78, 80]. Additionally, reports of AC expression and activity in the striatum are scarce and do not discriminate between pre- or post-synaptic localization [82, 83]. There is potential for a more direct relationship between AC1 and AC8 in the mediation of the presynaptic DA terminals response to ethanol being analyzed here. The blunted phosphorylation of exocytotic machinery discussed earlier could be also be occurring in the NAc in response to ethanol, which would explain the lack of DA release in the DKO animals.

5.4.3 DAergic METH-Stimulation is Similar in WT and DKO Animals.

Investigation of AC1 and AC8 in the literature has primarily focused on their roles in response to ethanol exposure due to the enhanced sensitivity to sedating doses of ethanol [78, 80]. There is also potential that these isoforms of AC are important in mediating effects of other substances of abuse, such as psychostimulants (like cocaine or amphetamines). Additionally, cAMP second messenger signaling pathways are important in long-term memory formation, which has implications in the propagation of addiction [83]. DiRocco *et al.* investigated the role of AC1 and AC8 in cocaine-sensitization using single knockout animals of each isoform, and DKO animals [83]. Acute administration of cocaine produced increased locomotor activation in DKO animals over their WT counterparts [83]. Acute cocaine also produced enhanced PKA phosphorylation in the striatum of WT but not DKO animals [83]. Further experiments suggested

that these AC isoforms are important for ERK activation, which leads to long-term neuroadaptations [83].

The characterization of DKO animals in response to METH has provided information opposite to that observed with cocaine. DKO animals have a blunted locomotor stimulation compared to WT littermates when METH is administered acutely *(personal communication with Dr. Conti)*. METH and cocaine both produce large extracellular concentrations of DA through slightly different actions involving the DA transporter; it is interesting that there is decreased locomotor activity in DKOs with one drug (METH) and increased activity with the other (cocaine), compared to WT mice. Cocaine blocks the DA transporter, leading to an increase in extracellular DA levels since the DA transporter is the primary clearance method for DA [5]. METH acts as a DA transporter substrate, vesicular monoamine transporter (VMAT) substrate, monoamine oxidase (MAO) inhibitor, and tyrosine hydroxylase (TH) activator, all of which lead to large amounts of DA in the synapse as well [5]. Given the similar pre-synaptic action of METH and cocaine to robustly stimulate DA, the opposing observations for the two drugs would suggest complex molecular interactions for AC1 and AC8 to regulate the behavioral responses differently.

In order to understand the differences in locomotor stimulation following acute METH, microdialysis was used to determine if there were differences in DA release in DKO animals. About 40 minutes after METH (5 mg/kg) injection, DA levels in WT and DKO animals were increased to a peak of about 2800% over baseline, with no difference between genotypes. The probe placement of these animals was analyzed in order to confirm that METH response variability was not a result of regional differences. The majority of probes were located in both of the NAc subregions of the core and shell together (Figure 5.5). Several of the higher

responding mice had their probes more posterior (Figure 5.5, bregma 1.10mm) than others however they were still in the NAc so they were not excluded. The similar DA release in WT and DKO mice following METH, with a difference in locomotor activation, indicates that there are downstream (possibly post-synaptic) alterations that change the behavioral response to METH in these animals. The inconsistencies with the similar pre-synaptic acting drugs cocaine and METH to produce large extracellular concentrations of DA, supports the importance of the cAMP second messenger signaling and the multitude of downstream systems it can act on. As mentioned in the DiRocco *et al.* paper, in which they examined one particular downstream pathway of AC1 and AC8 and noticed alterations. It is likely that despite the two drugs' similar pre-synaptic result on DA, their behavioral response is mediated in different ways by downstream effects of AC1 and AC8 promoted cAMP signaling [83].

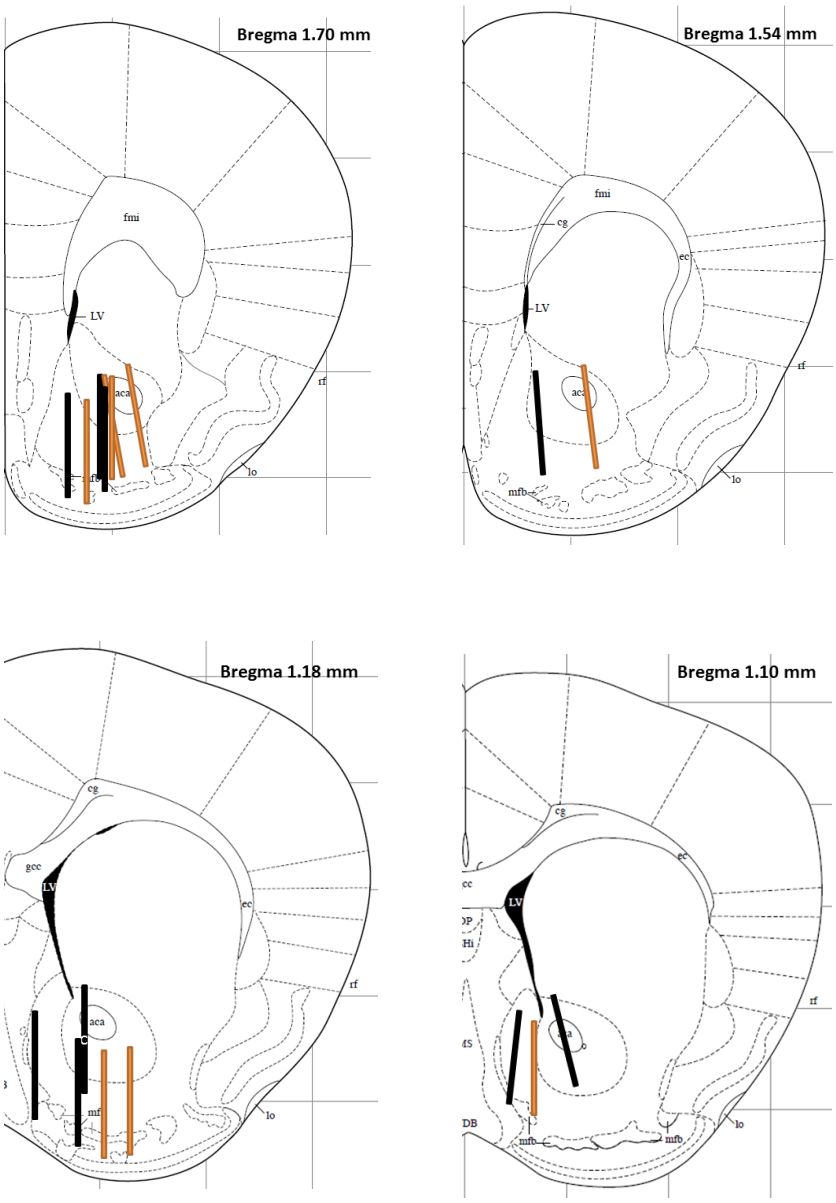

Figure 5.5 Adapted brain atlas images showing the microdialysis probe placement for mice that were given METH injections, with WT mice indicated in black and DKO mice in orange [54]. Slices vary in their anterior/posterior distance from bregma as indicated in the upper right-hand corner of each brain.

5.5 Conclusions

Analysis of the DA system using microdialysis is advantageous in that measurements are strictly pre-synaptic in the brain region of interest and they occur in an intact *in vivo* system which can simplify interpretations. Challenges arise when comparing microdialysis data to behavioral data and tissue studies, where post and pre-synaptic alterations aren't always distinguished. The DA system of DKO animals on a basal level (with no drug) appears to function normally, evidenced in the zero net flux and fast scan cyclic voltammetry studies. In experiments assessing pre-synaptic DA release, DKO animals were only affected differently from WT mice by the 2 g/kg dose of ethanol. Genotypic differences were not observed for the 1 g/kg ethanol dose (DA levels did not change after ethanol for both genotypes) or 5 mg/kg METH (both genotypes had similar increases in DA). In all conditions (no drug, ethanol, or METH) assessed, differences have been observed in DKO animals' behavioral response determined by locomotor activity (personal communication with Dr. Conti, [79]). The inconsistencies in DA response and locomotor behavior suggest important roles for these AC isoforms (1 and 8) post-synaptically and downstream from the DA nerve terminals of the NAc. The studies of downstream phosphorylation targets of cAMP signaling carried out in DKO animals with cocaine and ethanol support the post-synaptic role of cAMP signaling [78, 83], essentially showing that the AC1 and AC8 isoforms are crucial to the behavioral responses to these drugs and that seemingly different cAMP pathways are activated depending on the drug. Therefore, to fully understand the AC1 and AC8 roles, detailed molecular studies need to be carried out in relation to each specific drug. Finally, it would also be useful to determine a point in cAMP signaling that is important for mediating the different behavioral responses for the stimulants cocaine and METH, which both cause increased extracellular DA levels but with different behavioral outputs.

CHAPTER 6

Conclusions and Future Directions

The different investigations herein share the common overarching goal of understanding the effects of ethanol on the brain in order to aid in the development of therapies for those individuals struggling with alcohol use disorders. The complexity of understanding ethanol's action on the brain is indeed great, given the vast number of neural networks it acts on to produce neural adaptations [52]. Further complicating the ability to understand ethanol is the confounding factors of genetic and environmental influences that are associated with alcohol abuse and dependence.

6.1 Relating BDNF-TrkB Signaling Measures to Microdialysis Characterization of Ethanol Stimulation

Examining only male WT mice, recall that 24 hours after 7 days of DID, reduced BDNF-TrkB signaling (represented in Figure 6.1) was observed. An ethanol challenge administered at a corresponding time, showed that there was no longer an increase in DA levels, as previously observed under naïve conditions. Together, the reduced BDNF-TrkB signaling and DA tolerance to ethanol could suggest that reduced BDNF levels may indicate a reduction of input from the excitatory glutamatergic neurons of the cortex to the striatum and that this absence renders ethanol unable to elicit DA release. However, this hypothesis is challenged however when considering $BDNF^{+/-}$ mice, since they also show a similar tolerance to ethanol stimulation of DA without reduced BDNF-TrkB function after DID (compared to naïve $BDNF^{+/-}$). Taken together, findings from the BDNF-TrkB signaling and ethanol challenge experiments, summarized in Figure 6.1, would suggest that BDNF-TrkB alterations following repeated ethanol exposure are either

not responsible for the loss of ethanol-induced stimulation of DA or the downstream signaling of BDNFs action through TrkB is processed differently in the two genotypes.

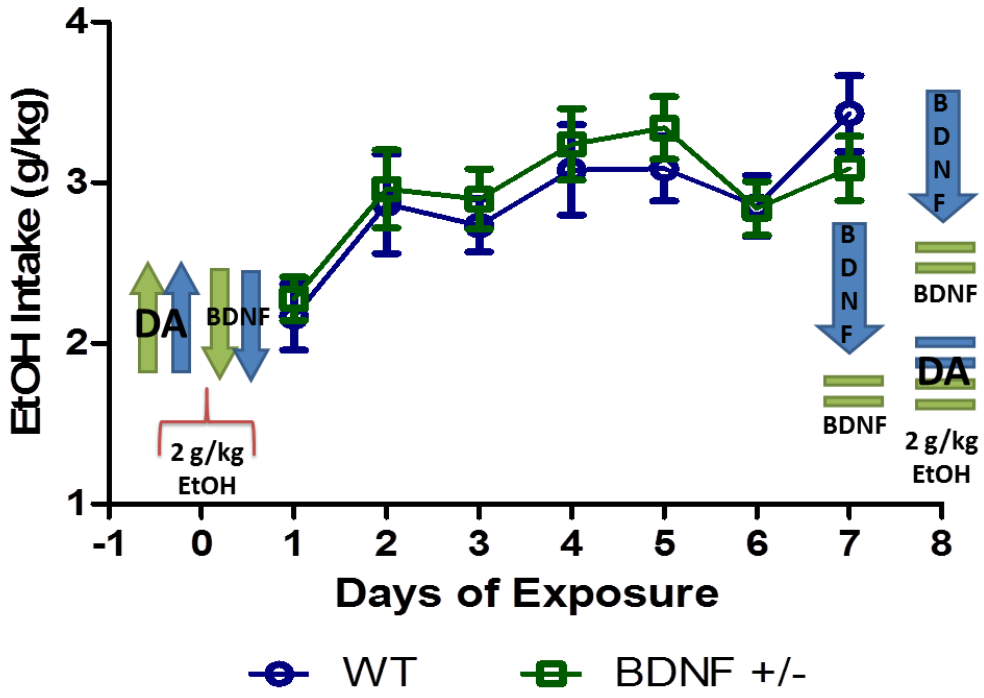

Figure 6.1 Seven day DID drinking data with a summary of the neurochemical measures made prior to and after DID exposure. Day 0 represents observations in naïve animals from the current study and previous findings with WT shown in blue and BNDF$^{+/-}$ mice in green [29]. The notations of increases, decreases, or equal levels are compared to control levels for non-treated mice of the same genotype.

6.2 Consideration of the DID Model

Acute reductions in BDNF levels have been observed 45 minutes after 2 g/kg systemic ethanol challenge, in both WT and BDNF$^{+/-}$ mice [29]. Together, the acute observations (from previous studies) and the reduced BDNF levels observed here in WT animals after repeated ethanol exposure, an initial hypothesis is that after the initial DID session BDNF levels are reduced in WT animals and the reduction persists over the course of the 7 days of DID. BDNF

levels in BDNF$^{+/-}$ mice are probably reduced after the initial DID session (based on an acute study by Bosse *et al*., [29]), but at some point during the 7 days of DID they appear to be compensated for and return to naive BDNF$^{+/-}$ mice levels. The reduction in BDNF-TrkB signaling in the WT animals could be responsible for the increase in consumption observed from day 1 to day 7. However, when considering BDNF$^{+/-}$ animals, it is interesting to note that they also increase ethanol consumption from day 1 to day 7, but without further reduction in BDNF-TrkB signaling. There is seemingly conflicting data between WT and BDNF$^{+/-}$ mice, where consumption is similar at day 7, but BDNF-TrkB signaling is attenuated in WT mice only (as compared to their own controls). It is possibile that the drinking model used is producing an addictive/dependent phenotype in the WT mice. If the BDNF neuroprotective pathway has been disrupted, then the WT brains could be more representative of an ethanol dependent brain. The reduced BDNF-TrkB levels in WT with enhanced consumption would further support the importance of BDNF's protective role in the onset of alcohol dependence. However, if 7 days of DID is creating this phenotype in WT mice, then we are comparing the BDNF$^{+/-}$ mice to a control group that we have caused dysfunction in, making this model less suited for our determination of the effect of low endogenous BDNF levels on susceptibility to alcohol dependence.

The potential recovery of BDNF to baseline levels (in reference to the genotype) over repeated exposures could also be interpreted as evidence of enhanced ethanol preference in our model which has been observed previously [26, 28]. The ability of BDNF levels to return to control levels in BDNF$^{+/-}$ mice during continued ethanol exposure may point to increased synaptic plasticity promoting ethanol reinforcement, as compared to WT mice who have attenuated BDNF-TrkB signaling after 7 days of DID. If the binge consumption is in fact causing deterioration of the BDNF homeostatic mechanism in WT mice, than exposure past 7 days could lead to a point where BDNF levels return to control while still having enhanced consumption,

similar to the observations in the BDNF$^{+/-}$ mice (Figure 6.2). If this deterioration of the BDN homeostatic mechanism were true, then it would suggest that changes in BDNF-TrkB signaling observed in both genotypes are indicative of addiction/dependence formation caused by the DID model. The restoration of BDNF-TrkB signaling to control during continued exposure to ethanol could be an important indicator that dependence forming neuroadaptations have occurred. It is possible that this dependence occurs very quickly in the BDNF$^{+/-}$ mice, and since no measurements were made earlier than 7 days we did not observe this. This hypothesis could be tested in the future by taking similar measures at an intermediate time point during the 7 days of DID and by extending the length of exposure to see if BDNF levels return to normal with continued exposure in WT mice; a suggested scheme is diagrammed in Figure 6.2. If this hypothesis is true, then expected outcome would be to that BDNF levels in WT mice would return to control levels even with repeated ethanol exposure, similar to the BDNF$^{+/-}$ mice (Figure 6.2). Furthermore, if we define our criteria for dependence as having normal BDNF and TrkB levels with continued ethanol exposure, it would be of value to test how long after ethanol cessation a single re-exposure to ethanol could again reduce BDNF levels. The length of cessation before BDNF levels can be reduced again could be interesting given the implications of BDNF's role in relapse [84]. A potential outcome for the cessation experiments (proposed in Figure 6.2) would be that after several days, re-exposure using DID would have WT mice essentially starting over as naïve animals, while BDNF$^{+/-}$ mice still experience enhanced consumption and no changes in BDNF after ethanol exposure. Preliminary data (*n* =1/genotype, Figure 6.3) collected for the development of a relapse drinking model, where a BDNF$^{+/-}$ mouse have enhanced consumption when ethanol was reinstated after 3 days off from DID. No concrete conclusions can be made from this observation due to the single *n*-value but the difference does warrant additional investigation. Furthermore, continued reinstatement may

indicate that the hypothesized return to normal function of BDNF-signaling (normal levels of BDNF and TrkB without ethanol) in WT animals is disrupted again, given the increase across the 4 days of re-exposure (Figure 6.3B).

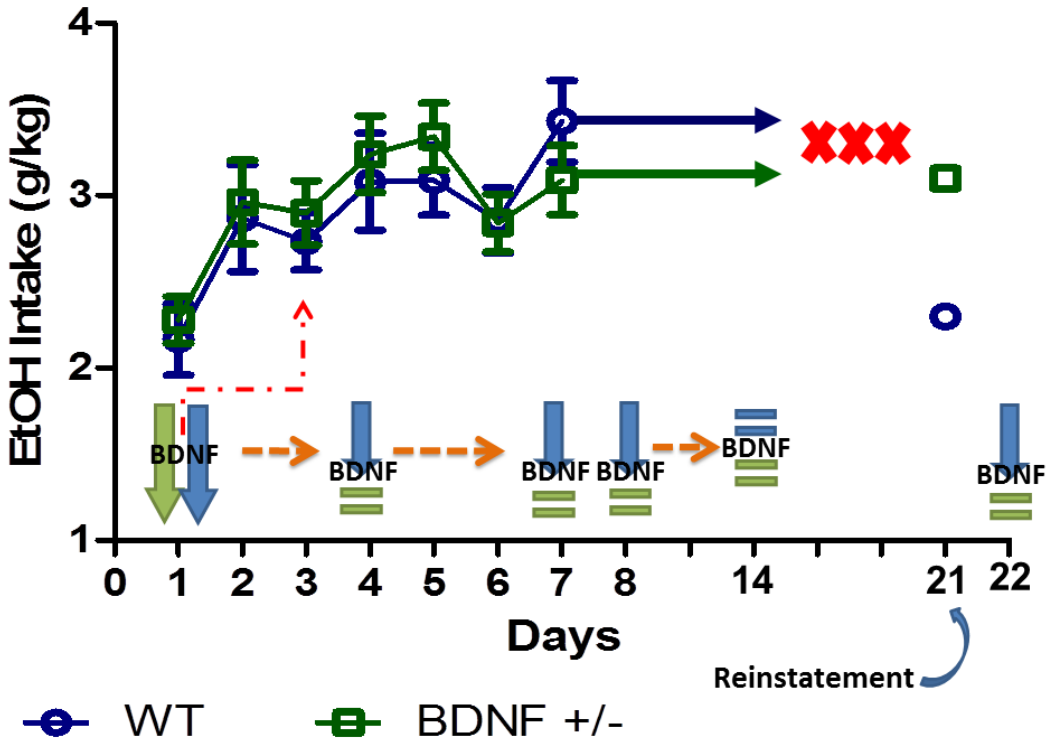

Figure 6.2 A schematic of proposed alterations to BDNF levels during different time points of DID exposure and after reinstatement following several days of no drinking. Representations of BDNF levels are in reference to control levels for the genotype, with the blue indicating WT changes and the green depicting $BDNF^{+/-}$ changes.

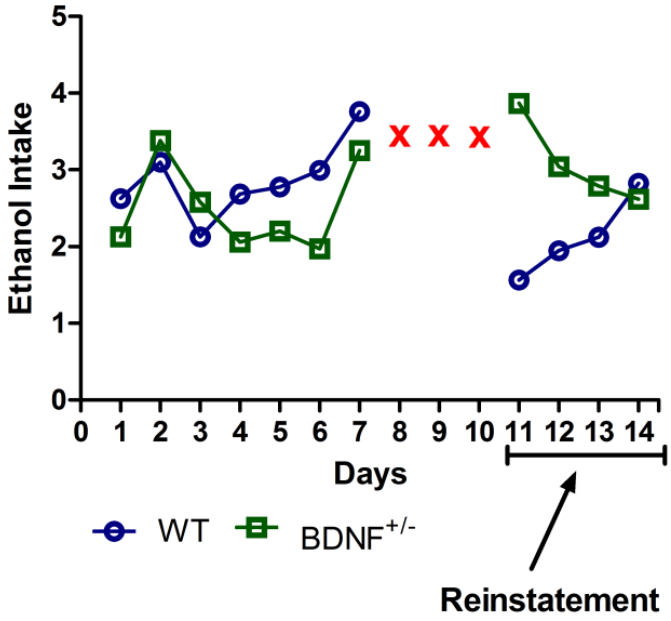

Figure 6.3. Pilot results of drinking data over 7 days (g/kg) followed by 3 days with no exposure (red x's) and initial reinstatement on day 11 followed by 3 subsequent DID sessions (*n* = 1 / group). Data for this experiment can be found in Table A.14 of the appendix.

6.3 Adenylyl Cyclase Involvement in DID Induced Tolerance to Ethanol Stimulation

Investigations using adenylyl cyclase 1 and 8 (AC1 & AC8) double knock-out (DKO) animals clearly illustrated the importance of AC1 and AC8 in ethanol stimulation of DA release (Chapter 5, Figure 5.3). While there are several possible explanations for the lack of DA response to ethanol after 7 days of DID in WT and BDNF$^{+/-}$ mice, the evidence of the roles of AC1 and AC8 in ethanol stimulated DA release makes AC an attractive target. The DKO studies were carried out in the NAc and therefore, to test this hypothesis, trends would need verification in the CPu. In addition it would also be interesting to assess the AC activity in the CPu of WT and BDNF$^{+/-}$ DID mice and see if there is a significant loss of AC function, which could explain the inability of ethanol to release DA after 7 days of DID (Chapter 3, Figure 3.2). Although it was previously suggested that BDNF-TrkB signaling was not involved in the observed ethanol tolerance, it could

in fact be mediating reduced AC1 & 8 activity via regulation of gene-transcription. However, the caveat of $BDNF^{+/-}$ mice having 'normal' BDNF-TrkB signaling and DA tolerance remains. If BDNF-signaling is responsible for alterations in AC function following DID through altered transcription of molecules that target AC, then this would suggest that BDNF-TrkB signaling may function differently in $BDNF^{+/-}$ mice compared to WT mice, something that has yet to be assessed in this mouse model. Alternatively, there may be inherent differences in AC1 & 8 function in WT and $BDNF^{+/-}$ mice. Previous experiments using microdialysis to assess ethanol-stimulated DA release in these mice showed blunted release in $BDNF^{+/-}$ mice as compared to WT [29]. This divergence was not observed in our study, potentially due to diurnal variation; it is postulated that the decreased neuronal tone during the dark cycle masked this genotypic difference [61, 62]. If AC1 & 8 function is reduced in $BDNF^{+/-}$ mice, then it may be that, despite BDNF-signaling restoration by the 7^{th} day of DID, AC function is not restored.

6.4 One Day DID Illustrates the Importance of Assessing Other Time Points Besides 7 days of DID

For the DID studies, the duration of ethanol exposure was 7 days, followed by microdialysis or tissue studies. Following the weeklong consumption, there were several interesting neuroadaptations observed, such as DA tolerance or reduced BDNF-TrkB signaling. However the time frame in which these striatal changes occur and whether or not they persist is unknown. It is also unknown whether these neuronal changes occurred after 1 day and remained consistent over the course of the exposure or if a gradual transition to these alterations occurred instead. Also, many of the striatal neuroadaptations were observed 24 hours after the last ethanol exposure, which leaves us asking how long before they return to normal, if ever. The importance of assessing at least one intermediate time point is evidenced

by preliminary microdialysis data that were collected 24 hours after one DID session in WT and BDNF$^{+/-}$ mice to assess their DA levels following an ethanol challenge (Figure 6.40). WT and BDNF$^{+/-}$ mice show similar responses to a 2 g/kg ethanol challenge under control or 7 day DID conditions, however the responses after only one drinking session are vastly different: BDNF$^{+/-}$ mice (Figure 6.4A) show attenuation in DA levels whereas WT mice (Figure 6.4B) show no difference (both compared to the response in control animals). Considering the aforementioned hypothesis that the BDNF$^{+/-}$ and WT mice undergo similar alterations with the DID procedure but that changes occur more rapidly in the BDNF$^{+/-}$ mice, this latest observation would be interesting to investigate further. Similarly if there is a role for AC in mediating the DA tolerance to ethanol stimulation, the tolerance at 1 day of DID in BDNF$^{+/-}$ mice could indicate that they have lower AC function and are more susceptible to alterations following ethanol exposure. Although these data were collected for only 2 mice for each genotype, it does highlight the importance of looking at other time points prior to the full 7 day exposure.

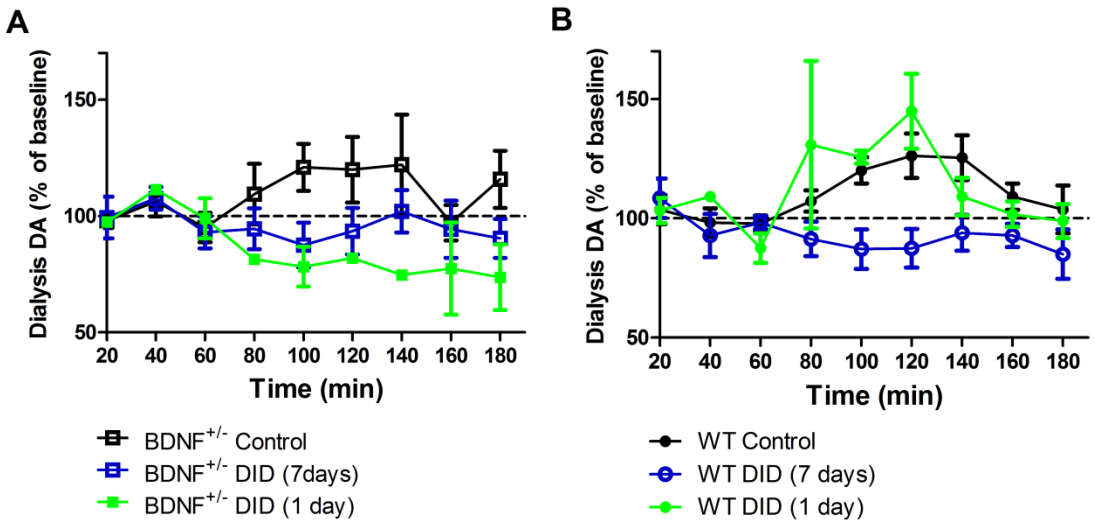

Figure 6.4 Dopamine response to a 2g/kg ethanol challenge in naïve and 7 day DID mice as previously reported (Chapter 3, Figure 3.2), with the addition of 1 day DID mice (n=2) for both **A**) BDNF$^{+/-}$ and **B**) WT mice. Data for the 1 day DID experiment can be found in Table A.15 of appendix.

6.5 General conclusions

Considering the discussion above regarding the BDNF$^{+/-}$ and DKO animals, several mechanistic proposals for further investigation can be suggested with regard to DA tolerance to ethanol-stimulation, the ramifications of altered BDNF levels and TrkB activation, and potential evidence of the DID model promoting an ethanol dependent animal. It is hypothesized that the DID model is producing an ethanol dependent animal in both WT and BDNF$^{+/-}$ mice, with the latter being affected much earlier in treatment. It is thought that initially, ethanol consumption causes attenuations in BDNF that lead to increased consumption in both genotypes and a potentially long-lasting reduction in function of AC1 & 8 in the BDNF$^{+/-}$ mice. Eventually, over the course of repeated exposure, the BDNF-signaling for BDNF$^{+/-}$ mice returns to normal for the genotype, but it is hypothesized that AC function is still reduced based on the continued tolerance to ethanol induced stimulation of DA. In the WT animals BDNF-signaling continues to be reduced with repeated exposure eventually leading to a hypothesized attenuation in AC activity similar to the BDNF$^{+/-}$ mice. The hypothesized decreases of AC1 & 8 are plausible given the DA tolerance to ethanol stimulation after 7 days DID and the divergence in response after 1 day of DID between the two genotypes. Finally, the alterations in BDNF-TrkB signaling in WT mice, with further investigation, could provide evidence that the DID model produces rapid induction of a dependent phenotype. Furthermore, the recovery of BDNF-TrkB signaling in the BDNF$^{+/-}$ animals should be investigated in terms of the long-term ramifications and what this recovery means behaviorally.

The findings presented here illustrate that there is still more to be understood about how different neural networks process and respond to ethanol and, conversely, how different exposure amounts and lengths are able to cause varying alterations in the brain. Continued

investigations into how alcohol is changing the brain and how different exposure methods have different effects will be important in understanding the human condition. No two alcoholics become addicted in the same fashion, nor did they have the same drinking patterns, as such there is no best practice for the animal models used to study alcohol abuse. Developments of models that better capture the human condition are strived for and for each new model developed, there is potential for different neuronal adaptations to be observed.

APPENDIX

This appendix provides the raw data used to make the plots throughout the dissertation and the blots used to make the histograms in Chapter 4.

Table A.1 Daily ethanol consumption (g/kg) for WT and BDNF$^{+/-}$ mice used in the first DID study described in Chapter 3. These data were used to create the graphs in Figure 3.1.

Day 1	Day 2	Day 3	Day 4	Day 5	Day 6	Day 7	Genotype
1.73	2.23	2.30	2.17	2.39	3.06	2.76	WT
3.05	2.17	3.78	3.48	3.53	2.74	3.43	
3.52	3.30	2.90	4.48	3.44	3.82	4.37	
2.07	3.13	2.28	3.20	2.62	2.27	3.67	
2.34	1.19	2.72	3.08	3.59	2.01	3.69	
1.61	2.88	2.33	2.09	2.53	2.82	2.65	
2.00	1.92	2.52	3.40	3.38	3.81	2.80	
2.41	2.08	2.70	3.26	2.64	3.37	3.00	
2.59	3.59	2.41	1.91	2.95	2.24	3.77	
0.63	2.87	4.03	3.93	4.47	2.77	4.34	
2.40	3.08	3.11	3.94	4.14	3.08	5.17	
2.46	3.02	1.96	4.11	2.55	3.53	2.84	
1.35	5.85	2.51	0.98	1.94	1.62	2.11	
1.80	3.02	3.09	2.55	3.11	3.15	3.19	BDNF$^{+/-}$
2.57	3.40	3.29	2.89	2.68	2.30	3.83	
1.67	2.50	2.61	3.43	4.00	3.15	3.45	
3.17	4.43	3.37	2.30	2.92	2.28	3.80	
1.89	2.22	2.36	2.11	3.42	1.95	2.15	
2.44	3.46	2.66	3.45	3.64	3.28	2.58	
1.85	2.76	3.23	3.83	3.99	3.30	3.35	
3.22	2.32	2.95	3.21	2.99	2.23	2.77	
2.07	1.81	2.81	3.65	3.12	3.24	4.35	
2.05	2.96	3.36	4.36	3.79	3.34	3.62	
2.48	3.41	3.61	4.15	4.10	3.94	2.72	
2.17	4.47	3.32	4.15	4.02	2.32	2.20	
2.26	1.74	1.00	2.04	1.65	2.46	2.14	

Table A.2 Uncorrected DA levels (in nM) over time used to create the baseline normalized plots from the ethanol challenge experiments in Figure 3.2 of Chapter 3 for WT and BDNF$^{+/-}$ mice.

20 min	40 min	60 min	80 min	100 min	120 min	140 min	160 min	180 min	Group
2.1	2.9	3.3	3.3	3.6	2.5	2.8	2.9	2.8	WT Control
	3.4	2.9	2.1	2.2	1.9	1.9	2.0	2.0	
1.1	1.1	0.9	0.8	1.6	1.3	1.2	1.0	0.7	
1.1	1.9	1.7	1.8	1.7	2.1	2.3	2.4	2.5	
	0.7	0.6	0.4	0.3	0.3		0.8	0.6	
4.8	3.9	3.8	4.4	4.4	5.2	5.6	4.2		
4.8	4.2	4.7	4.7	5.8	6.0	5.5	5.2	5.1	
4.2	4.5	3.9	4.4	4.4	4.5	4.8	5.0	5.6	
3.0	3.1	3.4	3.4	3.7	3.3	3.4	3.2	3.8	
4.9	5.0	5.2	5.8	6.2	6.0	5.5	5.3	5.7	
4.7	4.7	3.2	3.3	4.0	3.8	4.3	4.3	4.2	
	0.4	0.8	1.0		1.0	0.7	0.7	0.3	
0.4		0.4	0.5	0.4	0.8	0.8	0.4	0.3	
2.6	2.5	2.4	2.8	3.8	4.0	3.9	3.5	3.1	
0.7	0.2	0.5	0.3	0.3	0.3	0.4	0.3		WT DID
1.1	1.1		1.2	1.1	1.0	1.3	1.0		
2.3	3.7		2.5	1.7	1.6	1.8	3.2	1.5	
3.1	3.0	2.8	2.9		2.9	3.2	2.8	2.7	
1.7	1.2	1.4	1.2	1.3	1.5	1.2	1.4	1.1	
1.5	1.3	1.5	1.6	1.3	1.4	1.4	1.4	1.3	
1.4	1.4	1.2		1.5	1.4	1.4	1.3	1.5	
	4.4	4.7	4.9	5.0	5.3	5.3	5.0	4.6	BDNF$^{+/-}$ Control
2.3	2.1	2.4	4.7	3.9	4.8	6.2	3.2	3.0	
3.5	*3.8*	*4.0*	*4.2*	*2.2*	*2.6*	*2.1*	*2.5*	*2.3*	
2.4	2.8	2.2	2.5	2.4	2.7	2.6	2.7	2.8	
3.4	3.1	2.8	2.9	3.9	3.2	2.8	3.0	3.1	
4.7	6.2	5.5	4.4	4.4	5.9	4.6	4.4	5.3	
1.9	1.9	1.9	2.5	1.9	2.0	1.9	1.8	1.7	
	0.7	0.2	0.5	0.8		*0.2*	0.3	1.0	
4.3	4.6	4.9	4.9	5.7	5.7	5.4	4.8	5.3	
3.8	3.8	4.0	4.2	4.5	4.5	4.0	3.9	4.3	
	1.7	2.0	1.3	1.8	1.3	1.6	1.3	1.3	
1.2		2.2	2.4	1.9	2.5	2.0	2.9	1.7	BDNF$^{+/-}$ DID
4.4	6.0	4.3	4.4	5.1	5.0	5.9	4.9	4.6	
15.7	8.0	6.6	9.7		9.8	13.5	10.5	9.6	
1.3	1.4	1.0	0.9	1.0	0.9	1.0	1.0		
2.5	2.8	2.7	2.8	2.4	2.8	3.1	2.6	2.4	
2.4	2.5	2.7	2.4		2.7	2.7	2.3	2.1	
	3.9	3.0	2.1	1.6	1.5	1.5	1.2	1.7	
2.0	2.5			2.1	1.8	1.9	1.7	1.7	
1.2	1.6	1.2	1.3		1.1	1.5	1.2	1.8	

Table A.3 Uncorrected DA levels (in nM) over time used to create the baseline normalized plots from the 3 mg/kg METH challenge experiments in Figure 3.3 of Chapter 3 for WT and BDNF$^{+/-}$ mice.

20 min	40 min	60 min	80 min	100 min	120 min	140 min	160 min	180 min	200 min	220 min	240 min	Group
4.6	4.4	4.7	31.9	38.7	37.0	31.0	24.9	19.8	16.3			WT Control
1.9	1.9	1.5		2.8	2.0	2.2	1.6	1.3		1.1	2.5	
1.6	1.3	1.3		5.0	4.5	3.3	2.1	1.9	2.2	1.9	1.9	
0.4	0.6	0.6		7.8	5.3	2.8	2.1	0.6				
1.9	1.7	1.1	9.7	19.4		16.9	11.0	11.7	8.7	6.0	3.9	
1.2	1.4	1.2	10.5	27.1	7.9	4.1	2.3	1.6	0.2	0.2	0.1	
1.7	1.7	1.6	12.5	15.6	12.8	11.7	8.1	7.3	5.5	3.6	2.9	
1.0	1.3		15.3	29.8	24.1	16.9	12.8	11.5	10.4	8.9	7.1	
1.4	0.9		14.8		22.1	16.7	10.4	8.4	10.7	5.7	6.6	
0.4	1.1	1.2		17.2	10.7		5.6	5.4	4.3	3.1	2.0	
	0.7	0.5	3.7	30.3	24.5	19.9	11.5	11.6	7.1	6.7	5.3	
1.4	2.4	1.0	20.5	27.6	24.0	19.8	15.9	12.9	9.8	5.9	3.7	
3.5	3.7	3.3	12.1	21.1	13.5	10.0	5.8	6.6	5.3	4.6	4.1	
4.1	2.2	1.6	32.0	36.2	33.5	26.2	15.8	9.3	12.2	7.9	6.4	WT DID
	1.2	3.3	17.2	36.6	30.9	32.7	19.6	15.1	12.4	12.0	10.7	
1.7	3.2	2.7	29.1	54.8	37.6	31.0	23.7	12.2			4.9	
1.4	1.0		5.3	17.0	12.2	9.4	8.2	7.3	7.0	4.8	4.7	
1.5	1.1	1.0	19.4	42.0	38.2	33.4	22.4	20.6	17.5	19.7	13.2	
3.7	2.8	2.7	6.3	15.0	10.2	8.7	6.9	6.0	4.6	3.2	2.8	
2.4	2.4	2.4	17.8	19.8	13.5	12.2	9.7	6.7	5.9	4.5	3.5	BDNF$^{+/-}$ Control
2.7	2.0	0.7	58.9	88.4	60.6	38.3	40.5	28.4	10.7	21.2	18.0	
0.8		1.3	0.6	2.5	3.6	5.0	2.4	2.3	1.3	1.0	1.1	
0.3	1.0	0.8	3.8	3.8	4.3	3.1	3.0	1.7	1.2	1.3	0.9	
4.4	3.3	3.6	10.0	11.4	11.4	9.8	9.2	7.0	7.1	7.8	7.3	
4.3	4.6	2.4	11.8	21.2	18.2	11.8	10.6	9.4	9.0	9.2	6.8	
3.0	3.1	2.2		19.8	10.7	10.2	9.7	6.8	2.9	3.2	2.1	
1.6	1.6	2.0	10.7	17.4	17.6	15.7	11.8	9.2	7.8	5.8	4.3	BDNF$^{+/-}$ DID
12.6	11.1	10.5	16.6	20.1	16.4	15.7	14.4	11.8	9.8	9.5	9.4	
1.4	1.2	1.1	5.3	9.9	7.3	5.0	3.8	2.7	2.2	1.3	1.4	
3.7	3.7	3.6		65.7	48.3	28.5	24.3	16.2	12.3	9.2	8.1	
2.3	2.3	2.2	20.1	36.3	25.6	23.6	18.5	15.8	11.8	9.3	7.6	
2.1	2.5	2.3	23.4	56.3	48.7	43.3	36.1	28.2	25.0	23.6	18.8	
0.4	0.3	0.3	4.3	5.9	4.6	3.8	3.6	2.8	1.8	1.4	1.3	
15.1	15.5	13.0	17.8	28.0	24.6	28.6	25.0	18.6	16.3	13.5	10.8	
0.8	1.2	1.2	3.6	3.8	3.1	2.5			1.4	0.6		
4.2	2.3	0.9	8.3	15.0	8.9	6.4	4.4	3.0	3.5	2.5	2.7	

Table A.4 DA levels (in nM) calculated for 0, 5, 10, and 20 nM DA from the zero net flux plots. Note these data are not raw data from the experiment but they are the data used to make the plots (this is why there are negative values at 0 nM). The x-intercept and slopes obtained from linear regressions run on those plots. These plots can be found in Figure 3.4 of Chapter 3 for WT and $BDNF^{+/-}$ mice.

0 nM	5 nM	10 nM	20 nM	DA_{ext} (x-intercept)	Slope	Group
-0.7	0.4	1.4	3.4	2.6	0.28	WT Control
-0.7	0.7	2.1	5.0	12.8	0.15	
-1.9	-1.2	-0.4	1.1	12.2	0.30	
-4.8	-2.4	0.0	4.8	7.6	0.43	
-2.4	-1.0	0.4	3.1	8.7	0.28	
-3.3	-1.1	1.0	5.3	10.1	0.48	
-3.7	-2.2	-0.7	2.3	3.2	0.20	
-4.5	-3.0	-1.5	1.5	15.0	0.30	
-5.6	-3.9	-2.3	1.0	11.9	0.32	WT DID
-1.4	-0.1	1.1	3.7	5.5	0.26	
-3.8	-2.2	-0.6	2.6	1.6	0.59	
-0.9	2.0	5.0	10.8	7.6	0.25	
-1.9	-0.7	0.6	3.1	9.3	0.16	
-1.5	-0.7	0.1	1.8	16.9	0.33	
-3.2	-0.5	2.3	7.9	13.0	0.23	$BDNF^{+/-}$ Control
-4.6	-2.7	-0.7	3.1	5.8	0.56	
-1.2	0.6	2.4	3.1	11.9	0.39	
-1.4	0.2	1.9	5.2	3.3	0.36	
-1.5	-0.9	-0.2	1.0	4.3	0.33	
-3.0	-1.8	-0.7	1.6	11.9	0.13	
-1.7	-0.5	0.6	2.8	7.4	0.22	$BDNF^{+/-}$ DID
-1.6	0.0	1.6	4.9	5.0	0.32	
-2.2	-1.1	0.0	2.3	9.8	0.23	
-1.2	-0.4	0.4	2.0	7.7	0.16	
-2.5	0.0	2.5	7.6	4.9	0.50	
-4.8	-3.4	-1.9	1.0	16.7	0.29	

Table A.5 Uncorrected DA levels (in nM) over time used to create the baseline normalized plots from the quinpirole infusion experiments in Figure 3.5 of Chapter 3 for WT and BDNF$^{+/-}$ mice.

20 min	40 min	60 min	80 min	100 min	120 min	140 min	160 min	180 min	200 min	220 min	240 min	Group
2.0	2.0	2.0	2.8	3.3	3.0	2.4	1.7	1.9	1.4		1.0	WT Control
1.6	1.4	1.6	1.3	1.2	1.3	1.4	1.3	1.1	1.0	0.7	0.7	
0.5	0.7	0.7	0.7	0.9		0.8	0.5	0.6	0.6	0.4	0.2	
1.2	0.7	0.9	0.9	1.0	1.1	0.8	1.0	0.6	0.7	0.4	0.2	
1.7	1.2	1.5	1.4	1.3	1.4	1.9	1.2	0.9	0.8	0.6	0.4	
1.1	1.1	0.9	1.5	1.4	1.2					0.8	0.7	
4.8	3.3	2.8	2.4	2.2	2.1	2.2	1.8	1.7	1.4	1.2	1.6	
2.6	1.8	2.7	1.2	1.1	1.5	1.0	0.7	0.6	0.5		1.0	
1.3	1.0	1.3	1.8	1.6	1.5	1.4	0.9	0.8	0.2		0.2	
1.4	2.4	1.0	0.9	1.6	1.2			1.0		0.8	0.6	
1.7	1.6	1.8	1.8	2.0	1.8				1.7	1.6	0.7	
1.6	1.5	1.6	1.8	1.5	1.7	1.7	1.7	1.4	1.3	0.9	0.7	WT DID
1.2	1.4	1.4	1.7	1.8	1.4	1.3	1.1	1.1	2.2	1.0	0.8	
1.3	1.0	1.1	1.0	1.1	1.1	0.8	0.8	0.6	0.6	0.4		
1.5	1.4	1.6	2.4	1.4	0.9	0.7	0.9	0.7	0.6	0.4	0.3	
0.9	1.2		0.8	0.2		0.2	0.7	0.1	-0.1			
1.2	0.5	0.5	0.6	1.3		0.9	0.8	0.4	0.4	0.2	0.2	
1.8	1.6	0.9	0.7	0.9	1.0	0.6	0.7	0.6	0.3	0.4	0.3	
2.1	1.5	2.5	1.8	1.6	1.7	2.2	1.7	1.9	1.7	0.9	0.2	
1.0	1.0	0.9	0.5	0.6	0.8	0.9		1.0	0.8		0.7	
1.8	2.0	1.9	1.9	1.8	2.5	1.4		0.9	0.8	0.8	0.7	BDNF$^{+/-}$ Control
1.9	1.6	1.3	1.5	1.9	1.9	1.7	1.0	1.2	1.0	1.7	1.8	
1.9	0.5	0.9	0.7	1.0	1.0		0.6	0.9		1.0	0.2	
	0.9	0.9	0.4	0.9	0.8	0.7	0.2	0.2	0.3	0.0	0.1	
2.4	2.3	2.1	2.2	2.2	2.3	2.5	2.1	2.0	1.9	1.8	1.9	
1.6	1.6	2.2	1.3	1.4	0.9	0.8	0.5	0.6	0.4	0.4	0.1	
1.1	1.1	1.3	1.1	1.3	1.1	1.0	0.8	0.6	0.6	0.4	0.5	BDNF$^{+/-}$ DID
3.8		4.3	5.1	4.9	4.0	4.4	3.6	3.4	3.5	3.1	2.8	
9.2	8.6	9.7	9.3	8.1	8.9	9.1	9.8	7.8	8.5	5.7	6.1	
0.8	0.6	0.8	0.9	1.0	0.9	0.8	0.7	0.6	0.5	0.3	0.5	
2.9	3.0	3.4	3.2	3.1	3.0	3.1	2.5	2.3	1.8	1.3	1.2	
1.9	2.1	2.7	2.6	2.6	2.8		2.1	2.1	1.5	1.1	0.7	
2.1	2.1	2.1	2.3	2.3	3.5	3.5	2.3	1.8	1.8	1.1	1.2	
11.1	14.7	12.2	14.6	11.7	13.1	13.1	12.5	12.7	10.8	8.4	9.7	
1.1	1.1	0.6	1.2	0.8		1.1	0.8	0.7		1.6	1.2	
1.5	1.7	1.1	1.4	1.2	1.1	1.5	0.9	1.2	0.9	0.4	0.7	
1.7	1.4	1.4	1.8	2.1	1.4	0.8	0.8	1.0	1.2	1.3	1.4	

Table A.6 Daily ethanol consumption (g/kg) for MALE WT and BDNF$^{+/-}$ mice used in the second DID study described in Chapter 4. These data were used to create the graphs in Figure 4.1.

Day 1	Day 2	Day 3	Day 4	Day 5	Day 6	Day 7	Genotype
1.47	2.38	2.04	2.54	2.31	2.36	3.59	
2.78	2.32	1.46	1.86	1.72	2.59	2.73	
2.34	3.06	2.58	1.86	1.89	2.78	4.14	
1.53	2.21	2.21	0.66	1.86	1.78	2.78	
3.27	3.25	1.86	2.08	2.89	3.56	3.23	
3.23	1.08		2.79	2.84	2.52	2.83	
2.26	1.87	1.76	1.86	2.3	4.51		WT
2.2	1.69	3.12	2.07		3.5	2.44	
3.9	2.68	2.82	4.05	5.15	3.06	2.64	
2.73	2.71	2.92	2.71	3.66	2.71	2.83	
3.14	2.64	3.89	1.39	2.02	2.67	3.12	
1.59	1.31	2.5	1.8	2.79	3.25	2.04	
2.23	2.46	2.8	3.45	3.48	4.29	3.13	
0.35	2.03	2.45	1.2	2.3	1.94	3	
2.07	1.81	2.81	3.65	3.12	3.24	4.35	
1.83	1.59	1.73	1.23	1.5	1.7	1.78	
2.15	2.94	1.3	1.57	2.22	2.1	1.8	
0.84	1.21	1.82	2.3	1.23	1.42	1.16	
1.26	1	1.6	1.97	1.69	3.21	2.26	
1.15	1.6	2.31	2.18	1.64	3.48	2.52	BDNF$^{+/-}$
1.32	3.47	3.3	2.76	2.55	2.92	2.14	
2.18	2.57	2.35	2.92	2.83	2.19	2.09	
2.87	2.49	2.05	2.38	2.7	3.51	3.12	
2.83	2.93	3.3	4.97	3.35	2.97	3.26	
1.44	1.91	1.32	1.44	4.07	1.57	2.73	
1.39	2.4	2.81	3.37	2.48	3.48	2.78	

Table A.7 Daily ethanol consumption (g/kg) for FEMALE WT and BDNF$^{+/-}$ mice used in the second DID study described in Chapter 4. These data were used to create the graphs in Figure 4.1.

Day 1	Day 2	Day 3	Day 4	Day 5	Day 6	Day 7	Genotype
4.02	2.68	3.96	4.97	4.44	4.55	2.84	WT
3.56	1.73	2.32	2.75	3.02	3.1	1.99	
3.91	3.21	2.56	3.26	2.93	4.07	1.79	
2.63	2.9	2.98	3.37	2.18	2.95	4.09	
3.46	3.96	2.37	4.63	2.08	4.5	3.76	
2.23	3.2	3.46	3.07	2.75	2.98	3.35	
2.55	1.78	2.33	4.28	3.19	4.87	4.77	
3.75	3.79	4.42	3.52	4.44	3.71	4.36	
3.48	3.04	4.09	3.43	3.2	2.42	3.53	
4.3	2.25	4.08	2.68	2.37	3.36	4.18	
			2.68	3.15	3.43	3.51	BDNF$^{+/-}$
2.92	1.59	3.28	3.12	3.72	3.06	4.28	
3.77			3.13	4.27	2.89	3.93	
1.72	2.11	2.2	2.68	3.69	1.7		
2.15	3.61	3.52	3.11	2.73	2.7	4.1	
3.58	2.3	3	2.79	2.89	2.56	2.64	
1.18	2.64	2.57	2.62	2.86	2.3	1.93	
1.87	3.53	3.75	3.14	3.22	3.64	2.69	
4.04	2.83	1.83	3.77	2.33	2.73	3.85	

Table A.8 BDNF levels (ng/mg ww) used to make the raw data plots and the normalized data plots in Figure 4.2 of Chapter 4.

Male			Female		
BDNF (ng/mL ww)	**Genotype**	**Group**	**BDNF (ng/mL ww)**	**Genotype**	**Group**
20.6	WT	Control	42.8	WT	control
30.37			15.46		
24.3			11.2		
56.6			11.32		
15.15					
29.76	WT	30 min	24.3	WT	30 min
13.64			18.03		
9.44			7.87		
12.02	WT	24 hour	19.38	WT	24 hour
8.8			8.82		
30.06					
17.57					
8.95					
11.63					
7.29	$BDNF^{+/-}$	Control	6.92	$BDNF^{+/-}$	Control
7.41			9.04		
12.33			9.06		
12.89			8.97		
6.45			10.86		
4.76					
4.77					
4.72					
8.1	$BDNF^{+/-}$	30 min	4.73	$BDNF^{+/-}$	30 min
6.49			3.9		
4.8			5.47		
5.6					
5.44	$BDNF^{+/-}$	24 hour	0.06	$BDNF^{+/-}$	24 hour
7.28			1.31		
11.17					
8.86					
3.99					

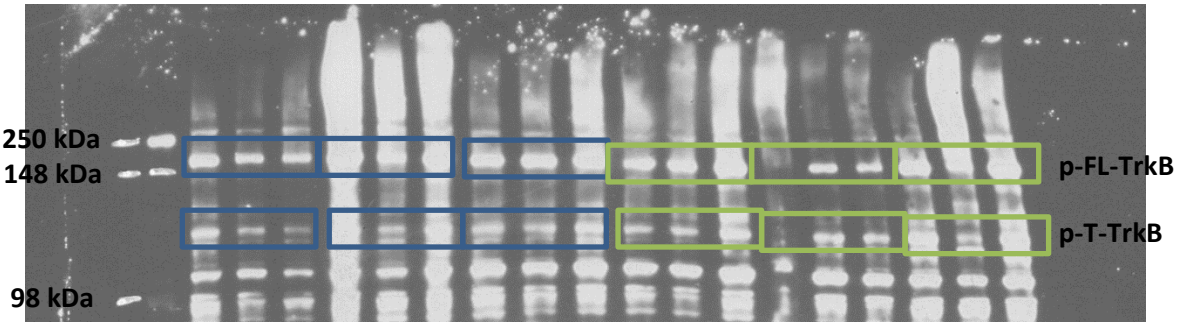

Figure A.1 Inversion of the film from the male blot for the phosphorylated receptor (p-FL-TrkB and p-T-TrkB). From left to right the blue boxes indicate WT: control, 30 min and 24 hours; the green boxes indicate $BDNF^{+/-}$: control, 30 min, and 24 hour. Figures 4.3 and 4.4 in Chapter 4.

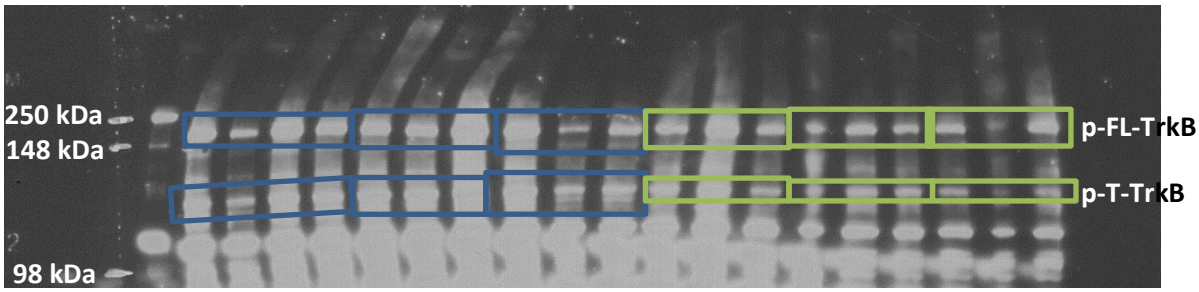

Figure A.2 Inversion of the film from the female blot for the phosphorylated receptor (p-FL-TrkB and p-T-TrkB). From left to right the blue boxes indicate WT: control, 30 min and 24 hours; the green boxes indicate $BDNF^{+/-}$: control, 30 min, and 24 hour. Figures 4.5 and 4.6 in Chapter 4.

Figure A.3 Image of blot for the total TrkB levels (FL-TrkB and T-TrkB) in male mice. From left to right the blue boxes indicate WT: control, 30 min and 24 hours; the green boxes indicate $BDNF^{+/-}$: control, 30 min, and 24 hour. Figures 4.3 and 4.4 in Chapter 4.

Figure A.4 Image of blot for the total TrkB levels (FL-TrkB and T-TrkB) in female mice. From left to right the blue boxes indicate WT: control, 30 min and 24 hours; the green boxes indicate BDNF$^{+/-}$: control, 30 min, and 24 hour. Figures 4.5 and 4.6 in Chapter 4.

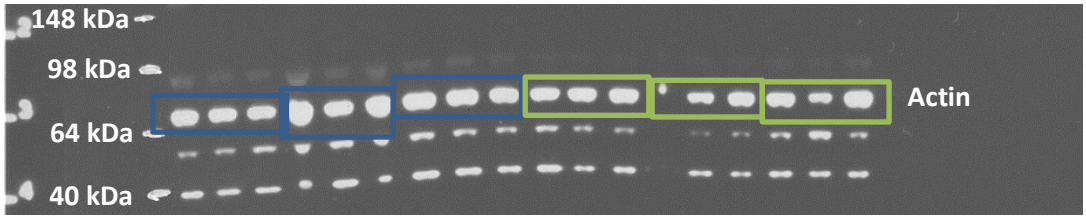

Figure A.5 Image of blot for the actin loading control for male mice. From left to right the blue boxes indicate WT: control, 30 min and 24 hours; the green boxes indicate BDNF$^{+/-}$: control, 30 min, and 24 hour. Figures 4.3 and 4.4 in Chapter 4.

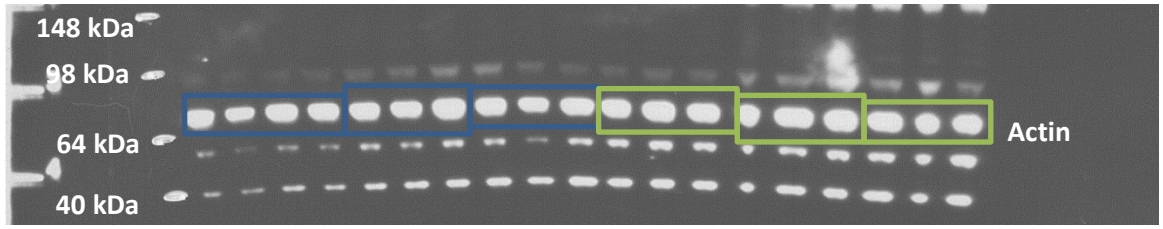

Figure A.6 Image of blot for the actin loading control for female mice. From left to right the blue boxes indicate WT: control, 30 min and 24 hours; the green boxes indicate BDNF$^{+/-}$: control, 30 min, and 24 hour. Figures 4.5 and 4.6 in Chapter 4.

Table A.9 Values obtained from the western blot for male mice, used to create the histograms in figures 4.3 and 4.4 in Chapter 4.

p-FL-TrkB	p-T-TrkB	FL-TrkB	T-TrkB	Actin	Genotype	Group
53.973	49.877	38.254	59.905	45.988	WT	Control
44.151	26.624	31.254	60.622	42.66		
50.684	15.183	21.223	74.693	40.561		
24.308	11.253	118.493	160.113	63.774	WT	30 min
48.368	18.448	35.43	135.03	47.107		
26.279	17.975	66.9	129.935	56.035		
59.716	47.298	52.708	125.817	61.246	WT	24 hour
62.686	37.9	56.408	112.816	55.807		
60.826	38.219	67.661	103.899	47.216		
46.1	13.228	40.492	72.645	42.457	$BDNF^{+/-}$	Control
55.159	24.537	47.708	61.627	43.533		
43.965	33.637	74.123	63.823	46.985		
6.937	-0.505	57.292	62.462	10.347	$BDNF^{+/-}$	30 min
39.502	57.64	71.092	55.763	31.538		
38.134	43.846	44.516	52.758	41.456		
51.141	53.03	38.408	73.012	43.826	$BDNF^{+/-}$	24 hour
35.104	13.259	25.584	107.598	26.081		
40.927	36.868	73.061	116.213	52.419		

Table A.10 Values obtained from the western blot for female mice, used to create the histograms in figures 4.3 and 4.4 in Chapter 4.

p-FL-TrkB	p-T-TrkB	FL-TrkB	T-TrkB	Actin	Genotype	Group
68.616	70.563	21.222	50.651	53.339	WT	Control
51.161	59.742	19.113	46.426	41.813		
80.565	82.439	26.097	72.421	57.091		
75.932	83.139	32.341	79.057	55.061		
64.392	73.042	43.012	98.313	53.834	WT	30 min
70.427	87.284	41.164	79.133	52.576		
56.601	72.629	46.898	84.584	64.622		
84.174	89.27	56.142	97.349	56.436	WT	24 hour
45.466	74.036	40.097	85.595	46.762		
79.397	89.869	38.92	73.989	58.344		
63.891	70.878	37.841	49.908	58.101	$BDNF^{+/-}$	Control
71.173	75.912	51.881	52.989	62.992		
65.426	62.995	40.977	86.815	61.213		
38.019	36.949	60.113	86.862	46.661	$BDNF^{+/-}$	30 min
72.667	74.918	95.443	137.246	78.224		
49.622	57.216	68.932	119.452	71.494		
63.344	47.591	49.807	120.702	67.268	$BDNF^{+/-}$	24 hour
9.874	1.719	32.954	127.046	46.254		
53.957	30.545	36.443	122.81	56.117		

Table A.11 DA levels (in nM) calculated for 0, 2.5, 5, and 10 nM DA from the zero net flux plots. Note these data are not raw data from the experiment but they are the data used to make the plots (this is why there are negative values at 0 nM). The x-intercept and slopes obtained from linear regressions run on those plots. These plots can be found in Figure 5.2 of Chapter 5 for WT and DKO mice.

0 nM	2.5 nM	5 nM	10 nM	DA_{ext} (x-intercept)	Slope	Genotype
-0.33	0.17	0.68	1.69	1.64	0.17	WT
-0.57	-0.13	0.30	1.17	3.26	0.13	
-1.36	-0.10	1.15	3.67	2.71	0.50	
-0.50	0.25	0.99	2.48	1.66	0.30	
-0.90	-0.05	0.80	2.51	2.65	0.34	
-1.02	-0.47	0.07	1.16	4.68	0.22	
-1.99	-1.18	-0.36	1.27	6.12	0.33	
-1.05	0.07	1.20	3.46	2.33	0.45	DKO
-0.62	0.08	0.79	2.20	2.21	0.28	
-0.46	0.14	0.75	1.97	1.91	0.24	
-0.96	-0.30	0.36	1.68	3.65	0.26	
-1.12	-0.01	1.09	3.31	2.53	0.44	
-0.46	0.30	1.06	2.58	1.52	0.30	
-0.34	-0.09	0.17	0.67	3.35	0.10	
-2.20	-0.26	-0.31	1.58	5.24	0.34	

Table A.12 Uncorrected DA levels (in nM) over time used to create the baseline normalized plots from the ethanol challenge experiments in Figure 5.3 of Chapter 5 for WT and DKO mice. For the 1 g/kg dose a 180 minute fraction was not collected.

20 min	40 min	60 min	80 min	100 min	120 min	140 min	160 min	180 min	Genotype	Dose
0.30	0.39	0.25	0.16	0.13	0.20				WT	1 g/kg
	0.35	0.28	0.34	0.32	0.27	0.16			WT	
0.60	0.45	0.37	0.27	0.41	0.16	0.31	0.27		WT	
1.36	1.47	1.46	2.06	2.91	1.38	0.94	1.36		WT	
2.08	1.50	1.44	1.77	1.45	1.14	1.40	1.18		WT	
0.44	0.46	0.30	0.38	0.30	0.14	0.27	0.51		WT	
0.41	0.55	0.34	0.47	0.19	0.46	0.43	0.37		WT	
0.51	0.32	0.44	0.47	0.46		0.48	0.47		DKO	
0.23	0.45	0.34	0.41	0.20	0.32	0.34	0.30		DKO	
1.26	1.82		0.95	1.20	1.30	1.05	0.98		DKO	
1.60	1.76		1.24	1.29	0.88	1.01	1.08		DKO	
0.28	0.18	0.23	0.25	0.27	0.24	0.13	0.24		DKO	
0.77	0.66	0.76	0.83	0.92	0.81	0.59	0.43	0.52	WT	2 g/kg
0.86	1.01	0.67	0.70	2.14	1.63	1.30	1.06	1.43	WT	
0.35	0.24	0.14	0.29	0.16		0.19	0.19		WT	
	0.49	0.47	0.53	0.58			0.38		WT	
0.13	0.10		0.12	0.16	0.06	0.17			WT	
0.12	0.08	0.03	0.20	0.21	0.18	0.21	0.10	0.07	WT	
0.16	0.19	0.26	0.32	0.37	0.27	0.30			WT	
0.76	0.74	0.88	2.09	0.46	0.72	0.53	1.27	0.63	WT	
2.13	1.55	1.44	2.01	1.85	2.40	2.04	1.60	2.07	DKO	
0.52	0.51	0.66	0.49	0.45	0.59	0.48	0.47	0.51	DKO	
	0.58	0.48	0.56	0.59	0.46		0.56	0.43	DKO	
0.44	0.34	0.35	0.42	0.38	0.31	0.38	0.37	0.59	DKO	
0.60	0.40	0.36	0.40	0.35	0.38	0.37	0.38	0.39	DKO	
0.56	0.63	0.54	0.55	0.62	0.46	0.39	0.41	0.58	DKO	
	1.72	1.00	0.82			0.38	0.35	0.23	DKO	

Table A.13 Uncorrected DA levels (in nM) over time used to create the baseline normalized plots from the 5 mg/kg METH challenge experiments in Figure 5.4 of Chapter 5 for WT and DKO mice.

Time	WT								
20 min			0.07	0.20	0.53	1.52		1.23	
40 min	0.73	0.27		0.16		1.28	2.63	1.48	0.60
60 min	0.52	0.34	0.19	0.20	0.74	1.51	2.51	1.13	0.48
80 min	5.55	2.22	0.63	1.55	5.11	6.30	6.88	2.99	26.33
100 min	20.55	3.11	13.27	2.78	14.16	14.66	17.64		50.11
120 min	19.22	2.94		4.92	11.43	12.01	14.43	3.67	19.73
140 min	16.22	3.00	7.47	4.28	9.08	9.39		4.00	20.57
160 min	10.68	2.94	3.57	3.80	6.24	8.06		1.31	14.25
180 min	8.08	2.38	2.27	1.08		5.89	5.31	2.22	5.25
200 min	7.60	1.56	1.94	0.89		4.47	3.81	2.05	2.84
220 min	5.18	1.19	1.30	0.84	1.98	3.55	2.79	1.87	1.69
240 min	3.80	1.10	0.87	0.64	1.31	2.46	2.77	1.81	1.42
260 min	3.00	0.61	0.88	0.56	1.27	2.07	2.34	1.31	1.57
280 min	2.47	0.46	0.74	0.64	0.75	2.38		1.00	0.53
300 min		0.36	0.42	0.25		1.62	0.91		0.64
Time	**DKO**								
20 min	0.46	0.44	1.72	0.62	0.31	1.16	0.29	0.82	
40 min	0.36	0.45	1.07	0.50	0.40	1.00	0.10	0.74	
60 min	0.40	0.46	1.15	0.70	0.32		0.98	0.74	
80 min	2.71	0.89	14.65	11.39	5.78	6.12	1.99	12.68	
100 min	14.46	4.78	34.81	33.66	8.57	20.42	5.18	44.33	
120 min	7.56		25.12	31.94	7.19	18.68	5.81	33.55	
140 min	7.65	4.31	15.17		6.15	14.63	2.64	19.54	
160 min	4.46	2.17	14.88	15.76	4.12	10.26		15.25	
180 min	3.24	1.24	9.92	9.30	3.25	7.03		8.41	
200 min	2.10		8.41	7.71	2.63	5.42	0.93	6.45	
220 min	1.61	0.93	7.85	6.70	2.37		0.57	5.70	
240 min	1.34	1.16	8.84	6.58	2.37	3.42	0.31	4.56	
260 min				4.79	2.70	3.60	0.48	4.57	
280 min				3.56	1.96	1.94	0.30	4.39	
300 min				2.82	1.44	2.94	0.42	3.81	

Table A.14 Drinking data in (g/kg) for a pilot study where one WT and BDNF$^{+/-}$ mouse each went through 7 days of DID followed by a 3-day cessation and reinstatement. This data was used to make Figure 6.3 in Chapter 6.

Day	WT	BDNF$^{+/-}$
1	2.63	2.13
2	3.10	3.38
3	2.13	2.58
4	2.69	2.06
5	2.78	2.20
6	2.99	1.97
7	3.76	3.25
8	*X*	*X*
9	*X*	*X*
10	*X*	*X*
11	*1.56*	*3.87*
12	*1.95*	*3.04*
13	*2.12*	*2.79*
14	*2.83*	*2.62*

Table A.15 Baseline corrected DA levels (in %, ([DA]/[average DA])*100) over time used to create the plots from the 2 g/kg ethanol challenge experiments after 1 day of DID in WT and BDNF$^{+/-}$ mice. This data was used in Figure 6.4 of Chapter 6.

20 min	40 min	60 min	80 min	100 min	120 min	140 min	160 min	180 min	Genotype
108.6	110.1	81.3	166.0	128.4	160.7	117.0	107.1	91.7	WT
98.0	108.3	93.7	95.7	122.9	129.3	101.2	96.5	106.1	
97.5	112.0	90.5		86.8	83.3	76.4	97.2	87.9	BDNF$^{+/-}$
	110.9	107.7	81.4	69.8	80.6	73.0	57.7	59.7	

REFERENCES

1. Abuse, N.I.o.D. *Media Guide: How to find what you need to know about drug addiction*. 2014 December 2012 [cited 2014 May 1, 2014]; Available from: http://www.drugabuse.gov/publications/media-guide/science-drug-abuse-addiction.
2. Health, N.I.o., *Drugs, Brains, and Behavior The Science of Addiction*, N.I.o.D. Abuse, Editor 2010. p. 1-36.
3. Berke, J.D. and S.E. Hyman, *Addiction, dopamine, and the molecular mechanisms of memory.* Neuron, 2000. **25**(3): p. 515-32.
4. Administration, S.A.a.M.H.S., *Results from the 2010 National Survey on Drug Use and Health: Summary of National Findings.* NSDUH Series H-41, 2011. **HHS Publication No. (SMA) 11-4658**.
5. Sulzer, D., *How addictive drugs disrupt presynaptic dopamine neurotransmission.* Neuron, 2011. **69**(4): p. 628-49.
6. Administration, S.A.a.M.H.S., *Results from the 2012 National Survey on Drug Use and Health (NSDUH) H-47: Mental Health Findings*, in *National Survey on Drug Use and Health (NSDUH)*2013.
7. United States. National Institute on Alcohol Abuse and Alcoholism, United States. Dept. of Health and Human Services, and United States. Alcohol Drug Abuse and Mental Health Administration, *United States. Alcohol alert*: Rockville, MD.
8. Nestler, E.J., S.E. Hyman, and R.C. Malenka, *Molecular neuropharmacology : a foundation for clinical neuroscience*. 2nd ed2009, New York: McGraw-Hill Medical. xiv, 498 p.
9. Perry, M., Q. Li, and R.T. Kennedy, *Review of recent advances in analytical techniques for the determination of neurotransmitters.* Anal Chim Acta, 2009. **653**(1): p. 1-22.

10. Brady, S.T., et al., *Basic neurochemistry : principles of molecular, cellular, and medical neurobiology*. 8th ed2012, Amsterdam ; Boston: Elsevier/Academic Press. xxiv, 1096 p.

11. Chen, G., et al., *Striatal involvement in human alcoholism and alcohol consumption, and withdrawal in animal models.* Alcohol Clin Exp Res, 2011. **35**(10): p. 1739-48.

12. Gerdeman, G.L., et al., *It could be habit forming: drugs of abuse and striatal synaptic plasticity.* Trends Neurosci, 2003. **26**(4): p. 184-92.

13. Hyman, S.E. and R.C. Malenka, *Addiction and the brain: the neurobiology of compulsion and its persistence.* Nat Rev Neurosci, 2001. **2**(10): p. 695-703.

14. Albin, R.L., A.B. Young, and J.B. Penney, *The functional anatomy of disorders of the basal ganglia.* Trends Neurosci, 1995. **18**(2): p. 63-4.

15. Everitt, B.J. and M.E. Wolf, *Psychomotor stimulant addiction: a neural systems perspective.* J Neurosci, 2002. **22**(9): p. 3312-20.

16. Koob, G.F. and M. Le Moal, *Drug addiction, dysregulation of reward, and allostasis.* Neuropsychopharmacology, 2001. **24**(2): p. 97-129.

17. Ribrault, C., K. Sekimoto, and A. Triller, *From the stochasticity of molecular processes to the variability of synaptic transmission.* Nat Rev Neurosci, 2011. **12**(7): p. 375-87.

18. Sesack, S.R. and A.A. Grace, *Cortico-Basal Ganglia reward network: microcircuitry.* Neuropsychopharmacology, 2010. **35**(1): p. 27-47.

19. Kreitzer, A.C. and R.C. Malenka, *Striatal plasticity and basal ganglia circuit function.* Neuron, 2008. **60**(4): p. 543-54.

20. Moonat, S., et al., *Neuroscience of alcoholism: molecular and cellular mechanisms.* Cell Mol Life Sci, 2010. **67**(1): p. 73-88.

21. Davis, M.I., *Ethanol-BDNF interactions: still more questions than answers.* Pharmacol Ther, 2008. **118**(1): p. 36-57.

22. Goldstein, B.I., et al., *Pharmacotherapy of alcoholism in patients with co-morbid psychiatric disorders.* Drugs, 2006. **66**(9): p. 1229-37.

23. Uhl, G.R., et al., *Polysubstance abuse-vulnerability genes: genome scans for association, using 1,004 subjects and 1,494 single-nucleotide polymorphisms.* Am J Hum Genet, 2001. **69**(6): p. 1290-300.

24. Matsushita, S., et al., *Association study of brain-derived neurotrophic factor gene polymorphism and alcoholism.* Alcohol Clin Exp Res, 2004. **28**(11): p. 1609-12.

25. Joe, K.H., et al., *Decreased plasma brain-derived neurotrophic factor levels in patients with alcohol dependence.* Alcohol Clin Exp Res, 2007. **31**(11): p. 1833-8.

26. McGough, N.N., et al., *RACK1 and brain-derived neurotrophic factor: a homeostatic pathway that regulates alcohol addiction.* J Neurosci, 2004. **24**(46): p. 10542-52.

27. Jeanblanc, J., et al., *The dopamine D3 receptor is part of a homeostatic pathway regulating ethanol consumption.* J Neurosci, 2006. **26**(5): p. 1457-64.

28. Hensler, J.G., E.E. Ladenheim, and W.E. Lyons, *Ethanol consumption and serotonin-1A (5-HT1A) receptor function in heterozygous BDNF (+/-) mice.* J Neurochem, 2003. **85**(5): p. 1139-47.

29. Bosse, K.E. and T.A. Mathews, *Ethanol-induced increases in extracellular dopamine are blunted in brain-derived neurotrophic factor heterozygous mice.* Neurosci Lett, 2011. **489**(3): p. 172-6.

30. Baek, J.K., M.B. Heaton, and D.W. Walker, *Up-regulation of high-affinity neurotrophin receptor, trk B-like protein on western blots of rat cortex after chronic ethanol treatment.* Brain Res Mol Brain Res, 1996. **40**(1): p. 161-4.

31. Blochl, A. and C. Sirrenberg, *Neurotrophins stimulate the release of dopamine from rat mesencephalic neurons via Trk and p75Lntr receptors.* J Biol Chem, 1996. **271**(35): p. 21100-7.

32. Goggi, J., et al., *Modulation of neurotransmitter release induced by brain-derived neurotrophic factor in rat brain striatal slices in vitro.* Brain Res, 2002. **941**(1-2): p. 34-42.

33. Bosse, K.E., et al., *Aberrant striatal dopamine transmitter dynamics in brain-derived neurotrophic factor-deficient mice.* J Neurochem, 2012. **120**(3): p. 385-95.

34. Tang, A., et al., *Ethanol increases extracellular dopamine concentration in the ventral striatum in C57BL/6 mice.* Alcohol Clin Exp Res, 2003. **27**(7): p. 1083-9.

35. Di Chiara, G. and A. Imperato, *Ethanol preferentially stimulates dopamine release in the nucleus accumbens of freely moving rats.* Eur J Pharmacol, 1985. **115**(1): p. 131-2.

36. Volkow, N.D., et al., *Decreases in dopamine receptors but not in dopamine transporters in alcoholics.* Alcohol Clin Exp Res, 1996. **20**(9): p. 1594-8.

37. Volkow, N.D., et al., *Effects of alcohol detoxification on dopamine D2 receptors in alcoholics: a preliminary study.* Psychiatry Res, 2002. **116**(3): p. 163-72.

38. Volkow, N.D., et al., *High levels of dopamine D2 receptors in unaffected members of alcoholic families: possible protective factors.* Arch Gen Psychiatry, 2006. **63**(9): p. 999-1008.

39. Franklin, K.M., et al., *A single, moderate ethanol exposure alters extracellular dopamine levels and dopamine d receptor function in the nucleus accumbens of wistar rats.* Alcohol Clin Exp Res, 2009. **33**(10): p. 1721-30.

40. Bulwa, Z.B., et al., *Increased consumption of ethanol and sugar water in mice lacking the dopamine D2 long receptor.* Alcohol, 2011. **45**(7): p. 631-9.

41. Jacobs, E.H., et al., *Neuroadaptive effects of active versus passive drug administration in addiction research.* Trends Pharmacol Sci, 2003. **24**(11): p. 566-73.

42. Becker, H.C., *Animal models of excessive alcohol consumption in rodents.* Curr Top Behav Neurosci, 2013. **13**: p. 355-77.

43. Rhodes, J.S., et al., *Evaluation of a simple model of ethanol drinking to intoxication in C57BL/6J mice.* Physiol Behav, 2005. **84**(1): p. 53-63.

44. Rhodes, J.S., et al., *Mouse inbred strain differences in ethanol drinking to intoxication.* Genes Brain Behav, 2007. **6**(1): p. 1-18.

45. Thiele, T.E. and M. Navarro, *"Drinking in the dark" (DID) procedures: A model of binge-like ethanol drinking in non-dependent mice.* Alcohol, 2014. **48**(3): p. 235-241.

46. Sprow, G.M. and T.E. Thiele, *The neurobiology of binge-like ethanol drinking: evidence from rodent models.* Physiol Behav, 2012. **106**(3): p. 325-31.

47. Thiele, T.E. and M. Navarro, *"Drinking in the dark" (DID) procedures: A model of binge-like ethanol drinking in non-dependent mice.* Alcohol, 2013.

48. K.E. Bosse, J.A.B., B.D. Newman and T.A. Mathews, *Analysis of Neurotransmitters and Their Metabolites by Liquid Chromatography*, in *Liquid Chromatography: Applications*2013, Elsevier: New York. p. 541-609.

49. Childress, A.R., et al., *Limbic activation during cue-induced cocaine craving.* Am J Psychiatry, 1999. **156**(1): p. 11-8.

50. Justice, J.B., Jr., *Quantitative microdialysis of neurotransmitters.* J Neurosci Methods, 1993. **48**(3): p. 263-76.

51. Vithanarachchi, S.M., *Synthesis and Characterization of New Gd3+- Containing Complexes as Potential Targeted Contrast Agents for Magnetic Resonance Imaging*, in *Department of Chemistry*2014, Wayne State University.

52. Eckardt, M.J., et al., *Effects of moderate alcohol consumption on the central nervous system.* Alcohol Clin Exp Res, 1998. **22**(5): p. 998-1040.

53. Guillin, O., et al., *BDNF controls dopamine D3 receptor expression and triggers behavioural sensitization.* Nature, 2001. **411**(6833): p. 86-9.

54. Paxinos, G. and K.B.J. Franklin, *The mouse brain in stereotaxic coordinates*. 2nd ed2001, San Diego, Calif. London: Academic. xxv, 264 p.

55. Mathews, T.A., et al., *Gene dose-dependent alterations in extraneuronal serotonin but not dopamine in mice with reduced serotonin transporter expression.* J Neurosci Methods, 2004. **140**(1-2): p. 169-81.

56. Khalid, M., R.A. Aoun, and T.A. Mathews, *Altered striatal dopamine release following a sub-acute exposure to manganese.* J Neurosci Methods, 2011. **202**(2): p. 182-91.

57. Parsons, L.H. and J.B. Justice, Jr., *Quantitative approaches to in vivo brain microdialysis.* Crit Rev Neurobiol, 1994. **8**(3): p. 189-220.

58. Yoder, K.K., et al., *Dopamine D(2) receptor availability is associated with subjective responses to alcohol.* Alcohol Clin Exp Res, 2005. **29**(6): p. 965-70.

59. Mathews, T.A., et al., *No role of the dopamine transporter in acute ethanol effects on striatal dopamine dynamics.* Synapse, 2006. **60**(4): p. 288-94.

60. Ramachandra, V., et al., *The mu opioid receptor is not involved in ethanol-stimulated dopamine release in the ventral striatum of C57BL/6J mice.* Alcohol Clin Exp Res, 2011. **35**(5): p. 929-38.

61. Smith, A.D., R.J. Olson, and J.B. Justice, Jr., *Quantitative microdialysis of dopamine in the striatum: effect of circadian variation.* J Neurosci Methods, 1992. **44**(1): p. 33-41.

62. Castaneda, T.R., et al., *Circadian rhythms of dopamine, glutamate and GABA in the striatum and nucleus accumbens of the awake rat: modulation by light.* J Pineal Res, 2004. **36**(3): p. 177-85.

63. Hemmings, H.C., Jr., et al., *Emerging molecular mechanisms of general anesthetic action.* Trends Pharmacol Sci, 2005. **26**(10): p. 503-10.

64. Oh, S.S., et al., *The effects of anesthesia on measures of nerve conduction velocity in male C57Bl6/J mice.* Neurosci Lett, 2010. **483**(2): p. 127-31.

65. Westphalen, R.I., K.M. Desai, and H.C. Hemmings, Jr., *Presynaptic inhibition of the release of multiple major central nervous system neurotransmitter types by the inhaled anaesthetic isoflurane.* Br J Anaesth, 2013. **110**(4): p. 592-9.

66. Wang, H., et al., *Changes of learning and memory in aged rats after isoflurane inhalational anaesthesia correlated with hippocampal acetylcholine level.* Ann Fr Anesth Reanim, 2012. **31**(3): p. e61-6.

67. Linsenbardt, D.N., et al., *Tolerance to ethanol's ataxic effects and alterations in ethanol-induced locomotion following repeated binge-like ethanol intake using the DID model.* Alcohol Clin Exp Res, 2011. **35**(7): p. 1246-55.

68. Kamdar, N.K., et al., *Acute effects of naltrexone and GBR 12909 on ethanol drinking-in-the-dark in C57BL/6J mice.* Psychopharmacology (Berl), 2007. **192**(2): p. 207-17.

69. Li, Y.X., et al., *Enhancement of neurotransmitter release induced by brain-derived neurotrophic factor in cultured hippocampal neurons.* J Neurosci, 1998. **18**(24): p. 10231-40.

70. Huang, E.J. and L.F. Reichardt, *Trk receptors: roles in neuronal signal transduction.* Annu Rev Biochem, 2003. **72**: p. 609-42.

71. Logrip, M.L., P.H. Janak, and D. Ron, *Dynorphin is a downstream effector of striatal BDNF regulation of ethanol intake.* FASEB J, 2008. **22**(7): p. 2393-404.

72. Blurton-Jones, M. and M.H. Tuszynski, *Estradiol-induced modulation of estrogen receptor-beta and GABA within the adult neocortex: a potential transsynaptic mechanism for estrogen modulation of BDNF.* J Comp Neurol, 2006. **499**(4): p. 603-12.

73. Altar, C.A., et al., *Anterograde transport of brain-derived neurotrophic factor and its role in the brain.* Nature, 1997. **389**(6653): p. 856-60.

74. Wirkner, K., et al., *Mechanism of inhibition by ethanol of NMDA and AMPA receptor channel functions in cultured rat cortical neurons.* Naunyn Schmiedebergs Arch Pharmacol, 2000. **362**(6): p. 568-76.

75. Guo, W., et al., *Neuronal activity alters BDNF-TrkB signaling kinetics and downstream functions.* J Cell Sci, 2014.

76. Logrip, M.L., P.H. Janak, and D. Ron, *Escalating ethanol intake is associated with altered corticostriatal BDNF expression.* J Neurochem, 2009. **109**(5): p. 1459-68.

77. Yoshii, A. and M. Constantine-Paton, *Postsynaptic BDNF-TrkB signaling in synapse maturation, plasticity, and disease.* Dev Neurobiol, 2010. **70**(5): p. 304-22.

78. Conti, A.C., et al., *Adenylyl cyclases 1 and 8 initiate a presynaptic homeostatic response to ethanol treatment.* PLoS One, 2009. **4**(5): p. e5697.

79. Conti, A.C., et al., *Investigation of calcium-stimulated adenylyl cyclases 1 and 8 on toluene and ethanol neurobehavioral actions.* Neurotoxicol Teratol, 2012. **34**(5): p. 481-8.

80. Maas, J.W., Jr., et al., *Calcium-stimulated adenylyl cyclases are critical modulators of neuronal ethanol sensitivity.* J Neurosci, 2005. **25**(16): p. 4118-26.

81. Acworth, I.a.M.L.C., *The Measurement of Monoamine Neurotransmitters in Microdialysis Perfusates Using HPLC-ECD*, in *Neurodegeneration Methods and Protocols*, J.a.H.A.T. Harry, Editor 1999, Humana Press: Totowa, NJ. p. 219 - 236.

82. Conti, A.C., et al., *Distinct regional and subcellular localization of adenylyl cyclases type 1 and 8 in mouse brain.* Neuroscience, 2007. **146**(2): p. 713-29.

83. DiRocco, D.P., et al., *A role for calmodulin-stimulated adenylyl cyclases in cocaine sensitization.* J Neurosci, 2009. **29**(8): p. 2393-403.

84. Wojnar, M., et al., *Association between Val66Met brain-derived neurotrophic factor (BDNF) gene polymorphism and post-treatment relapse in alcohol dependence.* Alcohol Clin Exp Res, 2009. **33**(4): p. 693-702.

ABSTRACT

ALTERATIONS IN THE MOUSE STRIATUM FOLLOWING ACUTE AND REPEATED ETHANOL EXPOSURE

by

BROOKE DANIELLE NEWMAN

August 2014

Advisor: Dr. Tiffany Mathews

Major: Chemistry

Degree: Doctor of Philosophy

Brain-derived neurotrophic factor (BDNF) is an important neuromodulator that has implicated in regard to several neurological disorders, including alcohol addiction. BDNF is also an important modulator of dopamine (DA), a neurotransmitter that is heavily implicated in addiction with one of the DA rich brain regions being referred to as the reward center of the brain. One of the focuses in alcohol dependence research includes determining risk factors that make an individual more susceptible to becoming dependent. BDNF has been of interest as a risk factor due to its involvement in ethanol consumption and addiction evidenced in a vast number of studies using both human and animal models. The goal of this study was primarily to understand how low endogenous BDNF levels could lead a person to be more susceptible to alcohol dependence/ addiction. This was coupled with the goal of understanding ethanol's alterations on the striatal DA system. Using two different mouse models and both voluntary ethanol consumption along with acute exposure to ethanol via systemic injection several striatal alterations were observed. Seven days of voluntary binge-like ethanol consumption produce a tolerance to ethanol stimulation of DA release, which could be mediated by alterations in adenylyl cyclase (AC) isoforms. BDNF and its receptor (tyrosine kinase B, TrkB) are reduced in WT mice, but not in BDNF-deficient mice following DID. The alterations observed with BDNF and

TrkB could have important implications for the continued used of the DID model. Finally using double-knockout animals that lack AC1 and AC8 it was shown that these isoforms are necessary for ethanol-stimulation of DA. Together these findings show how quickly neuroadaptations can occur following ethanol exposure and provide several avenues for future investigations.

AUTOBIOGRAPHICAL STATEMENT

Education

Wayne State University, Detroit, MI 2009-2004
Ph.D. Candidate in Chemistry
Eastern Michigan University, Ypsilanti, MI 2005-2009
B.S., Biochemistry/Toxicology, Cum Laude

Training

Wayne State University, Detroit, MI 2009 – 2014
Adjunct Faculty (CHM 1020, Summer 2014)
Graduate Research Assistant to Dr. Tiffany A. Mathews (2009-2014)
Graduate Teaching Assistant (CHM 2290, 4 semesters)

Eastern Michigan University, Ypsilanti, MI 2007-2009
Undergraduate Research Assistant to Dr. Harriet Lindsay

Publications

Book Chapter:
Bosse, K. E., Birbeck, J. A., **Newman, B. D**., and T. A. Mathews, "Analysis of neurotransmitters and their metabolites by liquid chromatography," for *HBSS: Liquid Chromatography, Edited by S. Fanali, P.R. Haddad, C.F. Poole, P. Schoemaker, D. Lloyd.* ISBN: 978-0-12-415806-1.

Kaplan, S., Limbocker, R., Divis, J., Osterhaus, G., Newby, M., Newman, B., Mathews, T., and M. Johnson, "Impaired Striatal Dopamine Release and Uptake in Wistar Rats Following Treatment with Carboplatin," *submitted ACS Chemical Neuroscience*

Newman, B. D., Bosse, K. E., and T. A. Mathews, "Striatal Dopamine Tolerance to Ethanol Following Seven Days of Drinking in the Dark," *in preparation J Neuropharmacology*

Awards

Pre-doctoral fellowship NIH/NIGMS R25 GM058905 8/2011 – 7/2013
Training Grant: ***"Initiative for Maximizing Student Diversity" Fellowship (IMSD)***
Wayne State University, Detroit, MI

Thomas C. Rumble Graduate Fellowship 2009
Wayne State University, Detroit, MI

Neuroscience Scholars Program Inductee (Travel Award) 2013
Society for Neuroscience, Washington, DC

Eli Lilly/WCC Travel Grant Award 2012
American Chemical Society, Washington, DC